GENERATION OF AN EARLY WARNING SYSTEM FOR LANDSLIDE AND SLOPE INSTABILITY BY OPTICAL FIBER TECHNOLOGY

A THESIS SUBMITTED TO
THE GRADUATE SCHOOL OF NATURAL AND APPLIED SCIENCES
OF
MIDDLE EAST TECHNICAL UNIVERSITY

BY

ARZU ARSLAN

IN PARTIAL FULFILLMENT OF THE REQUIREMENTS
FOR
THE DEGREE OF MASTER OF SCIENCE
IN
GEOLOGICAL ENGINEERING

AUGUST 2015

Approval of the thesis:

GENERATION OF AN EARLY WARNING SYSTEM FOR LANDSLIDE AND SLOPE INSTABILITY BY OPTICAL FIBER TECHNOLOGY

Submitted by **ARZU ARSLAN** in partial fulfillment of the requirements for the degree of **Master of Science in Geological Engineering Department, Middle East Technical University** by,

Prof. Dr. Gülbin Dural Ünver ______________________
Dean, Graduate School of **Natural and Applied Sciences**

Prof. Dr. Erdin Bozkurt ______________________
Head of Department, **Geological Engineering**

Prof. Dr. Haluk Akgün ______________________
Supervisor, **Geological Engineering Dept., METU**

Examining Committee Members:

Prof. Dr. Erdal Çokça ______________________
Civil Engineering Dept., METU

Prof. Dr. Haluk Akgün ______________________
Geological Engineering Dept., METU

Assoc. Prof. Dr. M. Tolga Yılmaz ______________________
Engineering Sciences Dept., METU

Assoc. Prof. Dr. Kaan Sayıt ______________________
Geological Engineering Dept., METU

Assoc. Prof. Dr. Ayhan Gürbüz ______________________
Civil Engineering Dept., Gazi University

Date: 28.08.2015

I hereby declare that all information in this document has been obtained and presented in accordance with academic rules and ethical conduct. I also declare that, as required by these rules and conduct, I have fully cited and referenced all material and results that are not original to this work.

Name, Last name: Arzu ARSLAN

Signature :

ABSTRACT

GENERATION OF AN EARLY WARNING SYSTEM FOR LANDSLIDE AND SLOPE INSTABILITY BY OPTICAL FIBER TECHNOLOGY

Arslan, Arzu
M.S., Department of Geological Engineering
Supervisor: Prof. Dr. Haluk Akgün

August 2015, 134 pages

The purpose of this study is to develop an early warning system for all kinds of mass movements regardless of the failure mechanism and lithology type. For this purpose, an optical fiber system was preferred due to its superiority in field conditions and continuous data measurement capability.

Two different optical fiber systems, namely, the Optical Time Domain Reflectometer (OTDR) and the Brillouin Optical Time Domain Analyzer (BOTDA) were experimented with alternative fiber cables and their competency was investigated for a real case landslide located in a hazard prone region in Bahçecik Settlement Area in Kocaeli Province. Before the field experiment, the systems were tested first in laboratory scale. For the laboratory studies, a landslide simulation model having an inclination mechanism designed to represent a slope was used. After these experiments, their applicability in the field or for a real case was conducted. Experiments revealed that the OTDR allows sensitive measurement in laboratory scale but is not suitable for field application due to its energy loss based measurement nature. Therefore, the BOTDA system capable of measuring strain without power loss but detecting frequency shift was preferred for the field studies.

Once the measurements from the optical fiber system were gathered, it was necessary to compare these results with the displacements that occurred on the studied mass. The displacements that take place in a small scale laboratory landslide simulator are rather obvious; however this is not the case for field application. Therefore, slope stability analyses were conducted in order to compare the strain results collected from fiber cables with displacements on the moved mass. In order to accomplish this objective, a back analysis study was implemented to reach the mobilized shear strength parameters of the moved mass by utilizing three profiles. Then, the landslide was modeled based on deformation analysis via the finite element method to compute the displacements of the critical region within circular failure. The main purpose of the finite element analysis was to determine the most critical part of the failure region and to examine the sensitivity of the study by locating the optical fiber system at this region. Thus, the reliability of field results can be better understood. In conclusion, finite element modelling results showed that the displacement values calculated by modelling were in good agreement with those obtained through field monitoring with BOTDA.

Keywords: Optical Fiber System, Landslide Monitoring, Early Warning System, Slope Stability, Bahçecik Landslide, Kocaeli.

ÖZ

HEYELAN VE ŞEV DURAYSIZLIĞI ERKEN UYARI SİSTEMİNİN OLUŞTURULMASINDA FİBER OPTİK TEKNOLOJİSİNİN KULLANIMI

Arslan, Arzu
Yüksek Lisans, Jeoloji Mühendisliği Bölümü
Tez Yöneticisi: Prof. Dr. Haluk Akgün

Ağustos 2015, 134 sayfa

Bu çalışmanın amacı, kayma tipi ve litolojik birimden bağımsız bir şekilde tüm kütle hareketleri için bir erken uyarı sistemi oluşturmaktır. Bu amaçla, erken uyarı sistemi için fiber optik sistemler arazi koşullarında kullanım kolaylığı ve sürekli veri alma özellikleri sebebiyle tercih edilmiştir.

Çalışmalar sırasında, iki farklı fiber optik sistem, Optik Zaman Alanı Yansıma Ölçer (OTDR-Optical Time Domain Reflectometer) ve Brillouin Optik Zaman Alanı Çözümleyici (BOTDA-Brillouin Optical Time Domain Analyzer) kullanılarak alternatif fiber kabloların ve ölçüm sistemlerinin Kocaeli ili Bahçecik Mevkii'nde bulunan ve afete maruz bölge ilan edilmiş çalışma sahası için uygulanabilirliği sınanmıştır. Saha çalışması öncesinde sistemler ile laboratuvar ortamında çalışılmıştır. Laboratuvar çalışmaları sırasında tasarlanan ve arazi koşullarındaki duraysız bir şevi temsil edebilecek şekilde bir eğim mekanizmasına sahip olan heyelan simulasyon modeli kullanılmıştır. Sistemlerin arazi koşullarına uygunluğu tespit edildikten sonra sistemin heyelan sahasına uygulanması için çalışmalara başlanmıştır. Çalışmalar laboratuvar ölçeğinde OTDR ile hassas ölçümler alınabileceğini göstermiştir, fakat sistem enerji kaybı prensibi ile çalıştığı için saha uygulaması için yeterli olmadığı tesbit edilmiştir. Bundan dolayı, gerinimi enerji kaybı değil, frekans kayması ile belirleyen BOTDA sistemi arazi uygulamaları için tercih edilmiştir.

Fiber optik sistem ile ölçümler yapıldıktan sonra elde edilen sonuçların söz konusu kütle hareketi sonucunda oluşan deplasman değerleriyle karşılaştırılması gerekmektedir. Laboratuvar ölçeğinde yapılan çalışmalar sonucu oluşan deplasman değerleri açık bir şekilde belirlenebilmektedir, fakat durum gerçek bir heyelan sahası için böyle açık değildir. Bu sebeple, fiber optik sistemden elde edilen gerinim değerleri ile meydana gelen deplasmanların karşılaştırılması şev stabilitesi analizleri ile mümkün olmuştur. Bunun için, heyelan boyunca çizilmiş üç profilden geriye dönük çözümleme yapılarak kayma anında malzemenin sahip olduğu kesme dayanımı parametrelerine ulaşılmıştır. Daha sonra sonra heyelan, sonlu eleman yöntemi ile modellenerek dairesel kaymanın olduğu kritik bölgelerdeki deplasman değerleri hesaplanmıştır. Sonlu eleman yöntemi uygulanmasında esas amaç alanda en çok deplasmanın beklendiği kritik olan bölgelerin belirlenmesi ve fiber optik sistemin belirlenen bu bölgelere yerleştirilerek çalışmaların hasassiyetinin araştırılmasıdır. Bu sayede arazide yapılacak çalışmalardan elde edilecek sonuçların güvenilirliği daha iyi anlaşılacaktır. Sonuç olarak, heyelan alanında modelleme çalışmaları ile elde edilen deformasyon sonuçları arazide fiber optik yöntemlerle elde edilen izleme/gözlemleme sonuçlarıyla karşılaştırıldığında uyumlu oldukları anlaşılmaktadır.

Anahtar Kelimeler: Fiber Optik Sistemi, Heyelan İzleme, Erken Uyarı Sistemi, Şev Stabilitesi, Bahçecik Heyelanı, Kocaeli.

To My Beloved Family

ACKNOWLEDGEMENTS

I wish to express my sincere thanks to Professor Haluk Akgün, my supervisor for his great support, guidance and valuable advice he gave during my study. I would like to also thank Dr. Mustafa K. Koçkar as he was the one I bore when I had a problem whether scientific or personal, he always solved them. I am grateful to Mert Eker as he was with me all the time with his advices and helpfulness.

I owe to Dr. Murat Nurlu a debt of gratitude as he understood the potential of the subject and encouraged us to write a project proposal to Republic of Turkey Prime Ministry Disaster and Emergency Management Authority (AFAD). I also would like to thank Mr. Ahmet Temiz, Cenk Erkmen, M. Maruf Yaman and Ceren Deveci from Planning and Mitigation Department of AFAD. I am grateful to AFAD's National Earthquake Research Program (UDAP) for the financial support they provide, without this support getting these results would be impossible.

Mustafa Yurtsever from Geolab Geotechnics and Haydar Merdin and Mehmet Abdullah Kelam from HAMA Engineering, I thank you gentlemen for everything. I would like to point out that I am sure I could not find such an interesting topic if I had not met you and I could not complete this study without your support.

I would like to thank Selim Cambazoğlu, Karim Youesifibavil, Mustafa Kaplan, Kadir Yertutanol and Damla Gaye Oral for their endless support and valuable friendship during this study. I also would like to thank Aydın Çiçek from General Directorate of Mineral Research and Exploration.

I have to thank Dr. Lufan Zou from OZ Optics for his support about the theory and device usage and I would like to thank Prof. Dr. Kazuhiro Watanabe for sending sample fiber cables from Japan.

I place on record, my sincere thank to my love, for his continuous encouragement, support and great thoughtfulness.

At last but not the least I am extremely thankful to my family for their great support, patience and encouragement, especially to my brother, Ali.

I would like to thank everybody who directly or indirectly contributed and I also wish to ask for forgiveness if I miss to mention anyone undesirably.

TABLE OF CONTENTS

LIST OF TABLES

TABLES

LIST OF FIGURES

FIGURES

CHAPTER 1

INTRODUCTION

1.1 Purpose and Scope

Landslides are one of the most destructive natural hazards in the world and in Turkey. They are without a doubt a major natural hazard as important as earthquakes or floods (Akgün & Bulut, 2007; Gökçe et al., 2008). Republic of Turkey Prime Ministry Disaster and Emergency Management Authority (AFAD) have conducted a study in terms of the number of affected settlements, number of occurrences, number of events that caused evacuation, and the number of people evacuated for several hazards between the years of 1950 and 2008 for Turkey (Table 1). The study shows that landslides are the primary type of disaster when the number of the affected settlements, occurrences and evacuation events are considered. In most cases, landslides are perceived as disasters triggered due to earthquake, flood, volcanic eruption or typhoon. However, they generally have greater socioeconomic impacts than recognized as they are the element of multiple hazard disasters. Landslides cause great economic loss in many countries around the world and this loss seems to grow with the increase in population and the utilization of unstable hillside areas to overcome the increasing demand for settlement areas. Moreover, landslides not only result in loss of lives but they also cause damage to residential areas, industrial complexes, agricultural lands, forests, and affect water quality of streams resulting in substantial economic losses (Schuster, 1996).

Table 1: Hazards occurred in Turkey between 1950-2008 and their results (Gökçe et al., 2008)

Hazards	Number of Affected Settlements	Number of Occurrence	Number of Events That Have Led to Evacuation	Number of People Evacuated
Landslide	4161 (%34.18)	12794 (%42.63)	6347	63969 (%25.40)
Rock Fall	899 (%7.38)	2769 (%9.23)	1367	20836 (%8.26)
Flood	1861 (%15.23)	3873 (%12.91)	2249	26081 (%10.36)
Earthquake	2952 (%24.25)	5267 (%17.55)	4807	106838 (%42.42)
Others	665 (%5.46)	1076 (%3.59)	658	8200 (%3.25)
Snow Avalanches	207 (%1.7)	670 (%2.23)	292	4112 (%1.63)
Multiple Hazards	1427 (%11.73)	2967 (%6.89)	1058	19102 (%7.57)
Unclassified		1491 (%4.97)	704	2723 (%1.1)
Total	12172	30007	17482	251861

Studies regarding landslides have become more important with the realization of the correlation between the number of landslides and adversely affected structures. Due to these reasons, awareness about landslides and importance given to the concept of risk assessment have been increasing, and correspondingly, early warning systems have started to gain more attention (Li et al., 2012; Liu et al., 2010; Pei et al., 2011). Today, there are many techniques to monitor landslides and/or potential slope instabilities and they have their advantages and disadvantages. Inclinometers, tiltmeters, extensometers, ground based LIDAR, satellite images, and air photography are examples of techniques used for landslide monitoring (Savvaidis, 2003; Pei et al., 2011). Rather than early warning, these methods are used to detect subsequent deformation. Among these, optical fiber systems have superiority over aforementioned systems in terms of their easy and fast data transfer, smaller dimensions, light weight, sensitivity to strain and temperature change, wide band range, resistance to environmental and electromagnetic effects, low cost and real time monitoring properties (Wang et al., 2008; Gupta, 2012; Measures, 2001). Optical fibers have been used since 1800s but their usage in early warning systems of landslides is a fairly new concept (Al-Azzawi, 2007).

The purpose of this thesis is to develop an early warning system for landslides that is related to neither failure mechanism nor lithology type by combining the strain results collected from fiber cables with displacements on moved masses. For this purpose, optical fiber systems are preferred due to their superiority in field conditions and continuous data measurement capabilities. In this study two different optical fiber systems were experimented with alternative fiber cables and their competency for a real case landslide area was investigated. Before the field experiment, systems were tested first in laboratory scale and then in the field. For the laboratory studies, a landslide simulation model having an inclination mechanism designed to represent a slope was used. Field application of the system was performed in a landslide hazard prone region in the Bahçecik Settlement Area in the Kocaeli Province. The region is located in the south of the city where the topography is mountainous.

1.2 The Study Area

The study area is located within the borders of Kocaeli Province, Başiskele District, Bahçecik Settlement Area. The location map of the region is given in Figure 1.

Kocaeli is located within the Eastern Marmara Region of Turkey and it has an economic importance due to its industrial capacity. Kocaeli is an industrial city with factories pertaining to especially the chemical industry along with the metal, automotive, and machine industries. Kocaeli is bounded by the Black Sea and İstanbul from the north, Sakarya from the east, Bursa from the south and İstanbul and Yalova from the west.

Figure 1: Location map of the study area (Google Inc., 2015)

Kocaeli is one of the important cities of Turkey due to its high rank in the country economy, geographical position and population. According to Gökçe et al. (2008) Kocaeli does not rank first in terms of the number of the landslides that have occurred to date. Although that is expected to affect landslide hazard analysis positively, risk is higher than expected as Kocaeli is important in terms of economy, location, and population. As a result, Kocaeli is determined as one of the priority areas in terms of landslide hazard and risk.

North Anatolian Fault System (NAFS) is a right lateral strike slip fault that has a length of 1500 km and separates Anatolian Plate located at South from Eurasia Plate located at North.Kocaeli is one of the cities that affected from this fault system. Therefore, earthquakes should be considered as a major triggering mechanism for landslides occurred in Kocaeli. Distribution of landslides occurred around the study area and faults present can be seen in the Figure 2. According to Duman et al. (2006) landslides reactivated after 1999 İzmit earthquake has an effect on hazard distribution together with shallow landslides formed.

According to the Republic of Turkey Prime Ministry Disaster and Emergency Management Authority (AFAD) database, the reported landslides that have occurred between the years 1960 and 2006 in Kocaeli is given in Table 2 on a district basis. The numbers given may be uncertain since the table was prepared according to the reported events (Gökçe et al., 2008).

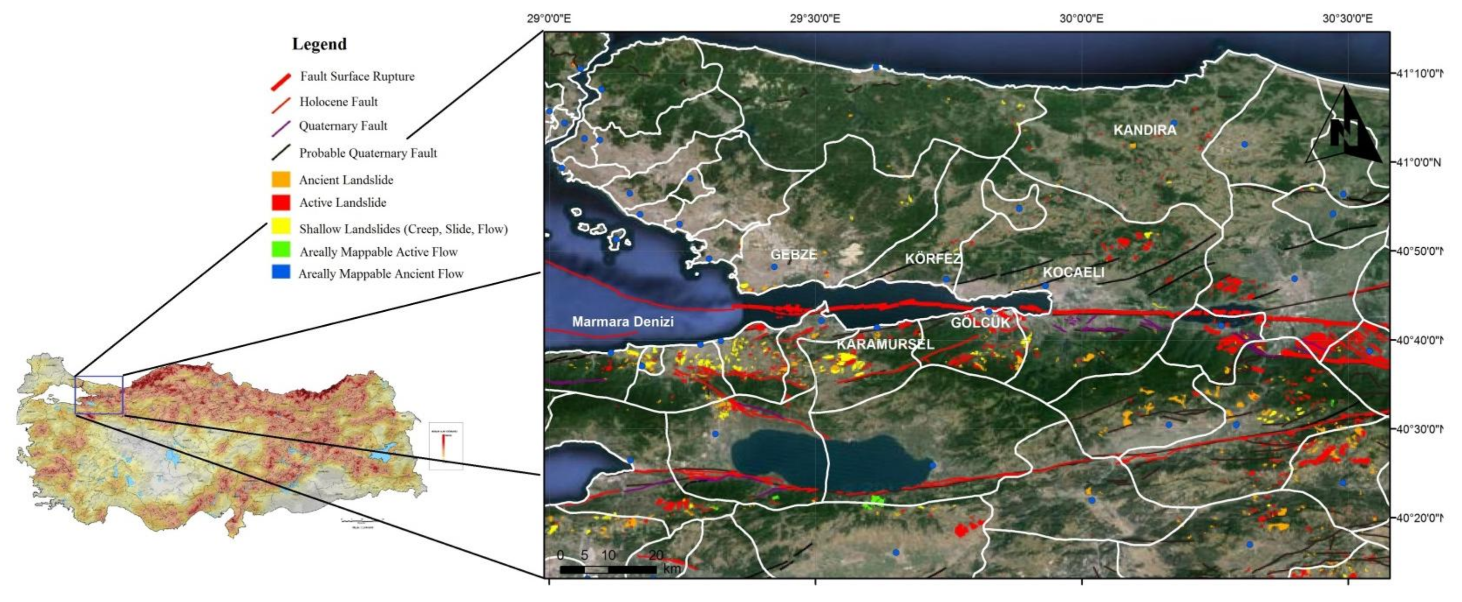

Figure 2: Distribution and types of landslides that have occurred and faults around the study area (Modified from Landslide intensity map of Disaster and Emergency Management Authority (AFAD) and landslide inventory map of General directorate of Mineral Research and Exploration (MTA)

Table 2: List of the landslides occurred in Kocaeli between 1960-2006 gathered from AFAD database (Gökçe et al., 2008)

Province	District	Number of Landslides
Kocaeli	Gebze	12
	Merkez	37
	Gölcük	12
	Kandıra	1
	Karamürsel	28
	Körfez	2
	Yarımca	4
Total Number of Landslides		96

The study area is located at the border of the Başiskele district. Başiskele is not present in Table 2 since it was founded in 2008, but it lies within the borders of Merkez where most of the landslides have occurred.

Landslides can be triggered by the intense precipitation, snow melt, earthquakes and human activities.. The climate and precipitation regime has an effect on landslides. Also, human activities that include construction of engineering structures like roads and tunnels have a remarkable impact in Kocaeli. In addition, seismic activity should be considered due to its proximity to the NAFS.

Apart from the economic importance of Kocaeli, the study area was selected due to its critical location in terms of landslide risk. In 2010, a landslide occurred and the region was announced as a hazard prone area by the AFAD in 19.02.2013 because the landslide was threatening a house that was located in its crown area (Figure 3).

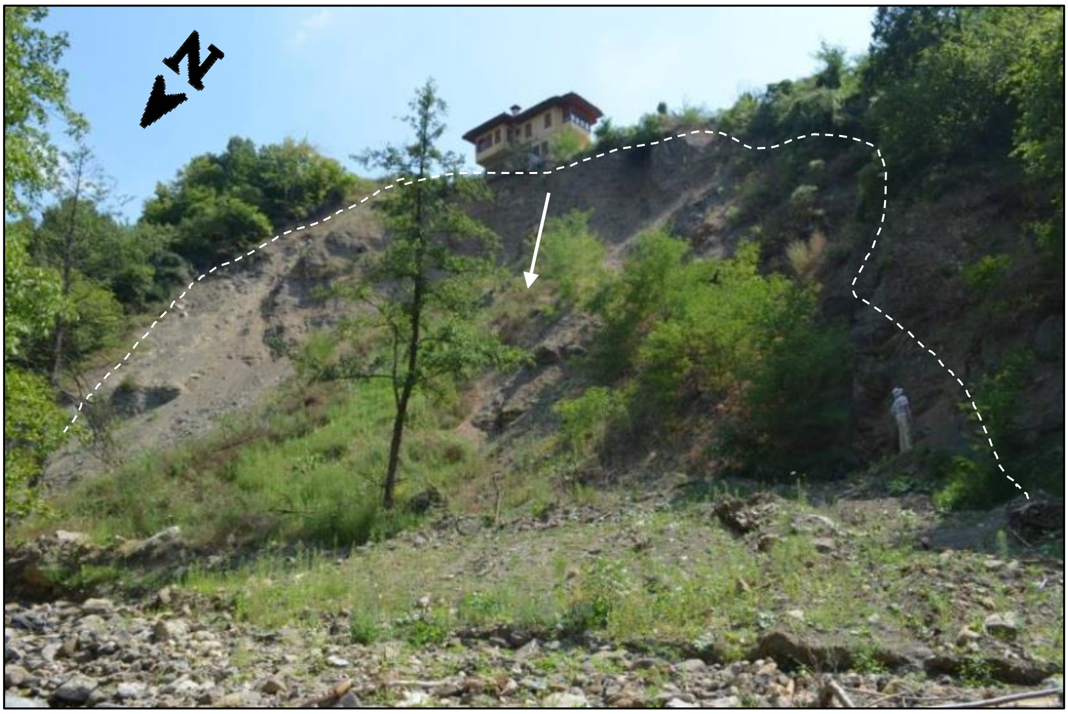

Figure 3: General geometry of the landslide and the house affected

Figure 4a through 4c give Google Earth images of the study area before and after the landslide as well as the house affected for the years 2009, 2011, and 2015, respectively. Field observations and measurements showed that the mass movement located at the study area has a width of 120 m and height of 40 m.

Figure 4: Appearance of the study area dated on a) 11.04.2009 (before), b) 05.08.2011 (after), c) 07.05.2015 (after).

1.3 Physiography

The catchment basin of the study area trapped by the Gulf of İzmit, İznik Lake and Sakarya River is formed by the plateaus with varying topographic heights. This area is geomorphologically differentiated from the Kocaeli Peninsula by the important topographic heights such as Naldöken (1125 m), Dikmen (702 m), Karlık (892 m) and especially Kartepe Mountain with an elevation of 1601 meters. Southern parts of Kocaeli have steeper slopes compared to the northern parts.

On the southern region, volcanic formations are abundant and these volcanic units composed of andesites and dacites are located within the catchment basin which is formed by the high mountains and plateaus, and extends through the NE and E direction until they reach Gölcük and Maşukiye. The regions where volcanic units located are the areas where events such as landslides and rock falls are expected.

On the southern part, the region between Hersek Delta and the western part of Gölcük is generally observed as a typical high cliff beach. Some low coasts are also present around Karamürsel, Ereğli and Yalıdeğirmendere. On the other side of the bay, on the east and west of this cliffed region, low coasts are observed in larger areas. On the eastern part, the coast between the Gölcük region and the end of the gulf of İzmit forms an alignment of transported sediments due to numerous streams. On the western part, the alluvial sedimentation that forms the Hersek and Laledere deltas penetrate towards the sea, thus forming the low coast at that region (Kocaeli Environment and Urbanization Directorate, 2011).

1.3.1 Climate

Kocaeli has a mild climate along the coasts of Black Sea and Gulf of İzmit, and harsh climate at mountainous regions. It can be said that Kocaeli has a transition climate between Mediterranean climate and Black Sea climate. Winters are not warm as Mediterranean climate and summers are not as wet as Black Sea climate. According to the Turkish State Meteorological Service (2014), the annual average temperature of the last 64 years is 15.0°C. January is the coldest month with an average temperature of 6.3°C and July is the warmest month with an average temperature of 23.7°C. The average values of temperature, sunshine duration, rainy days and precipitation is given in Table 3 on a monthly basis. In addition, the average monthly temperature and precipitation are presented in Figure 5.

Table 3: Average values of temperature, sunshine duration, and precipitation data in Kocaeli forthe 1950-2014 period (Turkish State Meteorological Service, 2014).

Value / **Month**	**Average Temperature (°C)**	**Average Highest Temperature (°C)**	**Average Lowest Temperature (°C)**	**Average Sunshine Duration (hr)**	**Average Rainy Days**	**Monthly Average Precipitation (kg/m^2)**
January	6.3	9.7	3.3	2.3	17.6	93.2
February	6.7	10.7	3.5	3	15.6	73.3
March	8.6	13.2	4.9	4.6	14.1	73.4
April	13.1	18.5	8.9	5.3	11.9	52.3
May	17.5	23.2	12.9	7.2	9.9	45.4
June	21.7	27.5	16.8	8.6	8.3	52.8
July	23.7	29.5	19.1	9.3	5.8	37.6
August	23.7	29.6	19.2	9.6	5.3	43.6
September	20.4	26.2	16.1	7.1	7.1	52
October	16	20.8	12.5	4.5	11.8	89.9
November	11.9	16.2	8.6	3.4	12.7	81.5
December	8.5	11.9	5.6	2.3	16.4	**108**

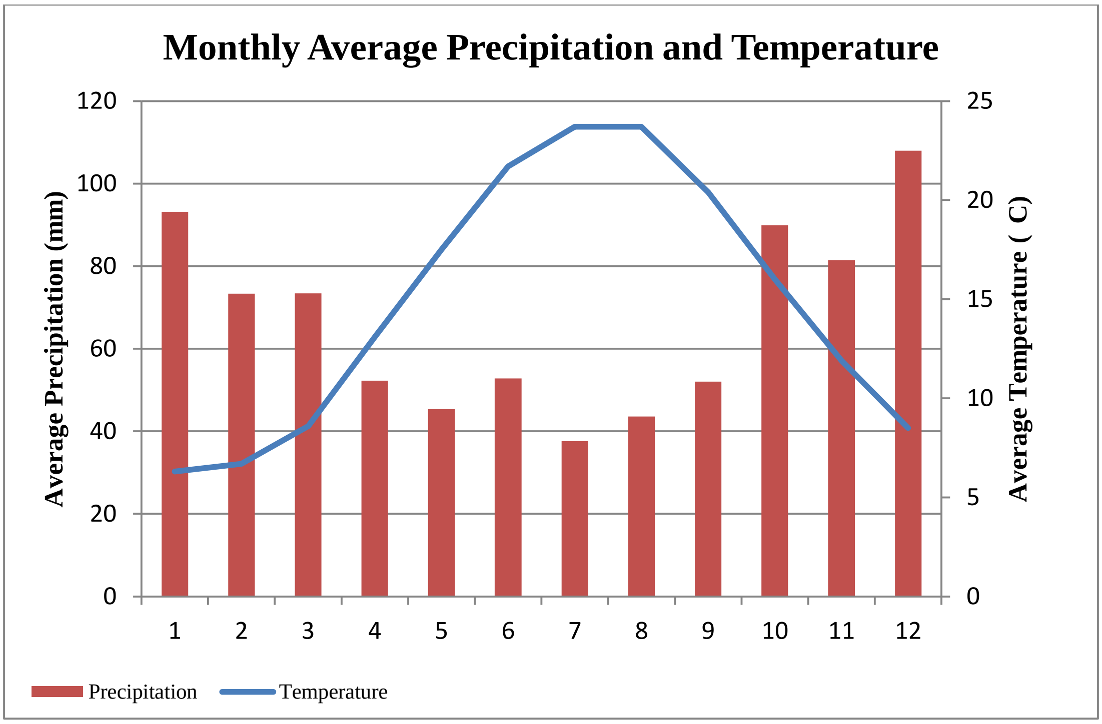

Figure 5: Monthly average precipitation and temperature values of Kocaeli between the years 1950-2014 (Turkish State Meteorological Service, 2014)

The annual precipitation distribution of Kocaeli for the years between 1981 and 2010 is shown in Figure 6. Accordingly, the average annual precipitation is 799.5 mm. The annual precipitation data shows that Kocaeli has received precipitation far over the average in the years 1981, 1997, and 2010 since 1981 with a nearly 14 years of recurrence period.

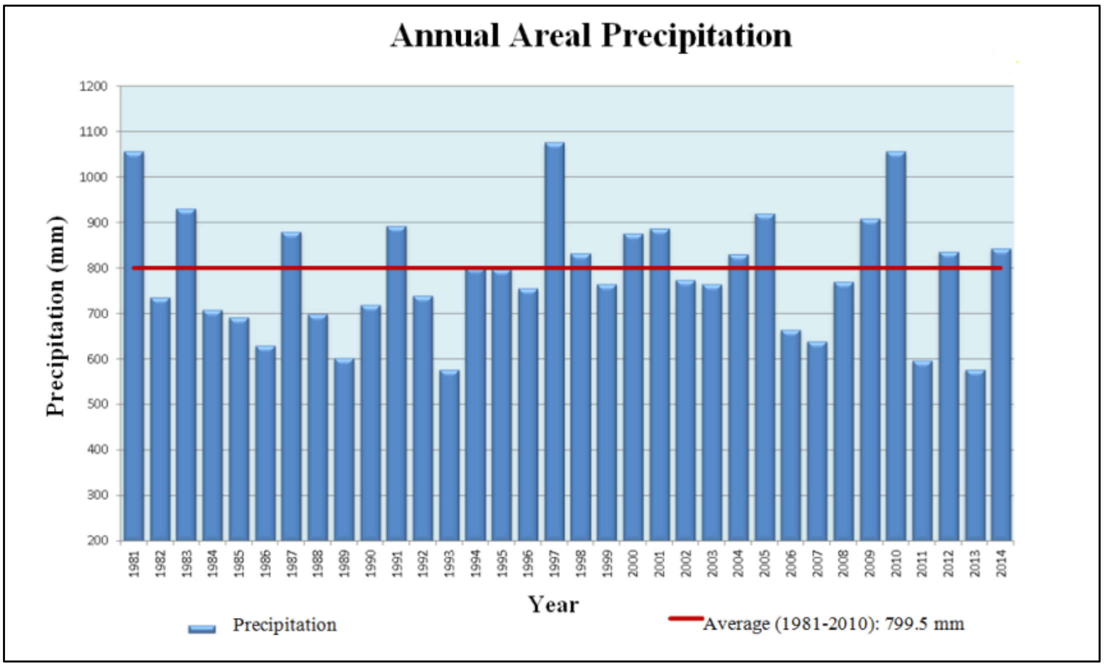

Figure 6: The annual areal precipitation of Kocaeli (Turkish State Meteorological Service, 2014)

From the data of Figure 6, it can be seen that the amount of precipitation in 2010 is higher than that of the preceding and following years. In addition, the average monthly precipitation values show that December has the highest amount followed by January. In 2010, the December precipitation of Kocaeli was measured as 124.5 mm which was drastically more than the average value of 108 mm. The daily precipitation data obtained from the Turkish State Meteorological Service database shows that thirteen days of December were rainy. The precipitation in this period varied from 0.6 mm to 28.4 mm and reached the peak value on December 10, 2010. The precipitation graphics of the related days are presented in Appendix A.

CHAPTER 2

GEOLOGICAL SETTING AND ENGINEERING GEOLOGICAL ASSESSMENT OF THE STUDY AREA

2.1 Introduction

Kocaeli is surrounded by the topographic heights of the Kocaeli Peninsula on the north, Armutlu Peninsula on the south and divided into two with the North Anatolian Fault System (NAFS) by the gulf of İzmit which is an extension of the Marmara Sea and also the sedimentary basin. This is the main reason why Kocaeli is examined in three different geomorphological regions which are the Kocaeli peninsula to the north, Armutlu peninsula to the south and the gulf of İzmit at the center (Kocaeli Environment and Urbanization Directorate, 2011).

Kocaeli has two geologically important tectonic and structural assemblies. One of them is the Kocaeli Peninsula containing the İstanbul Paleozoic and the Kocaeli Triassic units that are located at the north of the gulf of İzmit. According to Şengör and Görür (1983) the Kocaeli Peninsula was detached from the Moesia platform. The other assembly is the Armutlu Peninsula which is a part of the Sakarya Zone. Kocaeli is located on the tectonic assembly called the İstanbul Zone together with the İstanbul and Kocaeli Peninsulas which are natural extensions of each other. Also, the gulf of İzmit is located on the east west directional active graben where the North Anatolian Fault System and the Marmara Graben System are interacted.

The Sapanca Lake is located at the eastern part of Kocaeli while Kocaeli and Armutlu Peninsula are located at the north and south, respectively. The ages of the formations found in the Kocaeli Peninsula vary between Ordovician and Quaternary (Gedik et al., 2005) and the units of the Armutlu Peninsula are found in the age interval of Triassic to Quaternary and dominated by ophiolites and metamorphic units (Göncüoğlu et al., 1986). There is no chance to observe a continuity, concordance or correlation since these two units are separated by the North Anatolian Fault System.

2.2 General Geology and Seismotectonics

The units that outcrop in the Kocaeli Peninsula are composed of Paleozoic and Permian-Triassic aged allochthonous units, Late Cretaceous-Eocene aged semi-autochthonous units, and Oligocene-Miocene and Pliocene-Quaternary aged autochthonous units (Gedik et. al., 2005). There are two Paleozoic aged sequences and three Permian-Triassic sequences in the Kocaeli Peninsula. The units of these different aged sequences have originally deposited at various locations and later have come together as tectonic slices. The Paleozoic units were subjected to tectonic movements during terrestrial sedimentation and have located in their place as tectonic slices with transgressive Permian-Triassic units on them. At the Western Pontides, the age of this placement should be older than Late Jurassic as there are Late Jurassic-Middle Eocene aged units that rest unconformably on this unit. As the result of tectonism, faults rather than folded structures were formed in Kocaeli (Gedik et. al., 2005).

Armutlu Peninsula is situated in NW-Anatolia and composes the western part of the Pontides. The peninsula is bordered with two main branches of NAFS and it is approximately located on Mesozoic aged Intra-Pontide Suture. There are several different units representing the formations starting from Paleozoic outcropped within the borders of Armutlu Peninsula. Precambrian-Early Paleozoic aged Pamukova

Metamorphics compose the basement of the region. Sedimentary and volcano-sedimentary units that cover the basement are Early Triassic Taşköprü Formation, Late Paloecene-Middle Eocene aged İncebel Formation, and Eocene aged Sarısu Formation. Fıstıklı Granodiorite settled during Eocene. At the upper parts, Late Miocene aged Kılıç Formation, Late Miocene-Early Pliocene aged Yalakdere Formation, Pleistocene aged marine platform sediments and Quaternary alluviums (Akartuna, 1968; Göncüoğlu, 1990). These formations can be classified as two main geological units. One of them is pre-Cenomanian metamorphic basement that made up of Pamukova Metamorphics and İznik Metamorphics. Other geologic unit is a non-metamorphic cover with a discontinuous Cenomanian-Pliocene stratigraphic column. (Göncüoğlu et. al., 1992). Figure 7 shows a generalized regional geological map of the study area and its surroundings.

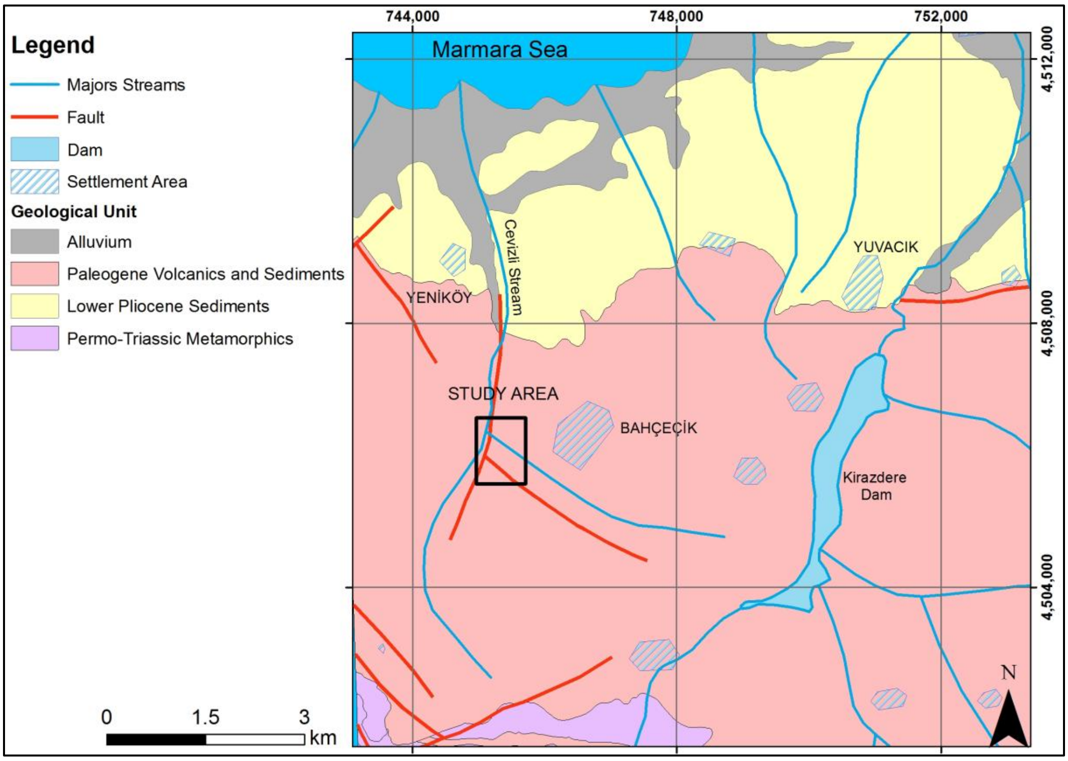

Figure 7: Regional geology map of study area (Modified from Gedik et. al., 2005)

Kocaeli is located in a region that is tectonically active and according to the study made by the Earthquake Research Center study of the Ministry of Public Works and Settlement in 1996, the study area is located in a first degree earthquake zone where the expected peak horizontal ground acceleration is greater than 0.40g (Figure 8).

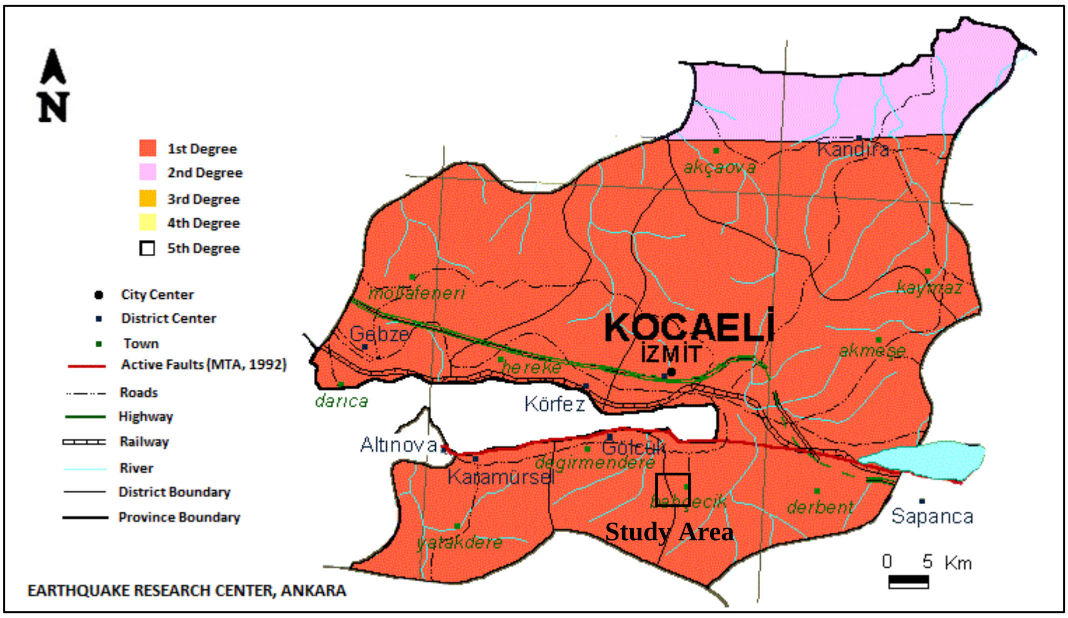

Figure 8: Map showing seismic zonation for Kocaeli (Earthquake Research Center, 1996).

The NAFS is one of the major tectonic structures of Turkey that disconnect the Eurasia Plate that is located at the north from the Anatolian Plate that is located at the south and has a length of 1500 km. The NAFS is a right lateral strike-slip fault system. Kocaeli and thereby the study area is located in the NAFS. This fault system has created a 125-145 km surface rupture as the result of the August 17, 1999 Kocaeli earthquake with a moment magnitude of 7.4 (Lettis et al., 2002; Barka et al., 2002). This surface rupture continues into the Marmara Sea (Emre et al., 1998; Barka et al., 2002; MTA, 2003; Harris et al., 2002; Duman et al., 2005, Emre et al., 2011). Another seismic source around Kocaeli is the fault zone created on November

12, 1999, namely, the Düzce earthquake with moment magnitude of 7.2. This fault zone has a length of 30 to 45 km (Duman et al., 2005). In addition, there is another seismic source created by the Abant (May 26, 1957, Ms=7.0) and in Mudurnu (June 22, 1967, Ms=7.1) earthquakes (Ambraseys and Zatopek, 1969). The Mudurnu earthquake has a 55 km long fault zone that overlaps 25 km of the Abant earthquake fault zone (Ambraseys and Zatopek, 1969). The 1957 Abant earthquake has a surface rupture with a length between 30 km (Barka, 1996) and 40 km (Ambraseys and Zatopek, 1969) that extends between the Abant Lake and Dokurcun. The surface rupture of the Bolu earthquake (February 1, 1944, Mw=6.8) that occurred near the study area continues between the Abant Lake and Bayramören (Ketin, 1969; Öztürk et al., 1985). Major earthquakes around the study region and their focal mechanism analysis are given by Figure 9.

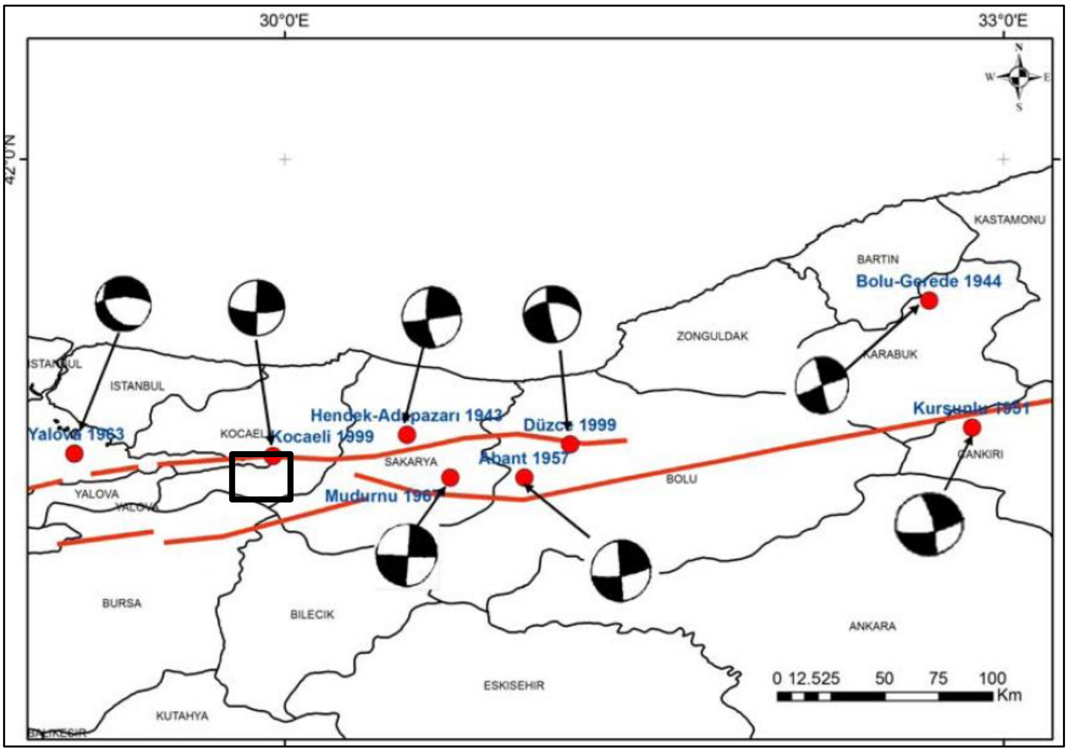

Figure 9: Major earthquakes and focal mechanism analysis within and around the study area along the NAFS (Cambazoğlu, 2012).

2.2.1 Local geology

The units that outcrop in and around the study area belong to the Sarısu and İncebel formations. As a consequence, only the details of the characteristics of these formations will be explained.

The Sarısu formation is a volcano-sedimentary sequence that is commonly observed in the middle part of the Armutlu Peninsula. It is composed of andesitic lava and agglomerate. The sequence is found most typically around the Sarısu Village and outcrops as a northeast-southwest oriented line that divides the peninsula into two pieces. The sequence contains different lithological order in different places due to development process of the volcanism. The formation generally starts with a 5-10 m thick sedimentary level onto metamorphic rocks. This level is composed of conglomerate, mudstone, sandstone and limestone. Conglomerate is made up ofquartz fragments and is grain supported. Mudstone contains quartz and limestone fragments. Limestone has the characteristics of packstone with lithoclastic, bioclastic, nummulite and quartz grains in it. This sedimentation is the 1000 meters thick part located on top of the basement sequence and is generally composed of pyroclastic and epiclastic rocks. Pyroclastics have normal, reverse or symmetrical grading while fine or coarse grained tuff has andesitic tuff and rock fragments in different sizes. Pyroclastic flow deposits are found in alternation with symmetrical graded or ungraded lahar deposits. Some levels of the sequence contain huge andesite blocks and pebbles of epiclastic deposits that probably have the characteristics of beach conglomerate. Lava flows within the sequence that are found at the upper levels and have a thickness of 5 meters show an alternation with pyroclastic rocks. Lava flows are composed of andesitic volcanic rocks with plagioclase, pyroxene and hornblende phenocrysts. Tuffs contain plagioclase, glass and fluidal textured volcanic fragments within a glass matrix. Lahar deposits which formed as a result of pyroclastic flow having normal or symmetrical grading have developed irregular unconformity planes by scratching the flow surfaces. All this sequence is cut by basalt dykes that are observed especially in the upper levels. Basalts have augite and plagioclase and appear to be much fresher than andesite.

The Sarısu formation is located on metamorphic rocks with a thin level of basal conglomerate, and has a tuff and sandstone alternation at its contact with the İncebel flysch. Limestone and sandstone specimens located at the lowest level of the volcanic sequence and metamorphic unconformity shows that the sequence developed starting from Lutetian (Erendil et. al., 1991).

The İncebel Formation is a Paleocene-Eocene aged formation seen generally at the south of Karamürsel. The formation unconformably covers the metamorphic units and forms a 3000 m thick sequence in the İncebel Village and dips towards northwest. The İncebel formation starts with a basal conglomerate layer composed of pebbles of the units that overlay and its color is observed to be purple, gray or yellow according to underlying unit. The İncebel formation is generally composed of a flysch sequence of sandstone, mudstone, marl, and conglomerate. However, it can contain volcanic lithologies, namely light colored tuffs and andesitic agglomerate in the upper parts of the sequence. Due to the presence of this volcanic level, the İncebel formation is interpreted to occur in alternation with the Sarısu formation (Göncüoğlu et al., 1992).

2.3 Engineering Geological Assessment of the Study Area

The study area is located within a valley that lies within the stream bed of the Sarılık Stream. A three-dimensional stratigraphic model of the region prepared by the Rockworks v.16 (Rockware, 2013) is given in Figure 10.

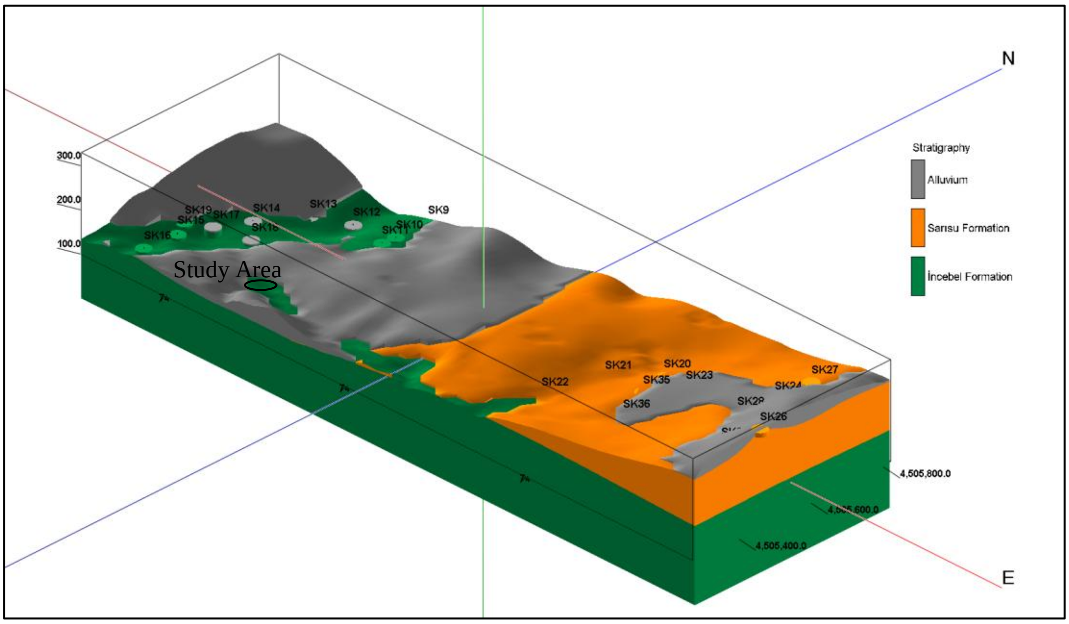

Figure 10: Three-dimensional stratigraphic model of the study area

A field study conducted in order to understand the general geological and engineering geological properties of the region revealed that the lithology in the study area consists of an alternation of sandstone and marl. Figure 11 shows a close-up view of the lithology. According to the field observations, this unit is correlates with the Paleocene-Eocene aged İncebel formation.

Figure 11: A close-up view of the İncebel formation

The sandstone marl alternation sequence contains scattered and non-persistent discontinuity sets. Small scale folds are observed in the field. As explained in Section 2.2, the study area is located within a tectonically active region, or in other words, in a shear zone. Figure 12 shows a view of the folded and sheared structures and discontinuities that are present within the sandstone-marl alternation sequence in the study area.

Figure 12: Folded structures and small scale non-persistent scattered discontinuities present in the study area

2.3.1 Engineering geological investigation

Several boreholes have been driven in the vicinity of the study area in previous geotechnical studies conducted by private companies. Table 4 gives the coordinates, depth and groundwater level of the boreholes located in the vicinity of the landslide region. The engineering geological borehole logs are given in Appendix-B.

Table 4: The coordinates, depth and groundwater level of the boreholes

Borehole Number	X	Y	Z	Depth (m)	Groundwater Depth from Surface (m)
SK5	492103.631	4503627.344	209.585	12.00	-
SK9	491609.017	4503564.437	136.944	12.00	3.00
SK10	491623.3	4503456.893	155.678	12.00	-
SK11	491624.15	4503416.77	159.929	12.00	-
SK12	491484.971	4503483.266	118.705	18.00	3.00
SK13	491402.697	4503446.256	119.547	18.00	3.00
SK14	491336.562	4503354.646	122.674	18.00	3.00
SK15	491287.681	4503189.871	145.695	10.00	3.00
SK16	491295.539	4503084.843	158.755	12.00	-
SK17	491313.861	4503264.014	138.109	21.00	4.00
SK18	491404.1	4503277.226	138.26	21.00	4.00
SK19	491256.442	4503243.465	133.987	10.00	4.00
SK21	492362.247	4503265.973	209.223	13.00	-
SK22	492295.662	4503154.601	192.723	12.00	9.00

The engineering geological characterization of the studied region was accomplished with 201 m of boring data resulting from a total of 14 boreholes. Note that these boring data were obtained from adjacent to the landslide location. According to the boring results, there is a 1-2 m thick soil cover on the upper levels of the İncebel formation and this soil cover is underlain by a sandstone siltstone marl sequence. The groundwater was encountered on nine of the fourteen boreholes at a depth generally varying from 3 to 4 m from the ground surface.

A sequence made up of sandstone and siltstone alternation occurs within the boundaries of the landslide. The sequence is generally tectonically deformed and disintegrated although in several locations of the landslide it outcrops as detached blocks (Figure 13). The sandstone has a yellowish brown color while the siltstone is greenish grey. They possess weak to very weak strength and are moderately to highly weathered (ISRM, 1981). The siltstone is weaker and more weathered than the sandstone layers. Scattered discontinuity sets are present in the area. Discontinuity surfaces are slickensided with clay infilling and possess small persistence according to ISRM (1981).

Figure 13: Disintegrated lithology and firm blocks of İncebel Formation

A discontinuity survey was utilized by collecting only local level of discontinuity data from detached blocks. The collected discontinuity data was plotted by using the

DIPS v.6 (Rocscience Inc., 2012) to understand whether there is any identifiable structural pattern of the pole concentration or not (Figure 14). The obtained scattered plot of discontinuities implies that discontinuities present in the region do not represent any identifiable structural pattern. Therefore, a circular type of slope failure is likely in the region (Hoek and Bray, 1981).

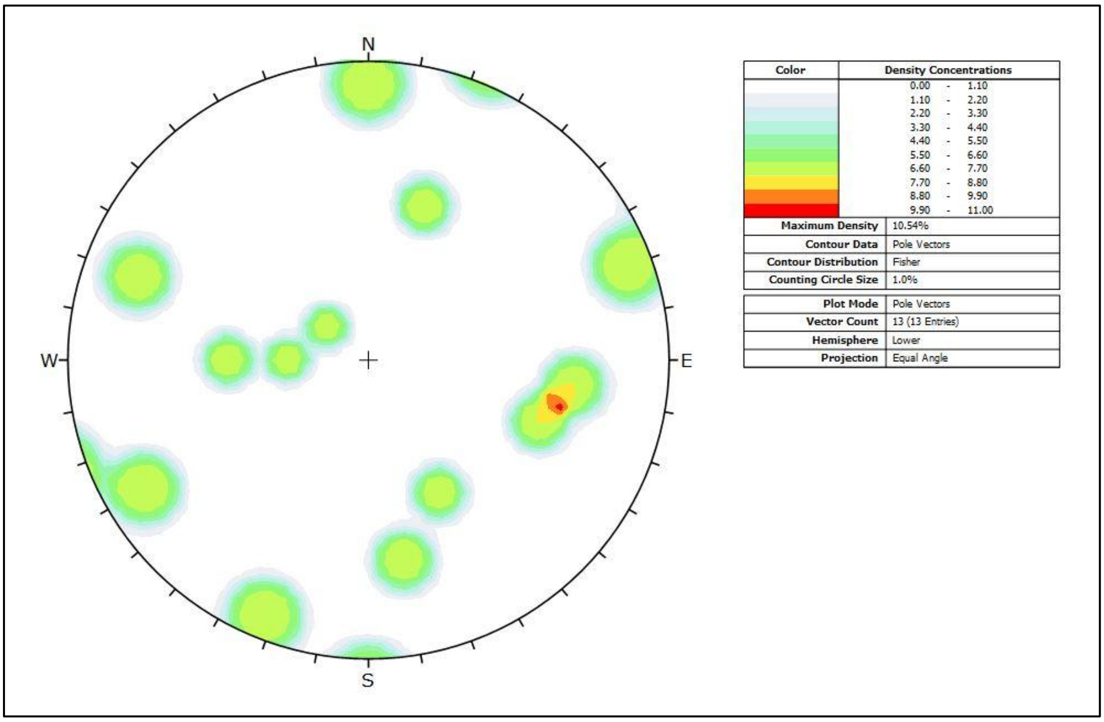

Figure 14: Pole plot of scattered discontinuities in the landslide area

From the boring data, the solid core recovery (SCR), rock quality designation (RQD) and point load strength values of the borehole cores along with the depth, groundwater depth from the surface and weathering condition is given in Table 5. Thereby, the SCR value ranges between 13% and 40% while the RQD is between 0% and 10% that classifies the unit as very poor rock (disintegrated/decomposed rock). The units are moderately to highly weathered (ISRM, 1981).

Table 5: Engineering geological characteristics gathered from borehole data

Borehole	Depth (m)	Ground Water Depth From Surface (m)	Point Load Strength Index (MPa)	SCR (%)	RQD (%)	Weathering Degree
SK5	12	-	-	13	0	Moderate to high
SK9	12	3	5.13	20	0	Moderate to high
SK10	12	-	0.27	21	3	Moderate to high
SK11	12	-	0.32	25	10	Moderate
SK12	18	3	2.81	40	10	Moderate
SK13	18	3	0.45	24	1	Moderate to high
SK14	18	3	4.98	22	3	Moderate
SK15	10	3	2.44	15	2	Moderate to high
SK16	12	-	-	17	0	Moderate to high
SK17	21	4	2.71	17	0	Moderate to high
SK18	21	4	4.31	18	0	Moderate to high
SK19	10	4	3.54	18	2	Moderate to high
SK21	13	-	0.1	20	4	Moderate to high
SK22	12	9	-	1	0	Moderate to high

Since the project site is located in a tectonically deformed zone and since the pole plot distribution shows scattering, the rock mass could be treated as an irregularly jointed, highly foliated and very deformable soil-like material, from an engineering geology point of view.

The Geological Strength Index (GSI) is a system of a rock mass characterization developed with the Hoek-Brown failure criterion to meet the need for a reliable input data into numerical analyses and analytic solutions for designing tunnels, slopes or foundations in rocks (Marinos et al., 2005). The GSI enables users to interrelate intact rock properties with in-situ rock mass values with respect to visual assessment of the rock mass, appreciating influence of geology on its mechanical properties (Marinos & Hoek, 2000). In the study area, the GSI value was selected as 20 (very poor category) according to field condition of the rock mass (Figure 15).

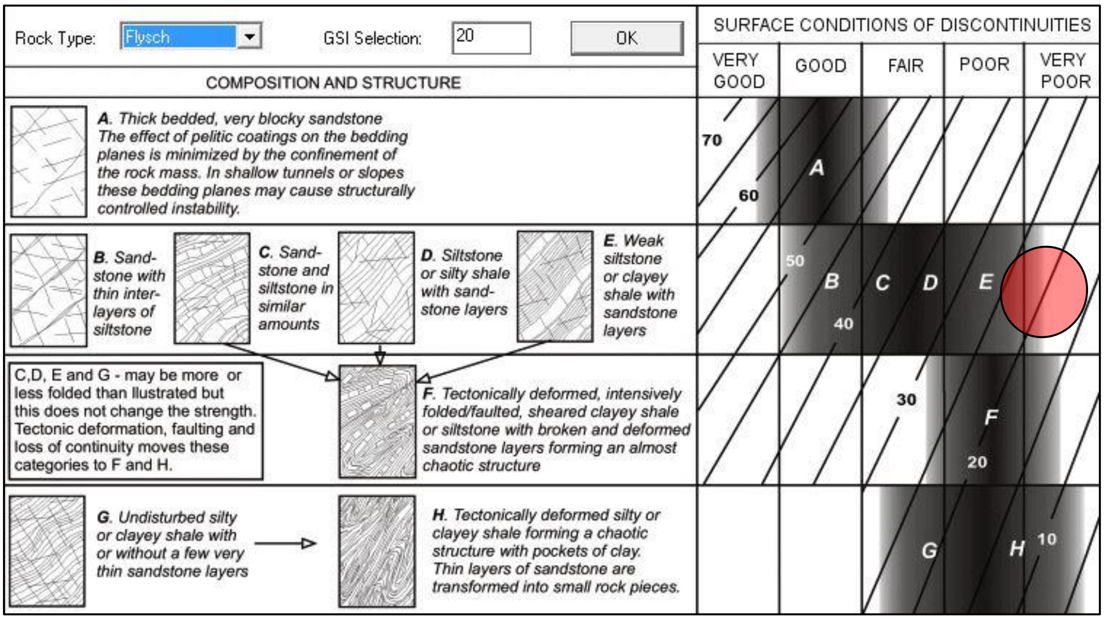

Rock Type: Flysch

GSI Selection: 20

A. Thick bedded, very blocky sandstone. The effect of pelitic coatings on the bedding planes is minimized by the confinement of the rock mass. In shallow tunnels or slopes these bedding planes may cause structurally controlled instability.

B. Sandstone with thin inter-layers of siltstone

C. Sandstone and siltstone in similar amounts

D. Siltstone or silty shale with sandstone layers

E. Weak siltstone or clayey shale with sandstone layers

C,D, E and G - may be more or less folded than illustrated but this does not change the strength. Tectonic deformation, faulting and loss of continuity moves these categories to F and H.

F. Tectonically deformed, intensively folded/faulted, sheared clayey shale or siltstone with broken and deformed sandstone layers forming an almost chaotic structure

G. Undisturbed silty or clayey shale with or without a few very thin sandstone layers

H. Tectonically deformed silty or clayey shale forming a chaotic structure with pockets of clay. Thin layers of sandstone are transformed into small rock pieces.

Figure 15: GSI table for heterogenous rock masses giving surface condition of discontinuities and composition and structure (Rocscience Inc., 2014)

Table 6 gives the results obtained from the RocLab v.1 (Rocscience Inc., 2014.). At the table sigt, sigc, sigcm, Erm, are the rock mass parameters representing rock mass tensile strength, uniaxial rock mass compressive strength, global rock mass compressive strength, and rock mass deformation modulus, respectively. Also, sigci, mi, GSI, D, and MR stand for unconfined compressive strength of intact rock, the intact rock parameter, the geological strength index, the disturbance factor and modulus ratio. In addition, m_b is a reduced value of material constant m_i, and s, and a are Hoek Brown constants.

Table 6: Geomechanical rock mass paramaters from the RocLab software (Rocscience Inc., 2014)

Rock Mass Parameters		**Hoek Brown Classification**	
sigt	-0.001 MPa	sigci	9 MPa
sigc	0.027 MPa	GSI	20
sigcm	0.410 MPa	mi	9
E_{rm}	100.78 MPa	D	0.5
Failure Envelope Range		MR	375
Application	Slopes	**Hoek Brown Criterion**	
Mohr-Coulomb Fit		mb	0.199
c	0.022 MPa	s	2.33e-5
ϕ	33.88°	a	0.544

GSI system applied by using field study observations and measurements was resulted with a cohesion (c) value of 22 kPa and internal friction angle (ϕ) value of 34 degrees. Figure 16 shows the rock strength analysis results of the GSI system from RocLab software.

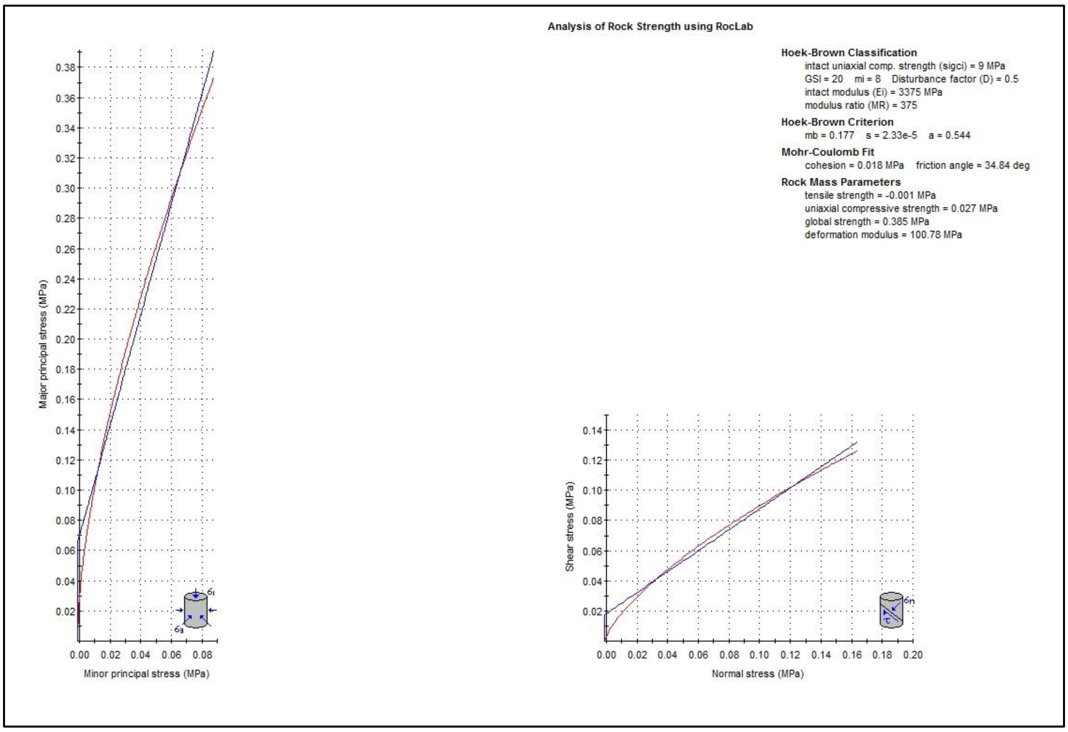

```
Analysis of Rock Strength using RocLab

Hoek-Brown Classification
        intact uniaxial comp. strength (sigci) = 9 MPa
        GSI = 20    mi = 8    Disturbance factor (D) = 0.5
        intact modulus (Ei) = 3375 MPa
        modulus ratio (MR) = 375
Hoek-Brown Criterion
        mb = 0.177    s = 2.33e-5    a = 0.544
Mohr-Coulomb Fit
        cohesion = 0.018 MPa    friction angle = 34.84 deg
Rock Mass Parameters
        tensile strength = -0.001 MPa
        uniaxial compressive strength = 0.027 MPa
        global strength = 0.385 MPa
        deformation modulus = 100.78 MPa
```

Figure 16: Analysis of rock strength from RocLab software.

CHAPTER 3

SLOPE STABILITY

3.1 Introduction

Cruden (1991) defines landslide as "the movement of a mass of rock, debris or earth down a slope."

The purpose of slope stability analysis is to reach safe and economic design of any related structure such as excavations, embankments, earth dams, and landfills. Slope stability analysis contains both identification of geological, material, environmental and economic parameters and understanding of nature, magnitude and frequency.

Slope stability analysis aims to:

- Understand development and form of a mass movement
- Analyze short-term and long-term stability
- Assess landslide possibility
- Find failure mechanism and effect of environmental factors
- Redesign with back analysis for planning, design and remediation
- Examine seismic loading effect.

Slope stability analysis takes into account factors such as topography, geology, material properties, and neutrality. A slope can be either a natural slope or a man-made engineered slope. Natural slopes are those formed as a result of landscapes and these could be triggered by changes in topography, groundwater level, stress, strength as well as seismicity and weathering. Engineering slopes originates from man-made structures like embankments, cut slopes and retaining walls (Abramson et al., 2002).

Slope movement occurs as a result of increase in shear stress or decrease in shear strength of the rock mass. Shear stress of a slope increases due to removal of support, overloading, transitory effects, removal of material from toe of the slope, and increase in lateral pressure. Reduction of shear strength is related to change in material properties, due to changes of weathering, pore pressure, and structural changes. In addition, preexisting discontinuities found in a slope region such as faults, bedding planes, foliations, cleavages, sheared zones, and dikes weaken the residual soil and the weathered bedrock (Abramson et al., 2002).

3.2 Modes of Failure

Varnes (1978) classifies landslides according to type of movement and type of material. Simplified version of Varnes classification is given in Table 7. Based on this table any landslide could be identified with two criteria: the first one describes the material and the second one describes the type of movement.

Table 7: Modes of slope failure (Varnes, 1978).

<table>
<tr><th colspan="2" rowspan="3">Type of Movement</th><th colspan="3">Type of Material</th></tr>
<tr><th rowspan="2">Bedrock</th><th colspan="2">Engineering Soils</th></tr>
<tr><th>Predominantly Coarse</th><th>Predominantly Fine</th></tr>
<tr><td colspan="2">Fall</td><td>Rock Fall</td><td>Debris Fall</td><td>Earth Fall</td></tr>
<tr><td colspan="2">Topple</td><td>Rock Topple</td><td>Debris Topple</td><td>Earth Topple</td></tr>
<tr><td rowspan="2">Slide</td><td>Rotational</td><td rowspan="2">Rock Slide</td><td rowspan="2">Debris Slide</td><td rowspan="2">Earth Slide</td></tr>
<tr><td>Translational</td></tr>
<tr><td colspan="2">Spread</td><td>Rock Spread</td><td>Debris Spread</td><td>Earth Spread</td></tr>
<tr><td colspan="2">Flow</td><td>Rock Flow</td><td>Debris Flow</td><td>Earth Flow</td></tr>
<tr><td colspan="2">Complex</td><td colspan="3">Combination of two or more principal types of movement</td></tr>
</table>

According to Varnes' classification, material composing a landslide can be rock or soil. Soil is further divided into two groups as debris and earth. Rock corresponds to a firm mass that was intact before the movement while soil could be described as an aggregate of solid materials like minerals and rocks that formed in situ due to the weathering of rock or that are allochthonous (i.e., transported from somewhere else). Soil has two subgroups based on particle size. 1) soil mass is called earth if 80% or more of the particles are smaller than sand-size particles (2mm) and 2) called debris if 20% to 80% of material are larger than 2mm. (Cruden and Varnes, 1996).

3.3 Methods of Slope Stability Analysis

Gathering information about engineering properties of material present at landslide area is a basic step of slope design. There are numerous analyses methods but none of them are applicable for all slope failures as the internal stress state of the region and the stress strain relation before and after a mass movement could not be defined with certainty. Today most of the methods use limit equilibrium analysis in which failure is assumed to be incipient with a safety factor of one. There are other complex methods such as finite element method (FEM) and boundary element method (BEM) which require a complete model of subsoils and extensive laboratory tests to determine soil's constitutive parameters. Due to its easy implementation limit equilibrium methods are preferred although they neglect stress-deformation increments or decrements of slope masses. Conventional slope stability analysis is based on the limit equilibrium concept and it gives a factor of safety which is a unitless measure of stability. Limit equilibrium formulation gives statistically indeterminate solution, so it is not possible to compare it with a closed form solution directly. However, factor of safeties obtained from different methods could be compared (Abramson et al., 2002).

Moment equilibrium is not satisfied by Janbu's simplified method while Bishop's simplified method does not satisfy horizontal force equilibrium. FS calculated by these two methods are 15% percent different than Spencer's and the Morgenstern-Price method which consider complete force and moment equilibrium. Bishop's simplified method for circular failure surface gives more or less the same result (difference is less than 5%) with more rigorous methods. But, Janbu's simplified method is used for noncircular failures and it underestimates the factor of safety as much as 30% compared to more rigorous methods. The methods which satisfy complete equilibrium such as Janbu's rigorous, Spencer or Morgenstern-Price methods are more complex (Abramson et al., 2002). Morgenstern-Price method is preferred as the method is applicable to both circular and noncircular failures and it satisfies force equilibrium in x and y and moment equilibrium to determine more realistic results. In this study, the limit equilibrium analysis was established by using this method.

One of the main purposes of this thesis study was to assess the deformation analysis by using finite element method and compare these data with the field monitoring results. In order to implement a finite element model rock mass strength parameters are needed (i.e., shear strength and elastic parameters). Additionally, geotechnical laboratory test results that were mentioned previously provide the index parameters of the intact rock, but the case dealt in the field is related to rock mass properties. GIS was used to overcome the data need and then, back analysis was conducted to determine shear strength parameters of the material. After mobilized shear strength parameters are determined by back analysis, it is important to reach deformation results that will be the correlative parameter with monitoring results.

3.4 Back Analysis

Stability analysis is performed to reach a factor of safety for slopes with known parameters in general, but they can be used to find shear strength values of a failed slope. In order to establish a back analysis, the slope stability analysis needs to be performed in a reverse order by a known factor of safety value; assumed 1 at the time of failure. This reverse order analysis is called back analysis (Bromhead, 1992).

Back analysis procedure develops an analytical model of a slope failed or about to fail and the model contains five components.

1. Landslide geometry with ground surface, slip surface, and material boundaries
2. Pore water pressures on the sliding surface at the time of failure (required for effective stress analysis)
3. External loads acting on the slope at the time of failure
4. Unit weights of the materials involved in the landslide
5. Strength of materials along the failure surface.

In general, the first four parameters could be evaluated by field and laboratory studies with certain accuracy and the fifth component could be obtained by back analysis by assuming that the factor of safety equals 1. Back analysis provides information about the shear strength parameters of a slope for future design that could not be reached by conventional laboratory tests (Abramson et al., 2002).

3.5 Mechanism of the Landslide in the Study Area

The data gathered showed that the units forming the landslide are classified as poor and very deformable soil-like lithology. It is known that the landslide occurred on December 10, 2010. There was heavy precipitation before and during the day the landslide occurred and the water level of the Sarılık stream increased with the precipitation that led to flooding.

Also, there was no sign of a seismic activity within a 100 km circle around the study area during the period of 01.01.2010 and 31.01.2011 according to the Kandilli Observatory and Earthquake Research Institute (KOERI) database (Figure 17). The data regarding the earthquakes that occurred in a 100 km circumference of the region is given in Appendix C. Hence, it could be concluded that the landslide was triggered by intense precipitation due heavy rainfall that caused the deformable soil-like landslide material to saturate and the increase of water flow at the toe of the slope leading to a landslide phenomenon.

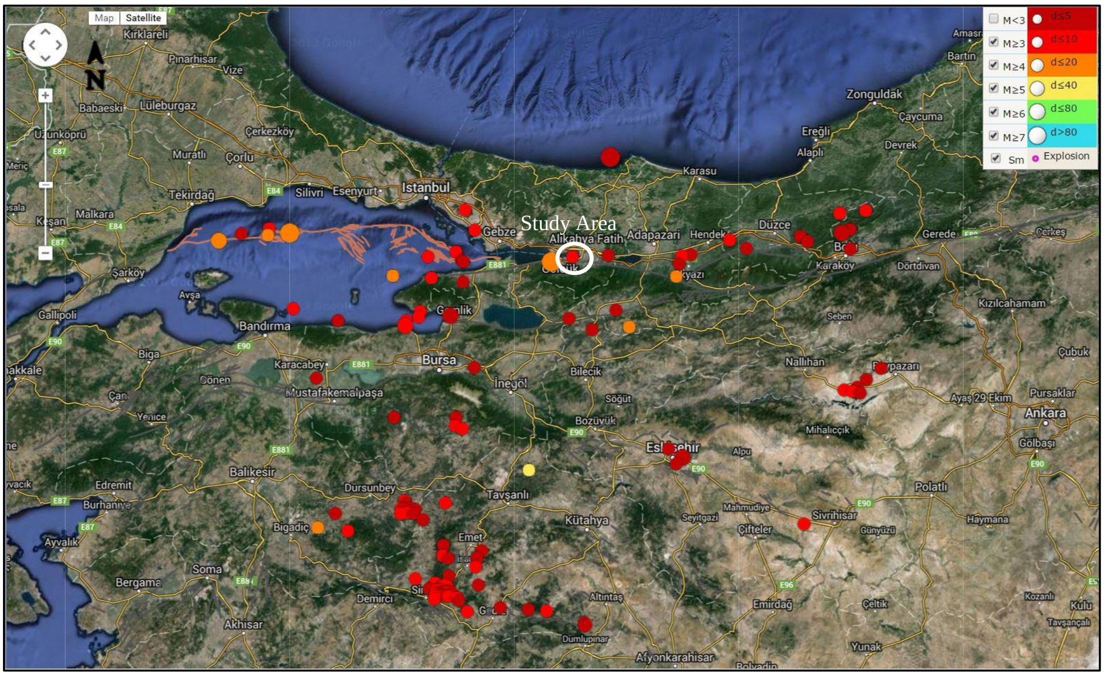

Figure 17: Earthquake catalogue of 2010 (KOERI http://www.koeri.boun.edu.tr/sismo/2/en/)

Deformational characteristics are important for characterizing the landslide and real case rock mass parameters are required to calculate the deformations. Hence the landslide has been modeled by finite element analysis that requires rock mass parameters (i.e., shear strength and elastic parameters) and these parameters could be calculated by back analysis along with the GSI results. Therefore, at first a back analysis was implemented to calculate the mobilized shear strength parameters of the landslide, and then the area was modelled through finite element analysis. To determine the landslide geometry prior to failure, a digital elevation model of the area was created from the topographical contours (Figure 18).

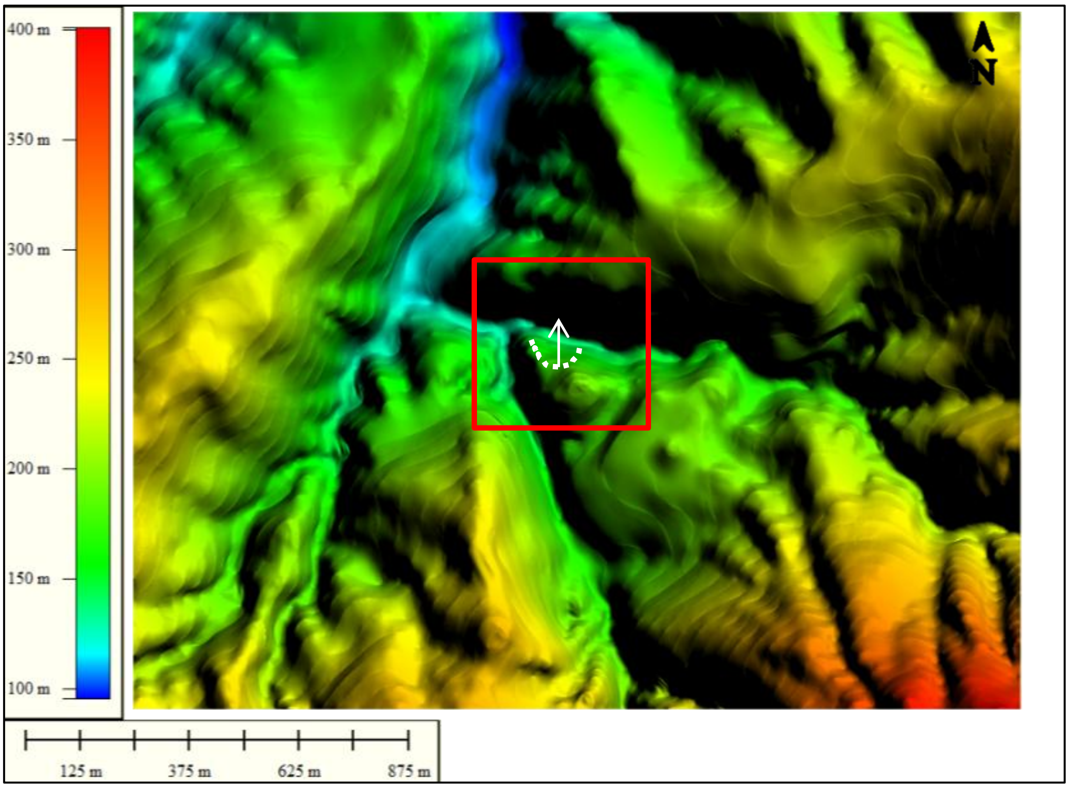

Figure 18: Digital elevation model of the study area and its surrounding

From the digital elevation model three cross sections (AA’, BB’, CC’) were created along the landslide that were parallel to the slope movement direction and the cohesion-internal friction angle pairs at the time of failure (i.e., satisfying a factor of safety value of 1.0) were computed. Figure 19 gives the location and orientation of the cross sections of the landslide.

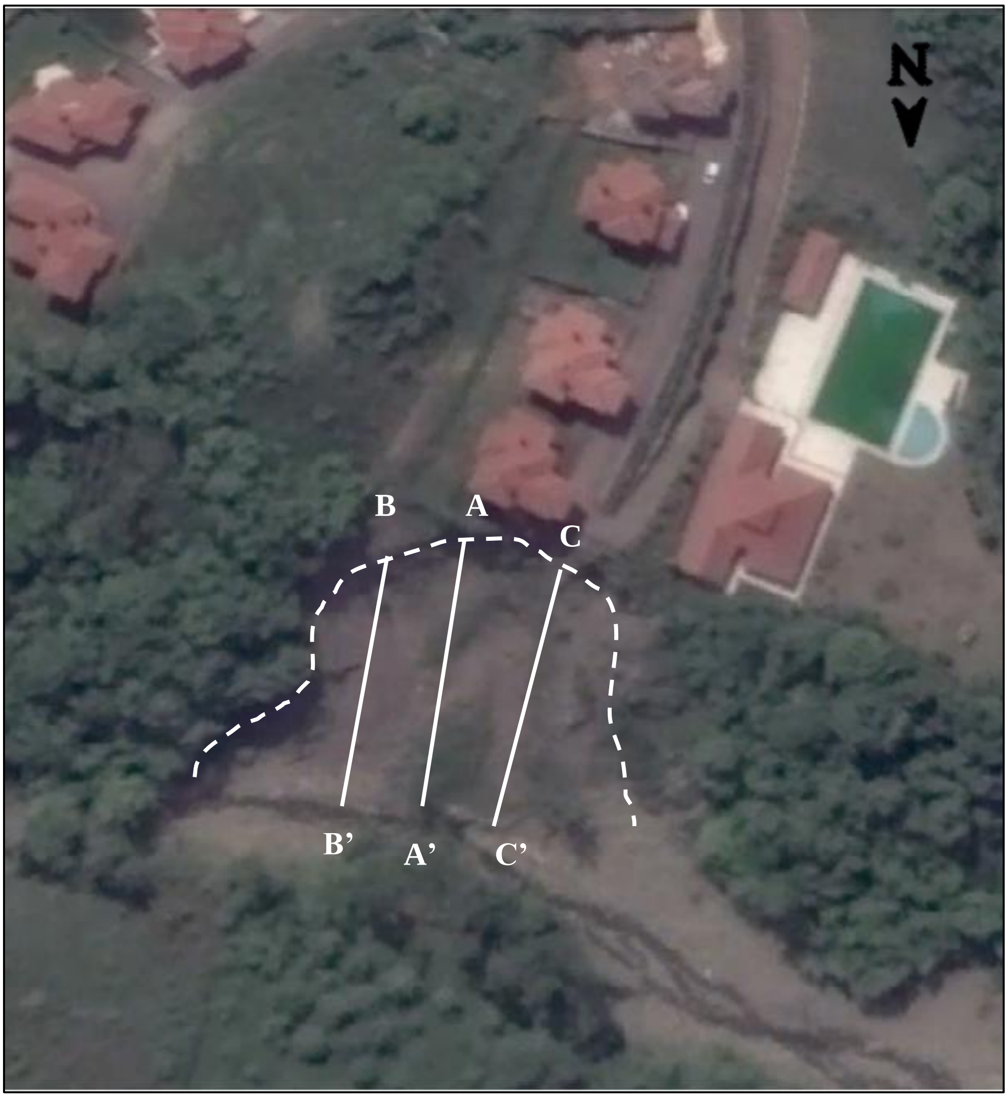

Figure 19: Locations and orientations of the cross sections of landslide.

Figure 20, Figure 21 and Figure 22 shows the profiles obtained by cross sections AA’, BB’ and CC’, respectively.

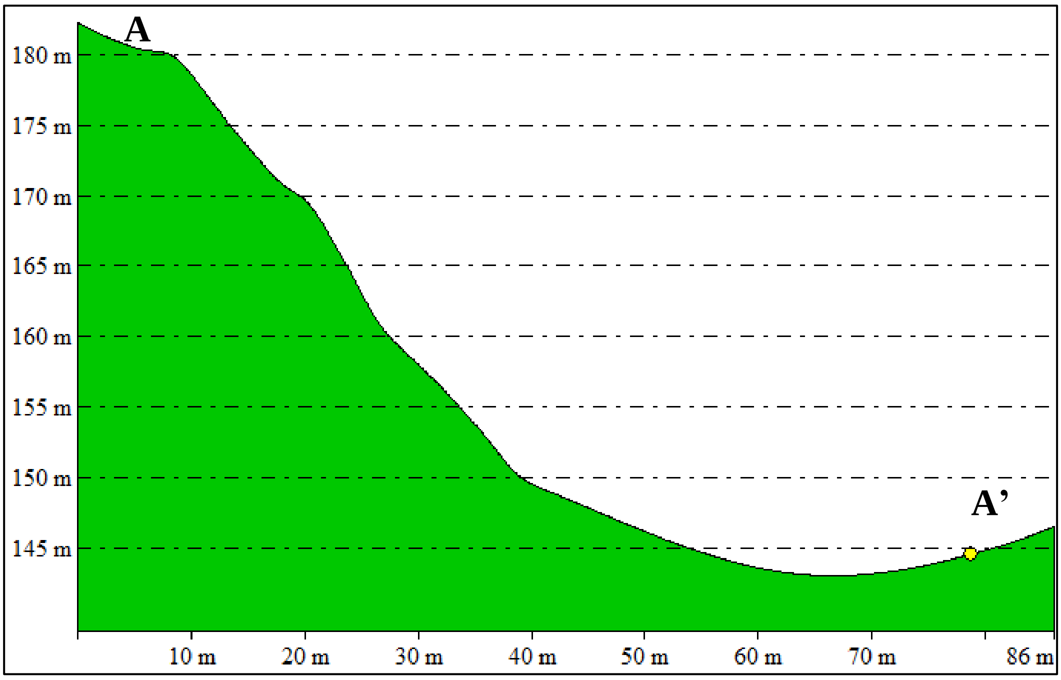

Figure 20: Profile along AA’

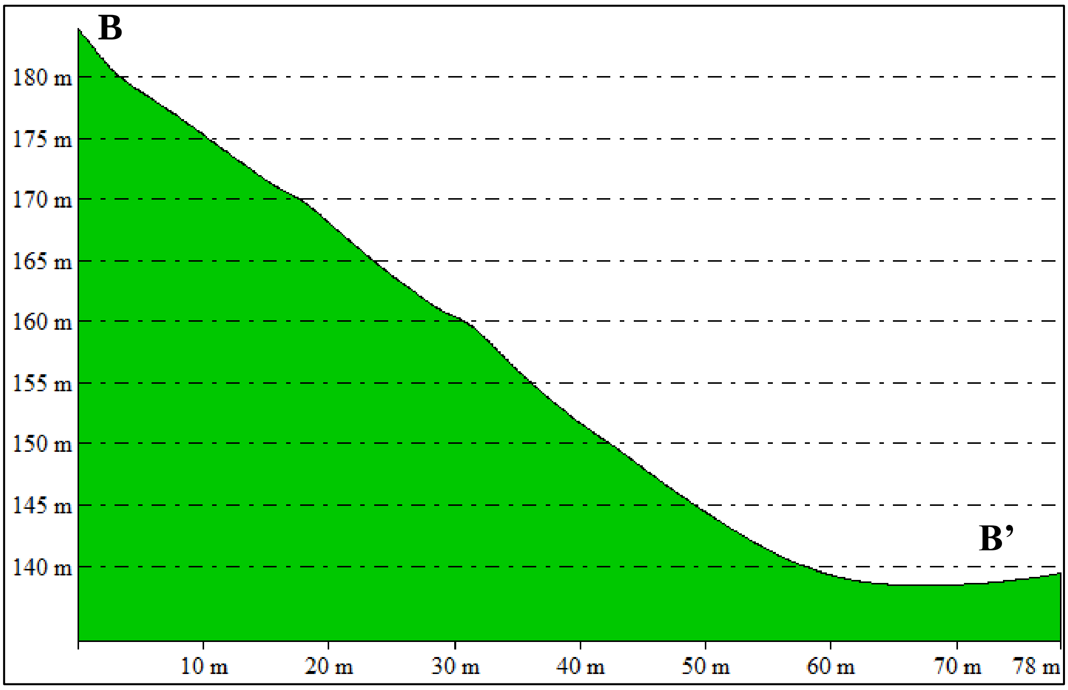

Figure 21: Profile along BB’

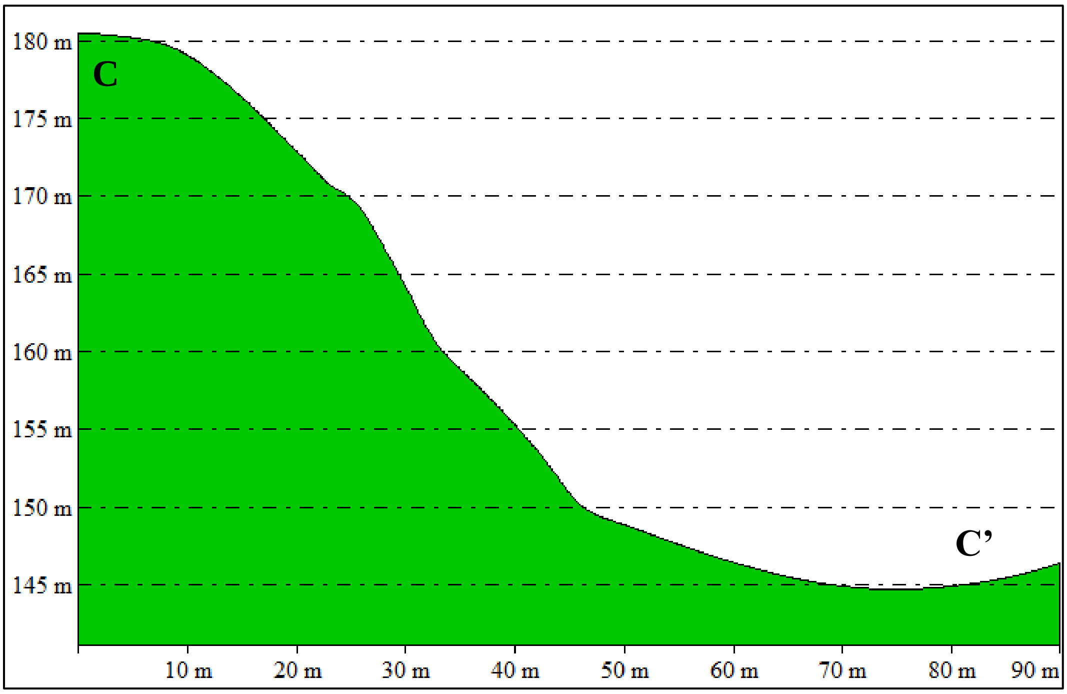

Figure 22: Profile along CC'

Once the cross sections were created, the back analysis was performed through limit equilibrium solution by the Morgenstern-Price method using the Slide v.6 software (Rocscience Inc., 2010). A fully saturated mass (representing heavy rainfall and flooding conditions) together with a 30 kPa of surcharge to represent the surcharge of the houses that are located in and behind the crown area (two-storey residential buildings). Figure 23, Figure 24 and Figure 25 represent the back calculated results of the limit equilibrium analyses of the cross-sections AA', BB' and CC'.

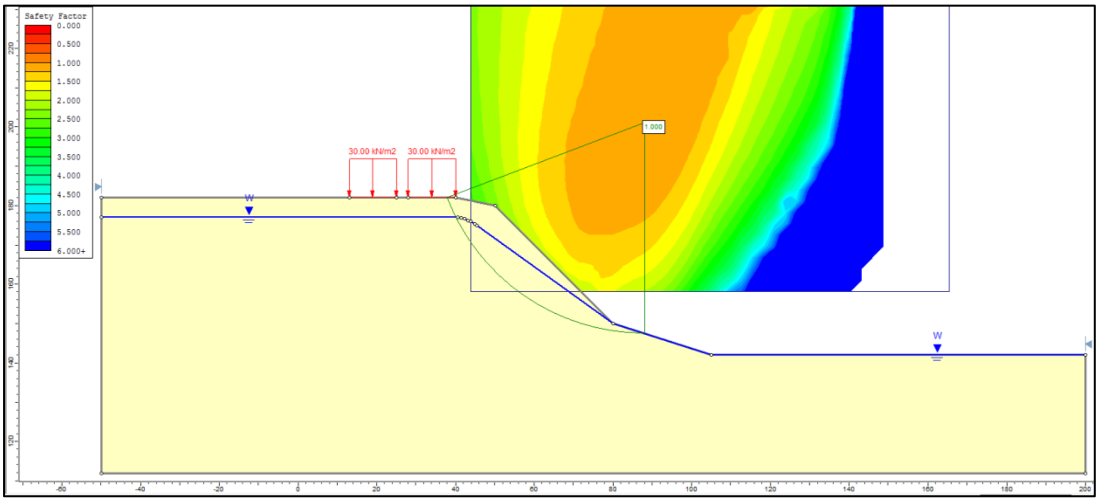

Figure 23: c'- ϕ' pair satisfying FS=1.0 for the profile AA'

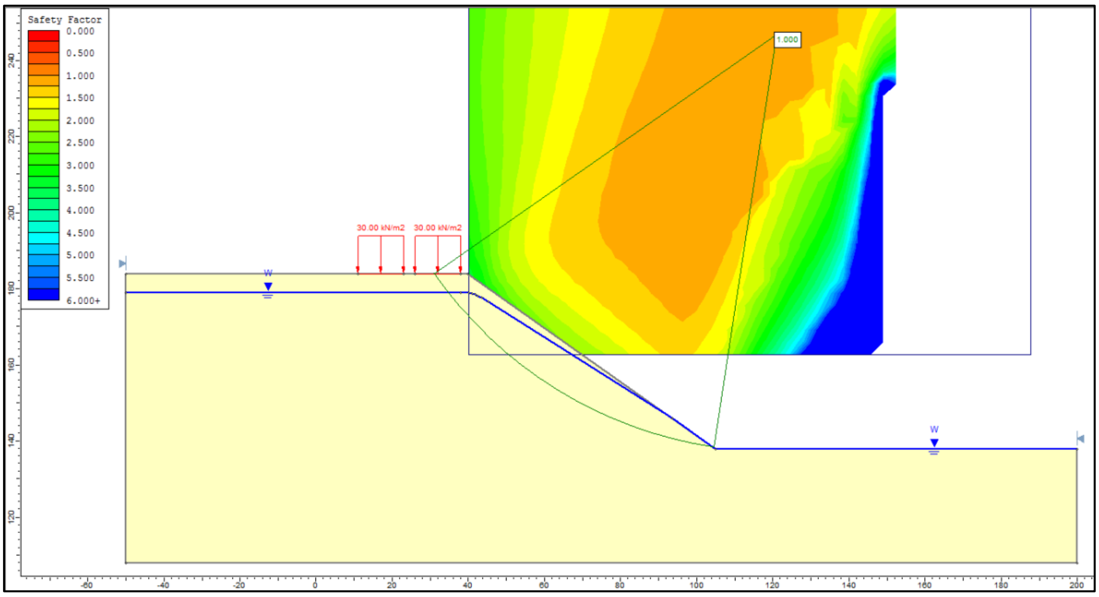

Figure 24: c'- ϕ' pair satisfying FS=1.0 for the profile BB'

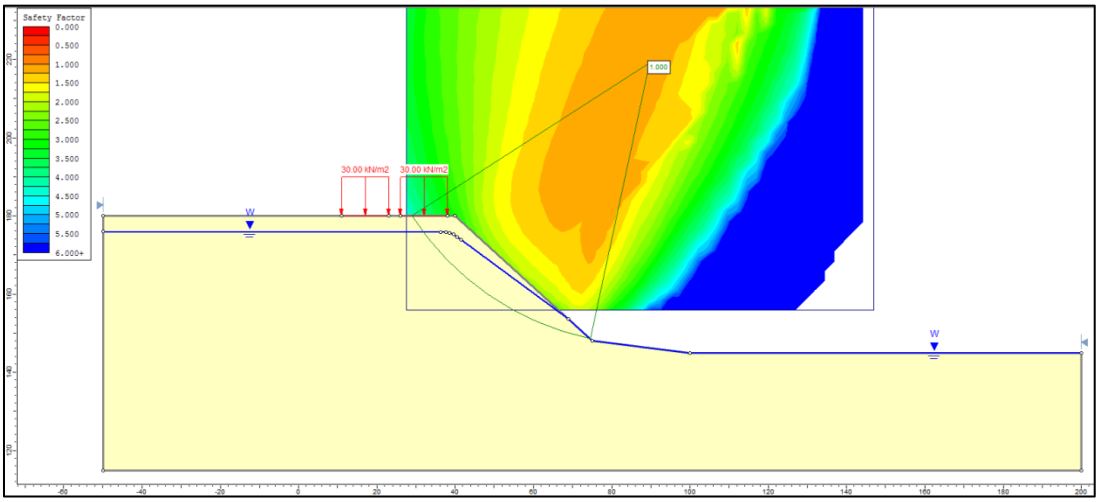

Figure 25: c'- ϕ' pair satisfying FS=1.0 for the profile CC'

The c'- ϕ' pairs calculated as the result of back analysis are tabulated in Table 8. In addition, a graphical representation of these pairs can be seen in Figure 26.

Table 8: c'- ϕ' pairs satisfying FS=1.0 limit equilibrium condition for the three sections

AA'		BB'		CC'	
c' (kPa)	**ϕ' (°)**	**c' (kPa)**	**ϕ' (°)**	**c' (kPa)**	**ϕ' (°)**
36	18.0	38	20.0	29	19.80
17	28.0	25	25.0	18	28.60
10	32.5	11	31.0	9	35.10
8	33.9	5	33.4	6	37.20

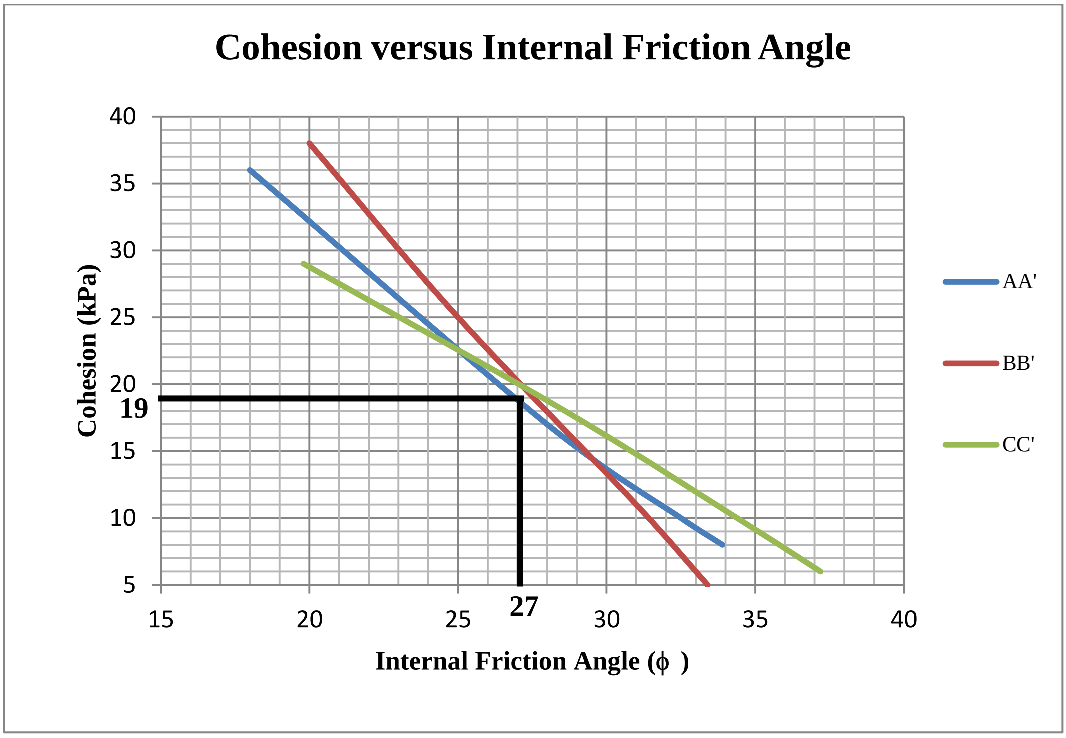

Figure 26: c'- ϕ' pairs obtained by back analysis

The center of gravity of the intersection triangle was selected to determine c and ϕ values from the back analysis graph where the c and ϕ values were determined as 19 kPa and 27°, respectively. The back analysis results provide the result of shear strength parameters at the time of failure and these results are relatively consistent with the values obtained from the rock mass calculation of GSI (c=22 kPa and ϕ = 34°).

In order to locate possible critical failure surface and to define the most critical part of the slope, deformation characteristic of the real case conditions of landslide was evaluated by using finite element method by the aid of Phase2 v.8 software package (RocScience Inc., 2011). For the landslide, deformable soil-like rock mass lithology without any preferred failure planes were modeled to be isotropic in the finite element analysis.

In order to understand the effect of groundwater in the landslide area, sensitivity analyses were performed with different scenario levels of groundwater. Figure 27 shows the deformation contours obtained by the finite element solution for the present case groundwater situation. Figure 28 displays the deformation contours for a partly saturated groundwater condition can be possible during a heavy rainfall precipitation. Lastly, Figure 29 gives the deformation contours for fully saturated condition that can be represented the worst case scenerio.

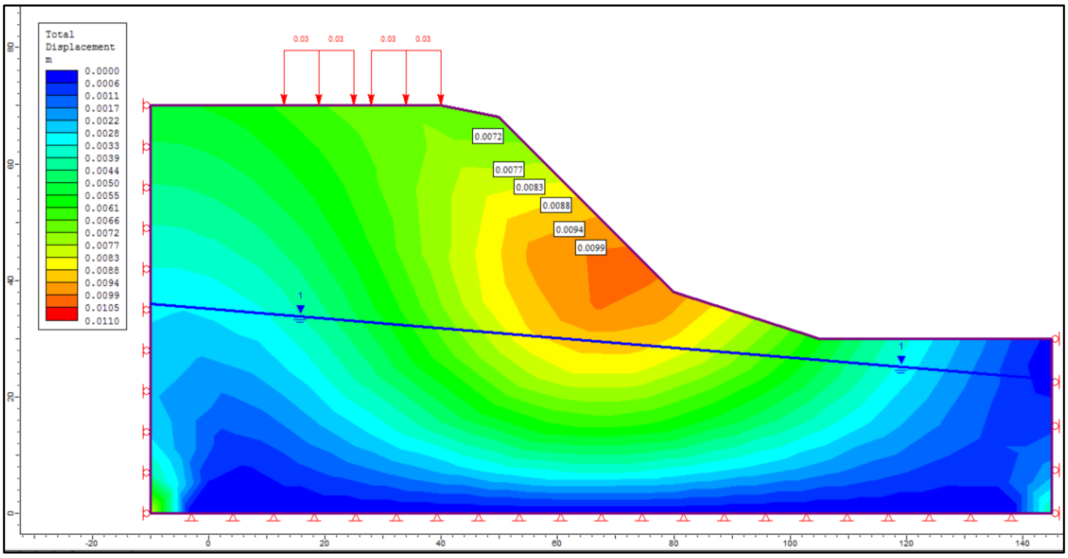

Figure 27: Displacement contours of the landslide for present situation

These different scenarios show that the larger deformations generally locate at the middle and toe part of the slope and deformation value near the surface of the landslide ranges from 7.20 mm to 9.90 mm (top to bottom) in the present case while it is in between 7.20 mm and 10.5 mm (top to bottom) for partially saturated and between 7.80 mm and 10.8 mm (top to bottom) for fully saturated model. Although these analyses performed to determine critical failure surface in terms of deformation, the results will be compared with the field monitoring data in the following chapters.

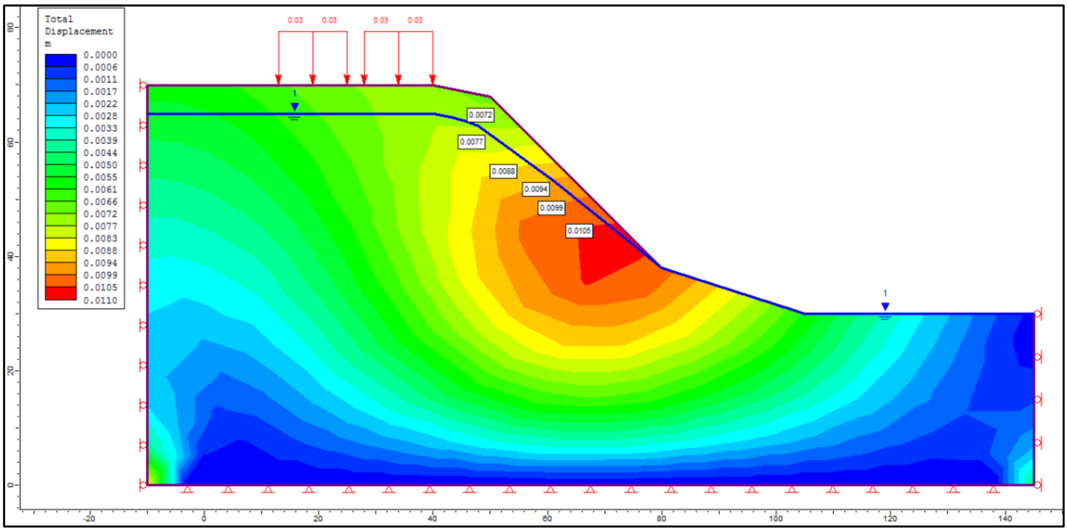

Figure 28: Displacement contours of the landslide for partially saturated condition

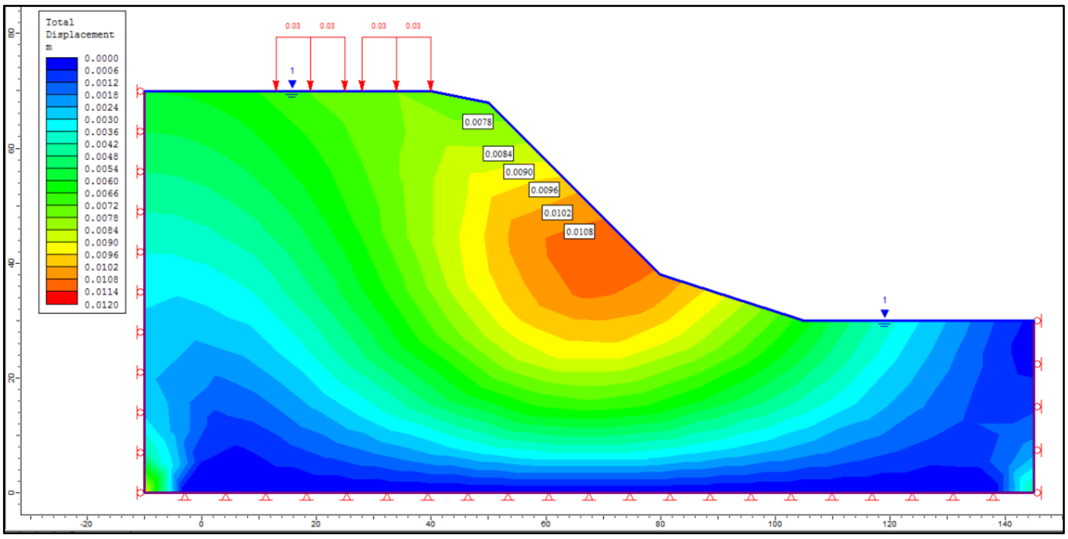

Figure 29: Displacement contours of the landslide for the worst case scenerio

CHAPTER 4

LANDSLIDE AND SLOPE MONITORING SYSTEM

4.1 Introduction

Although the history of optical fiber dates back to the 1700s with the invention of optical telegraph, it is being used in communication systems since 1977 (Al-Azzawi, 2007). Today optical fiber systems have many different areas of usage ranging from telecommunication to structural health monitoring, from monitoring of petroleum and natural gas pipelines to early warning systems of engineering structures. Some examples of these are telecommunication services such as cable television, high-speed internet, wireless transition, remote monitoring, surveillance; military application such as communication, command and control of ships and aircrafts, links for satellite ground stations; monitoring and sensing of engineering structures, gas and DNA sensors; lighting systems. Having such a large area of applications, requirements for fiber cables can be coated according to different requirements (temperature, chemicals or radiation resistant) to make them resistant to application environment.

4.2 Optical Fibers

An optical fiber is a transmission medium that conducts the light from cable’s one end to another in order to transfer it along a long distance. Optical fibers are thin cables composed of core and cladding, and their material is generally plastic or glass (silica). Fiber optic cables are made up of two main parts as core and cladding that covers the core. In addition to these two layers, a coating is coiled to protect the core and the cladding. Figure 30 shows the basic structure of an optical fiber cable.

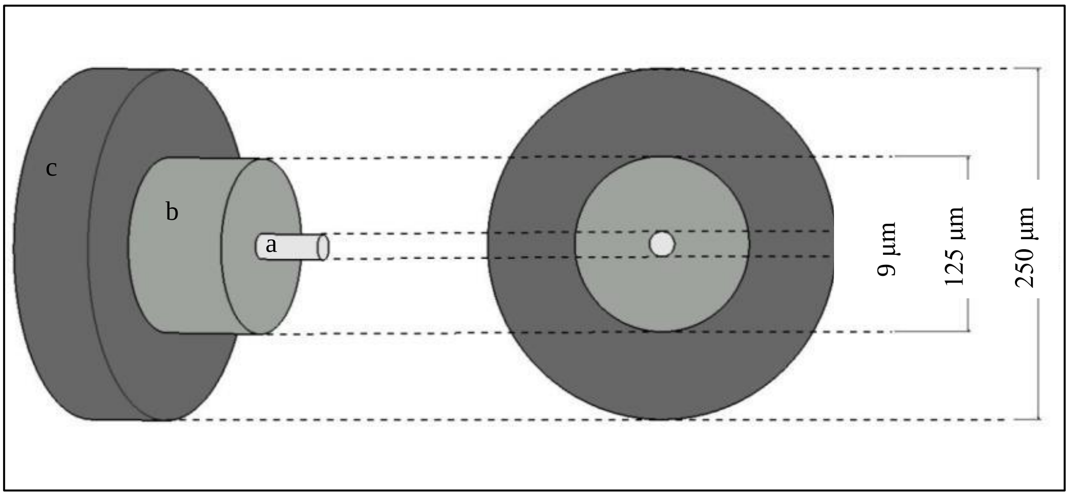

Figure 30: Basic structure of fiber cable; a) core, b) cladding, c) coating (Modified from Hayes, 2006).

Light's transmission through a fiber is based on the Snell's law (Snellius, 1621). Snell's equation explaining the relation between index of refraction and incidence angle of light is given by Equation 1. Also, critical angle calculation is given by Equation 2. Critical angle is a parameter related to total internal reflection. As the index of refraction of the core is slightly higher than that of the cladding, light launched through the cable travels within the core. This phenomenon is called total internal reflection (TIR). Figure 31 represents the light traveling between two mediums and shows the structure of the total internal reflection.

$$\sin\theta_2 = \frac{n_1}{n_2}\sin\theta_1 \tag{1}$$

$$\sin\theta_c = \frac{n_2}{n_1} \tag{2}$$

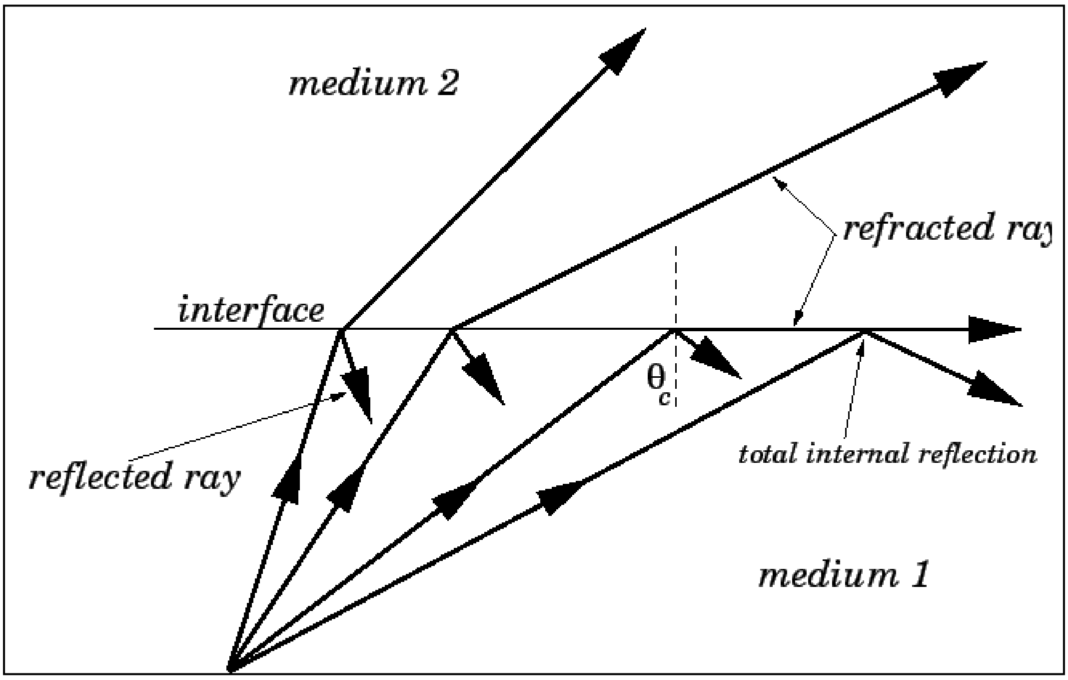

Figure 31: Light travel path possibilities between two medias (retrieved from http://farside.ph.utexas.edu/teaching/302l/lectures/node129.html)

In order to obtain data through a fiber optic system, the fiber cable itself can be used or sensitive regions, namely sensors can be deployed within the cable with a certain interval for the desired application. Optical fiber sensors can be classified into three groups as point, distributed, and quasi-distributed sensors. Point sensors measure changes from certain points on fiber cable. Conversely, distributed sensors make measurements along the cable, so they are capable of representing distribution of spatial changes. These types of sensors use Raman and Brillouin scattering principles. Quasi-distributed sensors are somewhere between point and distributed sensors; in such a way that information comes from certain points on the cable but data acquisition occurs along the cable (Grattan et al., 2000). Selection of sensors depends on the parameter to be measured (deformation, temperature, moisture, etc.), utilized device, and desired measurement sensitivity.

4.2.1 Classification of optical fibers

Although optical fibers are classified generally into two main groups as multimode and single mode cables they can be classified according to their production material, structure, function and performance.

According to the manufacturing materials, optical fibers can be classified generally as; silica fiber, compound glass fiber, plastic optical fiber, infrared fiber and crystal fiber. The most common materials used for fiber cable manufacturing are silica (SiO_2) and composite glass fiber composed of silicate, phosphate and fluorite. According to their structure, fibers are divided into step-index fibers, graded index fibers (GRIN), double cladding fibers (DCF), photonic crystal fibers (PCF), polarization maintaining fibers (PMF) and large aperture fibers. According to the function and performance, fibers are grouped into two categories as single mode fiber (SMF) and multimode fiber (MMF) (Fang et al., 2012). A single mode fiber has a core diameter ranging from 4 μm to 10 μm and this core diameter is small when compared to the wavelength of light. Due to the small core diameter, light could travel only in a single path or mode within a single mode fiber. On the other hand, multimode fibers have larger core diameter ranging from 25 μm to 150 μm allowing light to travel in many paths or modes (Iten, 2011).

4.2.2 Advantages of optical fibers

Optical fibers have superiority over conventional methods in terms of several characteristics, namely easy and fast data transfer, small diameter, light weight, sensitivity to strain and temperature change, wide band range, resistance to environmental and electromagnetic effects, and low cost (Wang et al., 2008; Gupta, 2012; Measures, 2001).

Powers (1997) gives the advantages of fiber optic as wide bandwidth, light weight and small size, immunity to electromagnetic interference, lack of electromagnetic interference crosstalk between channels, lack of sparking, compatibility with solid state sources, and low cost.

Bandwidth is the measure of the frequency range width of a medium that depends on carrier frequency. Optical fibers have higher frequencies than other methods which make them superior. Bandwidth of a fiber cable can be of several THz and this allows transfer of data from many different sources, so that they are applicable to a wide range of fields. Fiber optics have small dimensions and low density that allow them to be light and small in size. This property is an advantage in field application especially when the considered length is long. These physical characteristics result in an ease of the transportation of the cable since it is possible to install the cable in smaller areas. Electromagnetic interference is a problem for data transfer and it is almost impossible to avoid in electric related features and applications. Optical fiber technology is immune to electromagnetic interference which is why they can be implemented anywhere without being affected from electromagnetism. Furthermore, optical fiber cables are applicable to hazardous areas as they do not spark. Due to this characteristic, they can be safely used for any application without changing the application route. This property of optical fiber cables allows them to be utilized in flammable and toxic gas environments. Optical fibers are compatible with modern electronic components as a result of their material and dimensions (Powers, 1997).

The main superiority of the optical fibers are their capability to transport more data to in longer distances faster than any other medium (Hayes, 2006). Electromagnetic radiation does not affect optical fibers, thus allowing data transfer with smaller noise and error. Furthermore, unlike metallic conductors, utilization of fiber optics in the fields of sensor applications, medical applications, industrial applications, subject illumination, and image transport is possible (Hayes, 2006).

4.3 The Utilized Optical Fiber System

Today, optical fiber systems are being used to monitor buildings, bridges, tunnels, dams, slopes, pipelines, gas tanks, and ships for detection of changes in acceleration, chemicals/gases, color, distance, force, humidity, magnetic/electric field, movement/displacement, linear and angular position, pressure, and radiation (Altuğ, 2007). It is possible to detect these changes as chemical and physical properties affecting the intensity, scattering and polarization of light traveling within the fiber. These measurements are achieved by analyzing the amplitude, frequency, phase and polarization of the backscattered light.

Scattering is the dispersion and loss of incident light due to hitting any unexpected material such as irregularities caused from fiber production. There are three major scatter types concerning optical fibers; Rayleigh, Brillouin, and Raman. Rayleigh scattering is a linear scattering while Brillouin and Raman scatterings are nonlinear (Yücel et al., 2014). Rayleigh scattering is the result of very small irregularities within the fiber that have smaller dimensions than the wavelength of transmitted light. These irregularities show their effect in the refractive index as fluctuations. As a consequence, Rayleigh scattering occurs in almost all directions. Brillouin scattering could be identified as an interaction between acoustic wave and pumped wave. It is revealed as a result of the interaction of pumped light moving within the fiber and acoustic waves formed thermally and spontaneously. Raman scattering is the product of interaction between the light launched to fiber and molecular vibration modes of the medium. It could be described as scattering of light from phonons (Mafang, 2011).

An optical fiber system is not composed of only fiber cables but it also contains a device that launches light into the cable and collects backscattered light and in some cases sensitive regions called sensors. There are several different types of devices used with an optical fiber system. During this study, time domain reflectometry was used as a source and receiver.

4.3.1 Optical fiber system utilized with OTDR

Time domain reflectometry is a phenomenon based on a deformation on a cable due to any effect, and ground motion in the case of a landslide. The motion is determined by monitoring the pulsed light’s backscattering time (Yan et al., 2010). An Optical Time Domain Reflectometer (OTDR) is one of these devices that is invented by Barnoski & Jensen (1976). Its purpose is to detect, locate and measure events at any location on a fiber array. An OTDR sends the light to cable and collects backscattered light. By using amplitude, the return time of backscattered light can be determined (Fang et al., 2012). An OTDR gives the location of reflection that corresponds to a change in a cable due to any effect in terms of decibel (dB).

Decibel is a logarithmic unit and is used for the expression of the ratio of physical quantities. In the earlier years, power was measured in terms of milliwatts and loss was measured in decibels (dB). Over the years, dB started to be used for all measurements for convenience (Hayes, 2006). A decibel is a unit used for the comparison of power units and could be defined as the ratio of the input optical power to the output optical power (measured) for a certain wavelength. The number of decibels is defined with Equation 3 (Mohammed et al., 2013).

$$dB = 10log_{10}\frac{P_i}{P_o} \tag{3}$$

As the equation implies, dB is a logarithmic scale and every10 dB represents 10 times ratio. Therefore, 10 dB means a ratio of 10 times, 20 dB means a ratio of 100 times, 30 dB means a ratio of 1000 times and so on (Hayes, 2006).

4.3.2 Optical fiber system utilized with BOTDA

A Brillouin Optical Time Domain Analyzer (BOTDA) was the second device used in this study. It is again a distributed optical fiber sensor but it works with the Brillouin scattering principle. These systems are named as time domain systems as they use time interval between launched and backscattered light similar to the Optical Time Domain Reflectometer (OTDR) (Ohno et al., 2001). The main difference between the OTDR and the BOTDA is the adopted scattering principle, such that while the OTDR uses Rayleigh scattering the BOTDA uses Brillouin scattering. Brillouin scattering is a measure of a frequency shift caused from the difference between the launched and the backscattered light (Halley, 1987). The OTDR detects changes on the cable in terms of an energy loss (decibel loss), on the other hand, the BOTDA detects changes in terms of frequency (Thyagarajan and Ghatak, 2007).

Brillouin Optical Time Domain Analyzer (BOTDA) requires two laser beams having opposite directions in a fiber cable layout. One of them is the light launched to the cable and the other is the backscattered light. When the frequency difference between these two laser beams equals the Brillouin frequency of the fiber, a peak forms on the result graph (Xiaofei et al., 2011). The working principle of the Brillouin based time domain analysis can be seen in Figure 32.

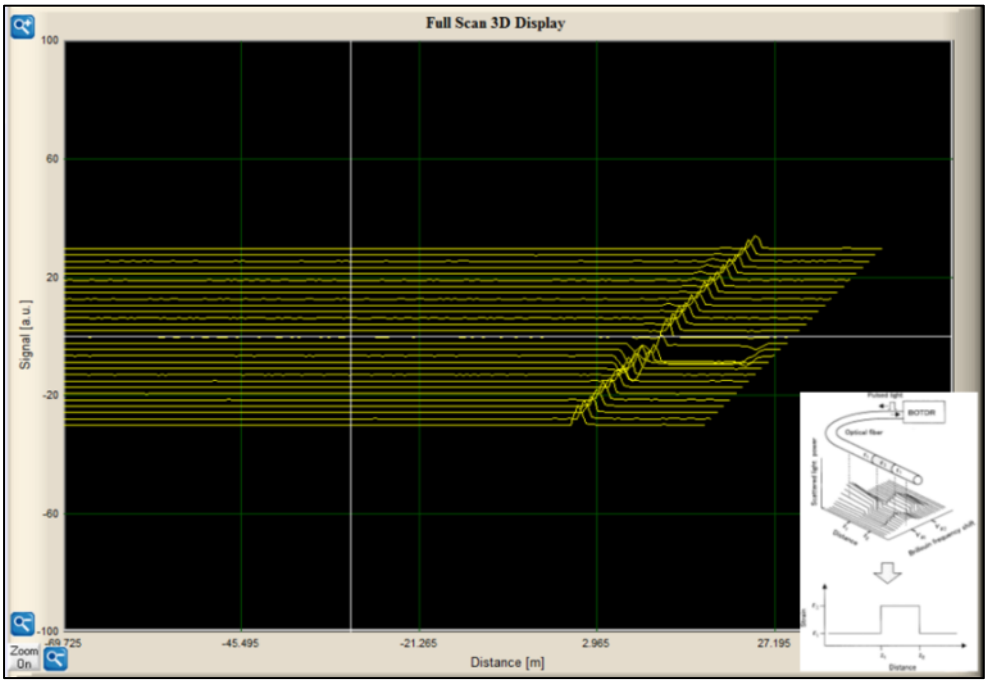

Figure 32: Measurement procedure of BOTDA taken from one of the experiments. The figure at the right hand corner is taken from Ohno et al. (2001)

Different from the OTDR, the BOTDA detects changes occurred within fiber array as a frequency shift and this difference is an advantage that will be explored and explained in the following sections. The BOTDA has advantages such as high precision, easy layout setting, strong anti-interference, and distributed mode (Shiqing and Qian, 2011). The BOTDA technology is preferred due to its high measurement precision, high measurement range and high spatial resolution in temperature and strain measurements.

There are two types of Brillouin sensors: Brillouin optical time domain analyzer (BOTDA) and Brillouin optical time domain reflectometer (BOTDR). In BOTDA, a pulsed pump light is launched from one end of the fiber cable while a probe light is launched from the other end (Horiguchi et al., 1989). In BOTDR, on the other hand, a pulsed light is launched from one end and Brillouin backscattered light is observed at the same end (Horiguchi et al., 1995). The device used during thesis study was a BOTDA which requires both ends of the cable for measurements.

As mentioned before, the Brillouin frequency shift is related to the launched light and the acoustic wave. Equation 4 shows the Brillouin frequency shift calculation.

$$v_B = 2nV_a/\lambda \tag{4}$$

where, n=refractive index

Va= velocity of acoustic wave

λ= wavelength of light

and velocity of acoustic wave is formulated as given in Equation 5.

$$V_a = \overline{E(1-k)/(1+k)(1-2k)\rho} \tag{5}$$

where, E=Young’s modulus

ρ= density of fiber

k=Poisson’s ratio

The Brillouin frequency is affected from temperature and strain as acoustic wave velocity is related to the material density, and this effect is the result of the material density that is dependent on temperature (thermal expansion) and deformation (strain) (Iten, 2011).

As the equations imply, the acoustic wave velocity, thereby Brillouin frequency is dependent on strain (Figure 33). If longitudinal strain, ε, occurs in an optical fiber so does Brillouin frequency shift. This relation can be represented by Equation 6.

$$v_B \;\varepsilon \;= v_B \;0 \;+ \frac{dv_B \;\varepsilon}{d\varepsilon}\varepsilon \tag{6}$$

Therefore, the Brillouin frequency shift can be used to determine the change in strain (Ohno et al., 2001).

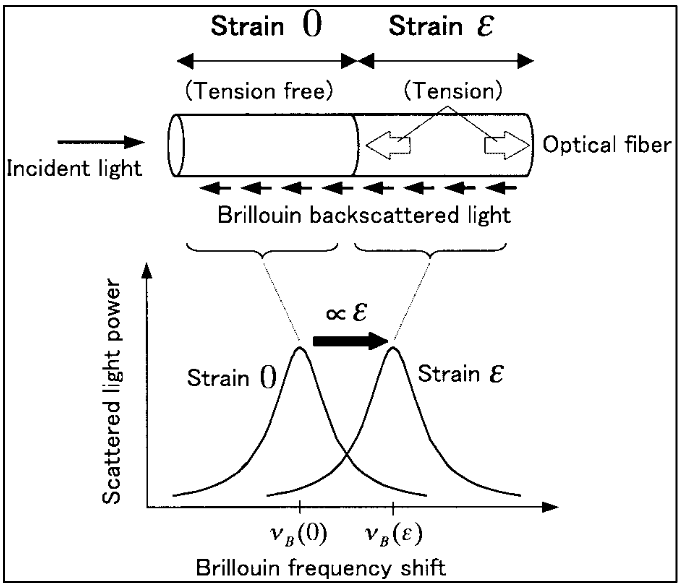

Figure 33: Brillouin frequency shift due to strain (Ohno et al., 2001)

The BOTDA operates in a similar manner to the OTDR method, i.e., the BOTDA uses time domain analysis by observing backscattered light. As a result, any Z distance where scattered light is generated can be determined by the relation given in Equation 7.

$$Z = \frac{cT}{2n} \tag{7}$$

where, c=light velocity

T= time elapsed between launching and backscatter

By using this equation, BOTDA detects the location of strain change. In addition, there is another important concept for accurate determination of location of change:

spatial resolution. Spatial resolution is a measure of accuracy of the location and can be formulized by Equation 8.

$$\Delta Z = \frac{c\tau}{2n} \tag{8}$$

where, τ=pulse width. As can be seen from the equation, higher spatial resolution ensures higher accuracy (Ohno et al., 2001).

CHAPTER 5

METHODOLOGY

5.1 Introduction

This study was initiated with the Techno-Initiative Capital Support Program of the Ministry of Science, Industry and Technology (Geolab Geotechnics, 2012) and continued with the Research and Development, Innovation and Industrial Application Support Program of the Republic of Turkey Small and Medium Enterprises Development Organization with the title of Risk Assessment, Monitoring and Early Warning System of Landslide and Slope Stability (HAMA Engineering, 2014). During these experiments a fiber optic system using an Optical Time Domain Reflectometer that is based on energy loss was used. The OTDR system was very sensitive as a point sensor and it was sufficient for laboratory studies, however its field application was not satisfying due to several reasons. In order to overcome the limitations of the OTDR, a new system based on Brillouin frequency shift was used owing to the support of the National Earthquake Research Program (UDAP) of the Republic of Turkey, Prime Ministry Disaster and Emergency Management Authority (AFAD) (Project No: UDAP-Ç-14-02).

Consequently, as two different procedures were followed to establish the monitoring system, studies performed during this thesis are explained below under two main headings; as studies with the OTDR (Section 5.2) and studies with the BOTDA (Section 5.3).

5.2 The OTDR Monitoring System

The Optical fiber system used during the initial stage of this study was composed of optical fiber cables, sensor embedded to the cable and the OTDR. As previously explained, an OTDR is a device that sends a laser into the cable and collects backscattered light (Fang et al,, 2012). The OTDR detects the location of reflection (decibel loss) by using the amplitude and the backscattered light's arrival time. A JDSU MTS 6000 model OTDR was used in this study (Figure 34).

Figure 34: Optical Time Domain Reflectometer (OTDR)

As mentioned before, there are two cable types according to their function and performance, namely 1) single mode fiber (SMF) and 2) multimode fiber (MMF). Their core sizes differ and multimode cables have larger core diameters than single mode ones. Larger core enables transfer of light arriving with different angles while single mode cables could only transfer light coming with a right angle. To compose the optical fiber system using OTDR, these two cable types were used together to form sensors. The sensors are the sensitive regions generated by splicing cables having different sizes and characteristics. Several combinations were tested and the optimum arrangement was found as placing a single mode fiber between two multimode fiber cables (Kelam et al., 2013). Figure 35 explains the structure of the sensor.

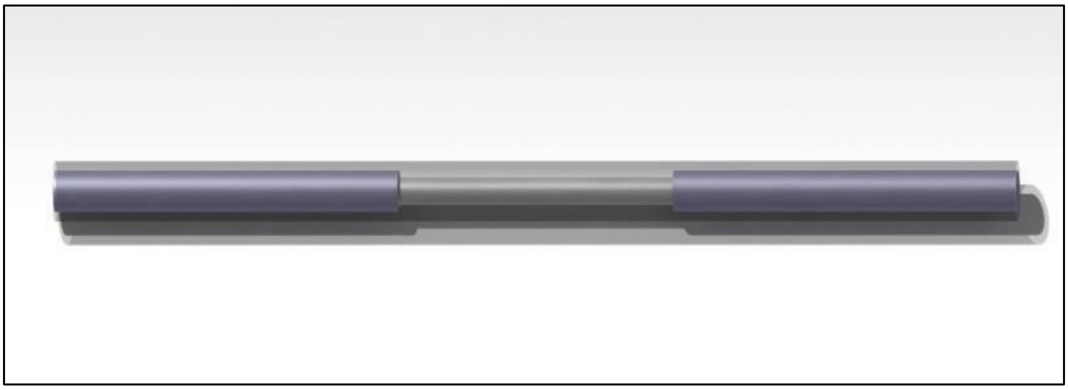

Figure 35: Basic structure of the heterecore

The logic behind the sensors is the mode difference in fiber cables where multimode cables have larger modes and higher core diameters than single mode fibers (Watanabe et al., 2000). Multimode cables can accommodate light coming with different angles as a result of their larger mode diameter while single mode cables transfer light with a right angle. Due to this diameter change, the light launched from the source (i.e., OTDR) travels through the multimode cable and some of the light is lost when it arrives to a sensor point as the fiber mode changes. This loss enables sensitive regions to be formed.

Figure 36: The utilized fusion splicer (Fujikura FSM 60S) to fuse two cables without signal loss

During the fusion process, a Fujikura FSM 60S model fusion splicer (Figure 36) was used to splice the cables and also the Fujikura CT-30 model high precision cleaver (Figure 37) was used to cut the cables at a right angle in order to minimize extra losses which may originate from the sensor itself.

Figure 37: Cleaver used to cut the fiber cables properly

During this study, several cable pairs were spliced and their sensitivities were analyzed in order to decide the most suitable cable pair. The OTDR shows changes in cable as decibel losses. Table 9 gives the decibel loss values of different cable pairs for certain displacements. In addition, graphs of given displacement values can be seen as Figure 38, Figure 39 and Figure 40.

Table 9: Losses of different cable pairs based on displacement

Displacement	Loss of 62.5-G652D-62.5	Loss of 62.5-DSF-62.5	Loss of 62.5-NZDSF-62.5
Initial	3,329	3,143	4,011
1cm	3,866	3,980	4,827
2cm	4,612	4,238	5,408
3cm	5,522	4,620	5,780
4cm	6,390	5,175	5,544
5cm	7,127	5,315	6,084
6cm	7,330	5,434	6,351
7cm	7,623	5,336	6,481
8cm	8,367	5,400	6,487
9cm	7,789	5,377	6,516

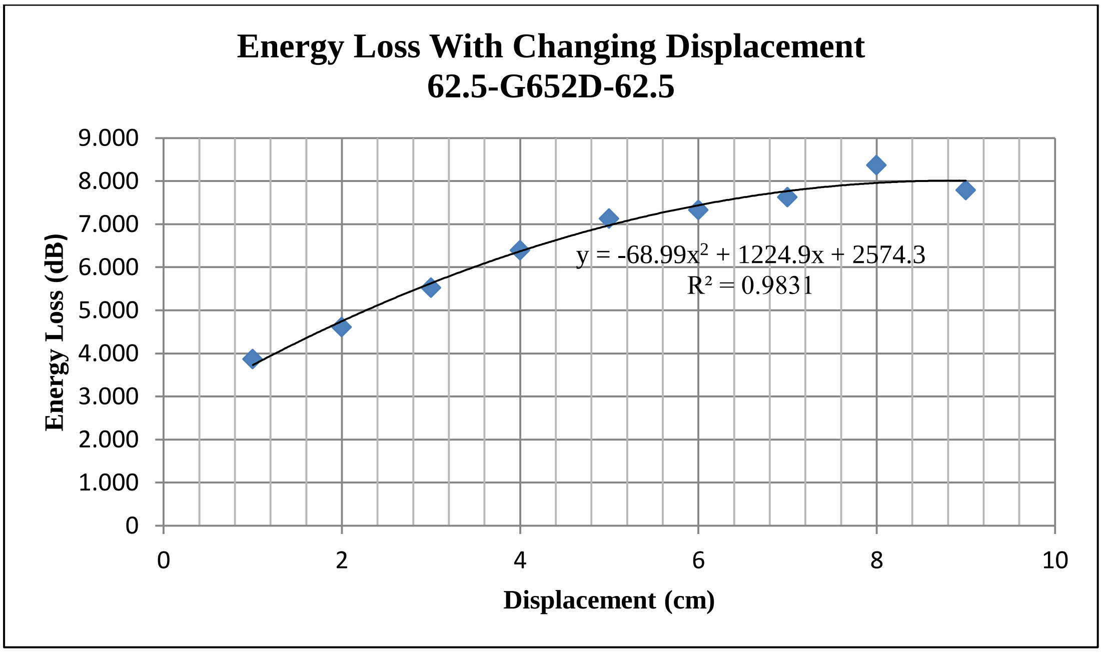

Figure 38: Energy loss and displacement relation for the cable pair of 62.5 and G652D

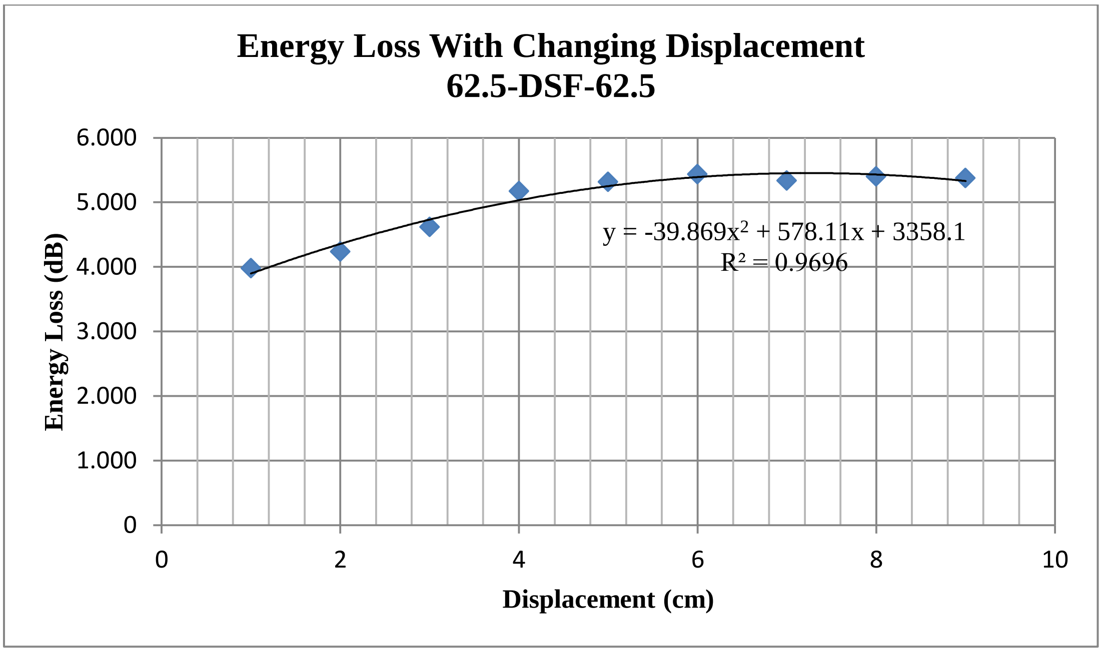

Figure 39: Energy loss and displacement relation for the cable pair of 62.5 and DSF

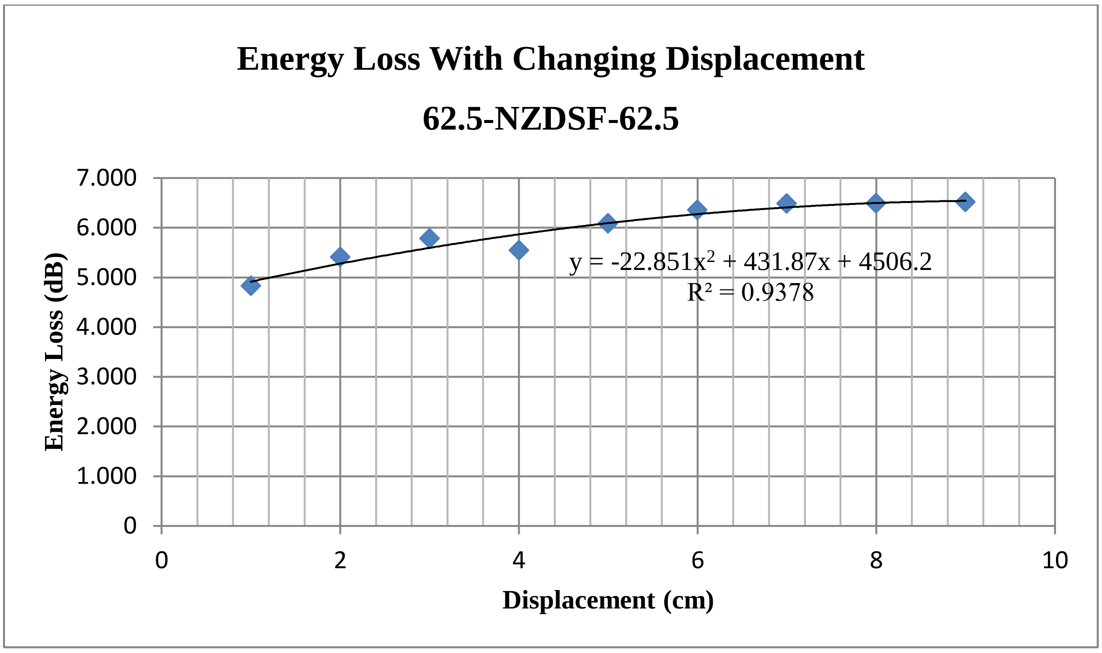

Figure 40: Energy loss and displacement relation for the cable pair of 62.5 and NZDSF

As Table.9 and Figure 38, Figure 39 and Figure 40 indicate the 62.5 and G652D fiber cable pair was the most sensitive one due to its higher loss that resulted from the same effect.

After the cable pairs were selected, the system with heterecores was first tried in a laboratory scale prior to the field application. The aim was to check the system by implementing it into a small scale area. In addition, this step gave an opportunity to understand unexpected situations that could be encountered in the field. Laboratory studies conducted on a laboratory scale experimental set-up called landslide simulator has been designed for this study to represent an ordinary soil slope in order to observe the performance and reliability of the optical fiber sensors, to test their sensitivities and to calibrate the collected OTDR data by performing deformation measurements. A landslide simulator is basically a large container composed of two identical trays each having a length of 2 m and width of 3 m. The depth of the tray changes linearly between 0.2 to 0.4 m representing the toe and the scarp of a slope. Both of the trays had an inclination mechanism that gave an opportunity to study with either single or both trays. Figure 41 presents a sketch of one of these trays. The inclination mechanism of the trays is operated with a manual pulley hoist. The trays can be moved vertically to create an inclination of a desired angle up to 45° to represent ideal mass movement conditions for the material used. The trays have a foot that holds the simulator 25 cm above the ground level. The base of the trays has three integrated barriers with a height of 20 mm to prevent any unexpected failure caused by material and tray interface. In addition, the side panels were designed with small holes on them to facilitate deployment of the optical fiber cables and their connections to the measurement device.

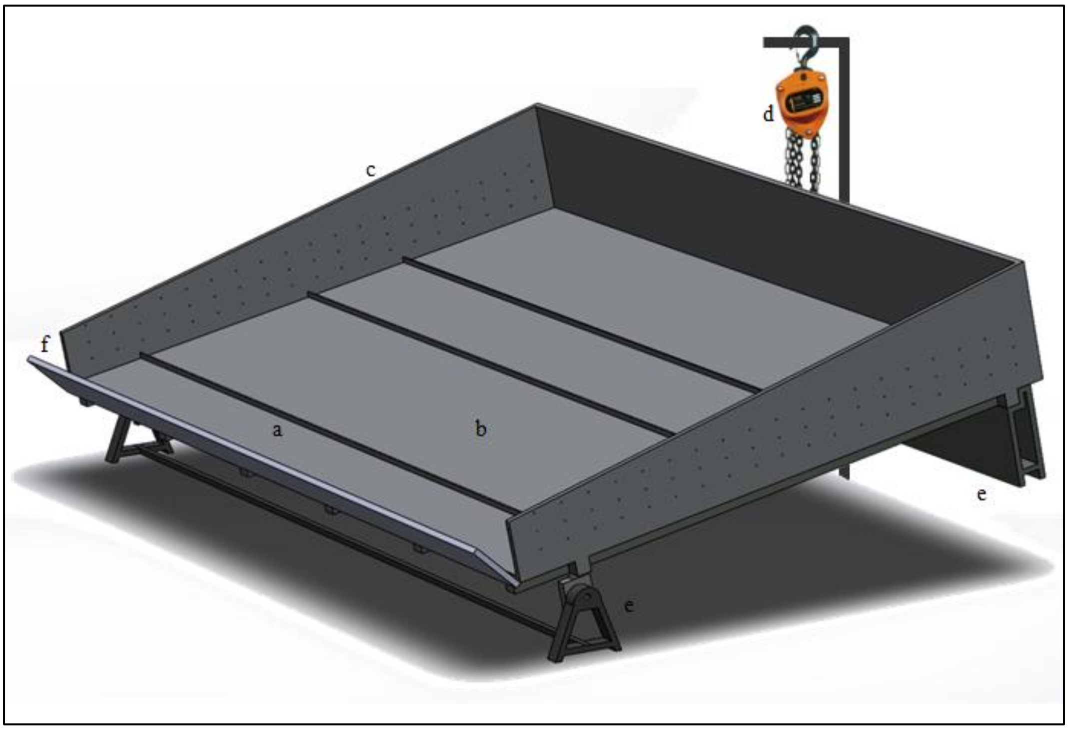

Figure 41: Representative sketch of laboratory experimental set-up. a) soil barrier having a height of 20 mm, b) soil-model interface, c) optical fiber cable holes, d) chain hoist to lift the model up and down in a controlled fashion, e) model feet for balancing, f) stopper to control mass movement

In order to study with laboratory landslide simulator the tray was filled with sand material and the sieve analysis results of the sand used are presented by Table 10 and Figure 42.

Table 10: Sieve analysis data

Test sieve		Mass retained (g)	Cumulative mass retained (g)	Cumulative % retained	Cumulative % passing
ASTM Sieves	Sieve Size (mm)				
No.4	4.750	23	23	4.637096774	95.36290323
No.10	2.000	175	198	39.91935484	60.08064516
No.20	0.850	138	336	67.74193548	32.25806452
No.40	0.425	73	409	82.45967742	17.54032258
No.60	0.250	46	455	91.73387097	8.266129032
No.140	0.106	34	489	98.58870968	1.411290323
No.200	0.075	4	493	99.39516129	0.60483871
Pan		3	496	100	0

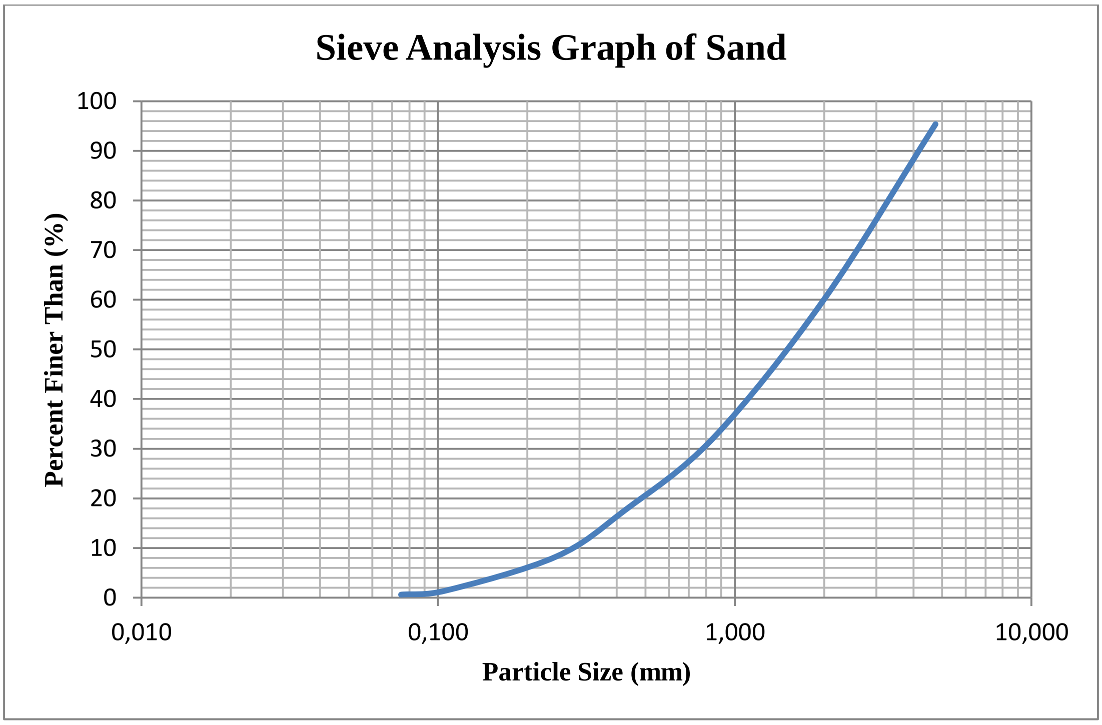

Figure 42: Sieve analysis result for the sand used

From the sieve analysis, D_{60}, D_{30}, and D_{10} values were calculated as 1.871, 0.750, and 0.269, respectively. By using these data, the coefficient of uniformity and the coefficient of curvature were calculated by using Equation 9 and Equation 10.

$$Cu = \frac{D_{60}}{D_{10}} = \frac{1.871}{0.269} = 6.955 \tag{9}$$

$$Cz = \frac{(D_{30})^2}{D_{60}D_{10}} = \frac{(0.75)^2}{(1.871)(0.269)} = 1.118 \tag{10}$$

As a consequence, the sand is classified according to unified soil classification system (USCS) as well graded sand, gravelly sands with little or no fines (SW). The USCS table is given in Appendix D.

Figure 43 and Figure 44 show the landslide simulator before and after movement based on inclination, respectively.

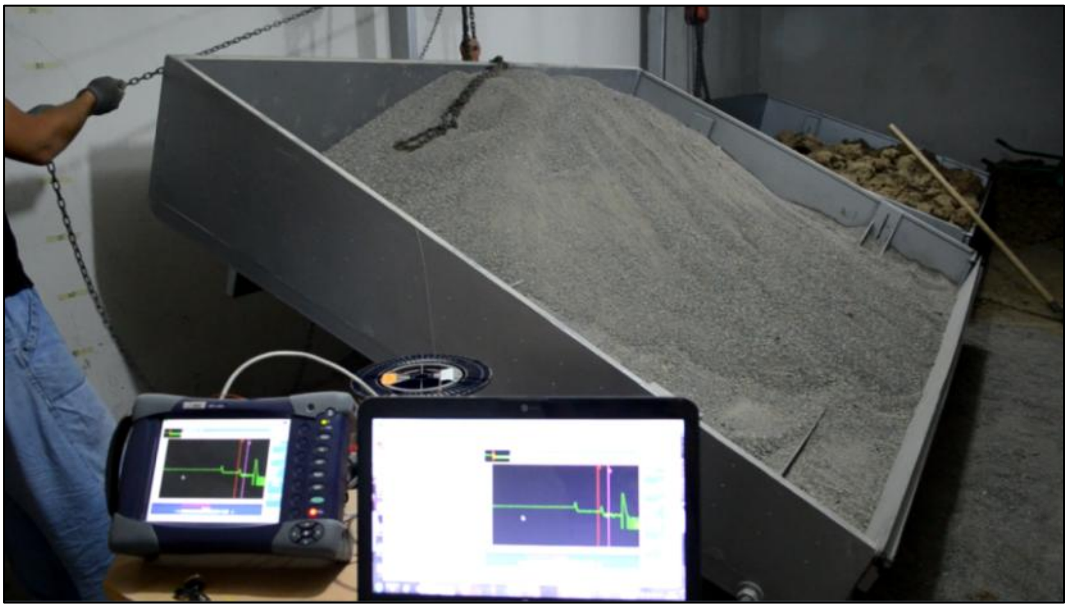

Figure 43: OTDR sytem measurement in landslide simulator before a movement based on inclination

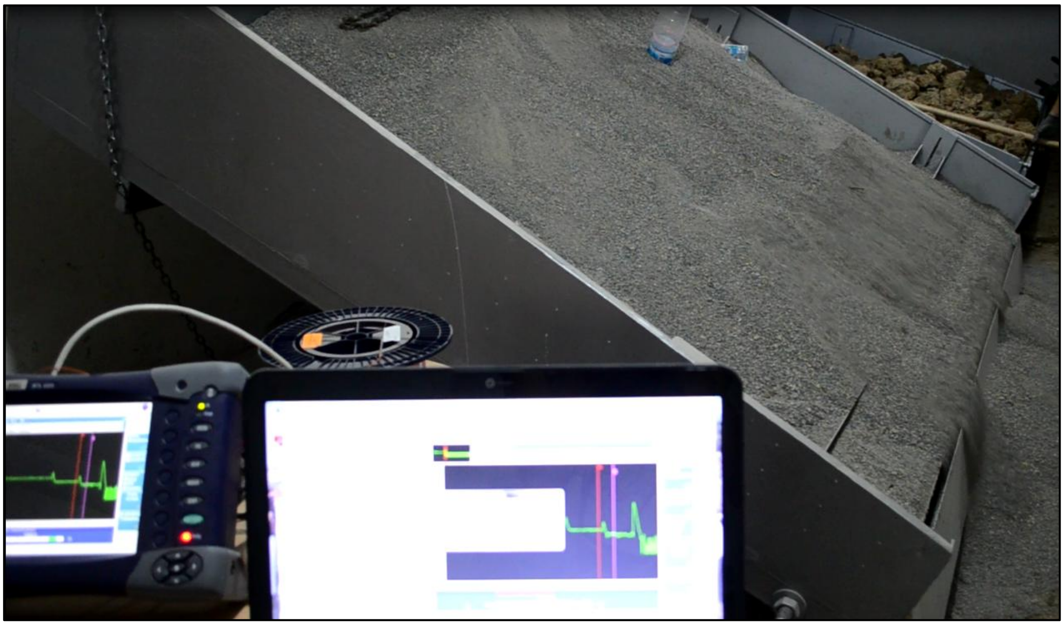

Figure 44: OTDR sytem measurement in landslide simulator after a small movement based on incination

Laboratory tests showed that the OTDR system is a sensitive and useful system for laboratory scale measurements. After the laboratory experiments were completed the aim was to implement the system to a landslide area. However, this aim could not be accomplished with the OTDR and this fiber optic setup due to the fragile structure of heterecores and the limited number of usable heterocores as a result of high energy loss. The laboratory test with the OTDR, on the other hand, allows finding a relation between the energy loss and displacement (Equation 11).

$$y = -68.99x^2 + 1224.9x + 2574.3 \tag{11}$$

Since the system constructed with the OTDR efficiently responses to the displacements occurred in a short distance that can be scanned by using three heterocore sensors, it is obvious that application of this monitoring system in large scale landslides is not that suitable because as shown in the table, even a single heterocore sensor reacts to a 1 cm displacement with a 3dB loss which indicates a power loss around 50%. It means that after the system senses a 3rd displacement, the maximum remaining power is around 10% of the initial one. That is why the device has had problems in taking measurements after the 3rd point and sensed the fourth point as the cable end (Arslan et al., 2014). This problem could be resolved by combining optical amplifiers to the sensors but that wouldn’t be a cost effective solution.

Because of this problem it was realized that to monitor a large scale area, the system utilized should be loss-independent which means that it should use a different parameter than the intensity of the light. All these facts directed the project to construct a new system by using BOTDA which enables to detect absolute and relative strains along an entire cable free of power loss by observing frequency shifts which will be given in detail in the following titles.

5.3 The BOTDA Monitoring System

It is possible to reach displacement results by using the OTDR by the correlation of the decibel losses recorded in a laboratory environment by the aid of a sensitivity analysis (Kelam et al., 2013). Unfortunately, the dB loss logic behind the OTDR makes its usage difficult in field applications as the power of light decreases with every loss. These disadvantages make calibration of the OTDR results complicated and less accurate. To overcome such negative effects and to increase efficiency and accuracy, Brillouin-OTDR (BOTDA) systems that detect strain and temperature changes have started to be used as an alternative (Wu et al., 2002).

The BOTDA requires two laser beams having opposite directions in a fiber cable layout. One of them is light launched to the cable and the other is backscattered light. A peak point manifests itself on the resulting measurement graph when the frequency difference between these two lasers coincides to the Brillouin frequency of a fiber (Xiaofei et al., 2011).

The strain and temperature changes cause the peak point to form in a different position than that of its former position. This change is observed as a frequency shift of the peak point. The BOTDA system is capable of acquiring measurements along a long fiber layout with a high accuracy. Due to this advantage, in addition to strain measurement, BOTDA can be used for monitoring of deformation in engineering structures (Xiaofei et al., 2011; Yin et al., 2010).

Studies were conducted with a Distributed Strain and Temperature Sensor (DSTS) device manufactured by OZ Optics, Ltd. Similar to the OTDR system studies, the BOTDA experiments were initiated in a laboratory environment with sensitivity measurements. As a result of these initial experiments, the relationship between displacement and strain that is presented in Table 11. Based on the relation given in the table third order polynomial equation is proposed in Figure 45.

Table 11: Displacement and strain relation

Displacement (cm)	Microstrain
6	78.27
8	219.49
10	219.50
12	282.77
14	282.73
17	379.69
20	628.43
22	843.44

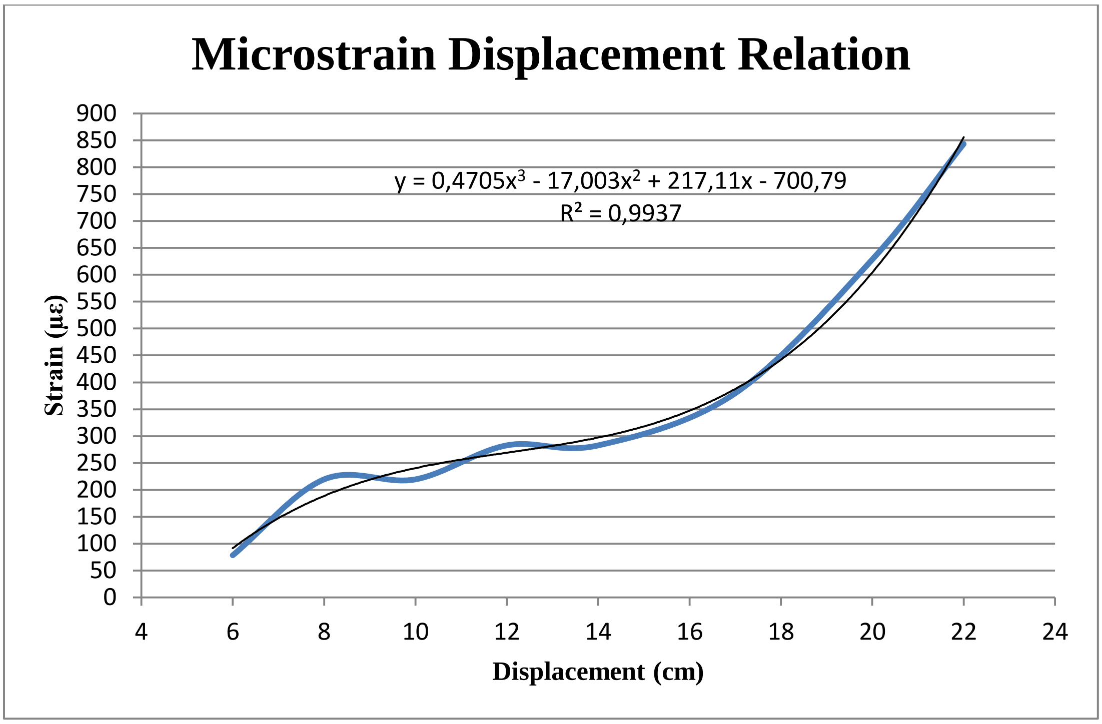

Figure 45: Strain changing with respect to displacement

After acquiring this calibration relationship, studies on the landslide simulator were initiated. Figure 46 and Figure 47 show before and after condition of the experiment, respectively.

Figure 46: Initial state of the BOTDA system on the laboratory simulator before sliding

Figure 47: Appearance of the BOTDA system after given inclination after sliding

As can be observed from the figures, mass movement occurred and the resultant strain was recorded by the BOTDA. Figure 48 shows the results acquired at the end of the experiment where the graph gives the strain resulting from slopes with varying inclination. Blue line represents initial strain present on fiber cable and red, green and yellow lines represents the strain conditions when the landslide simulator inclined to 10°, 20° and 30°.

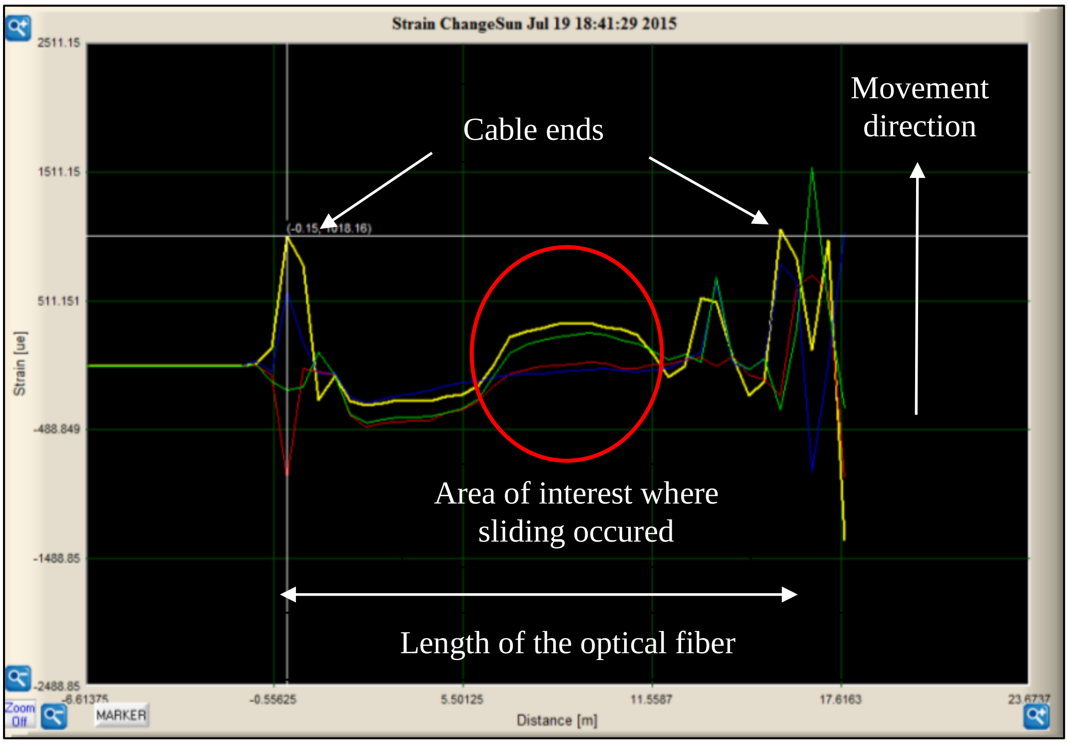

Figure 48: Microstrains formed due to changing inclination of the landslide simulator (red line represents the measurement taken at 10° inclination, green represents 20° and yellow represents 30° inclination).

5.4 Field Application of the Monitoring System

Field application of the system was implemented at the landslide region that is located in the Bahçecik Settlement Area of Başiskele District, Kocaeli Province, Turkey. The landslide in question is in a valley created by the Sarılık Stream and in its crown area there exists a two storey house which was evacuated. To monitor this slope, a fiber cable system starting from a point behind the crown was used. The cable system encircles the landslide, and then comes back to the starting point. In order to monitor shallow movements occurring on the slope, wooden stakes with a length of 2 m are used. Initially, the wooden stakes were driven 1 m on and around the failure surface. After that, the optical fiber cables were coiled around these anchored wooden stakes. During the construction of network between the stakes the optical fiber cable was deployed below 10 cm of the ground surface (Figure 49).

Figure 49: Close up view showing fixing of the cable on a wooden pole

Figure 50: A view of opening stage of guidance channels

Figure 50 shows the implementation procedure of the fiber cable between the two wooden poles. The cables were installed by opening guidance channels. Figure 51 and Figure 52 show the final configuration of the deployed system in the field. Figure 53 gives the appearance of the read out unit of the system in the container cabin.

Figure 51: Layout of the deployed fiber cables and fixing points (from toe to scarp)

Figure 52: Layout of the deployed fiber cables and fixing points (from scarp to toe)

A total of 15 stakes were used and the cable fixed to these poles covers the cable length between 2005 and 2056 meters. The stakes were tried to be deployed as equally spaced as possible. These stake locations were decided based on the deformation analysis explained and given in slope stability chapter (Chapter 3.5) in order to find the most critical region where the largest mass movement can occur (Figure 54).

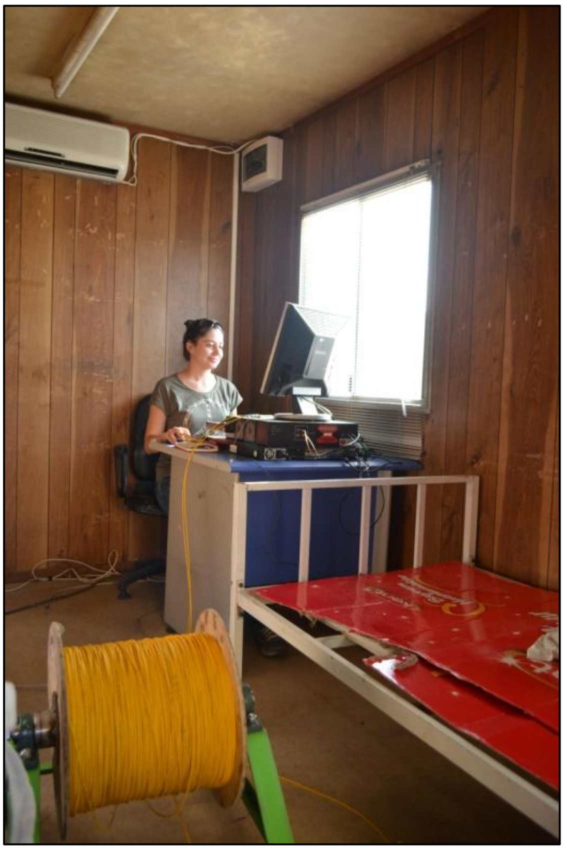

Figure 53: The monitoring unit of the field set up in the container

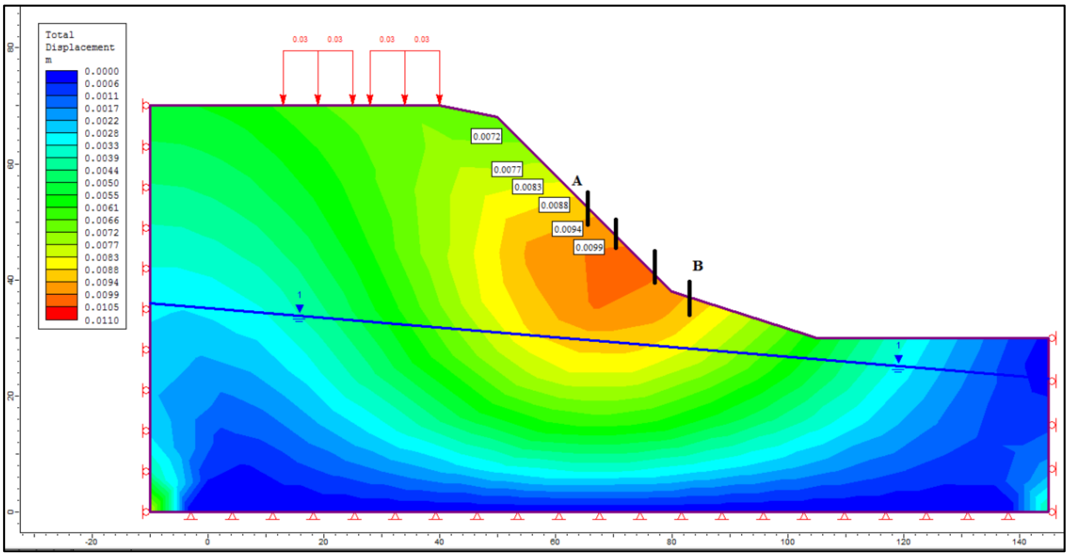

Figure 54: Landslide geometry shown together with deformation contours and cable fixing points

After the system was deployed, a base measurement was taken and the system was initialized to monitor the slope. Figure 55 gives the measurement of the entire cable length while Figure 56 shows the region where the cable was deployed into the landslide. In Figure 55 and Figure 56 letters A and B are the markers representing the borders of the deployed length. The optical fiber cable used for field application can be seen in Appendix E.

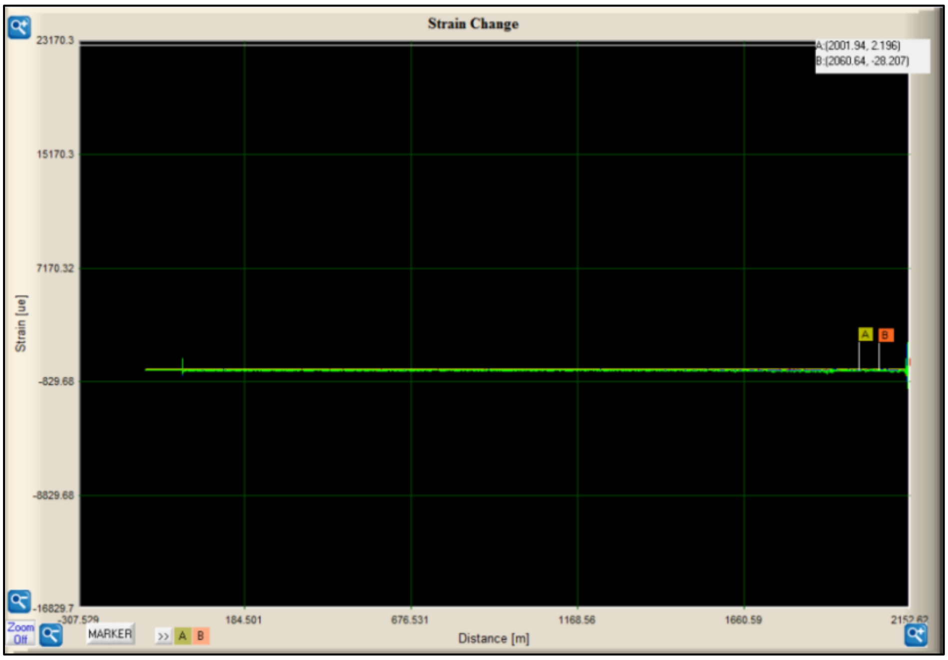

Figure 55: Baseline measurement of the whole cable

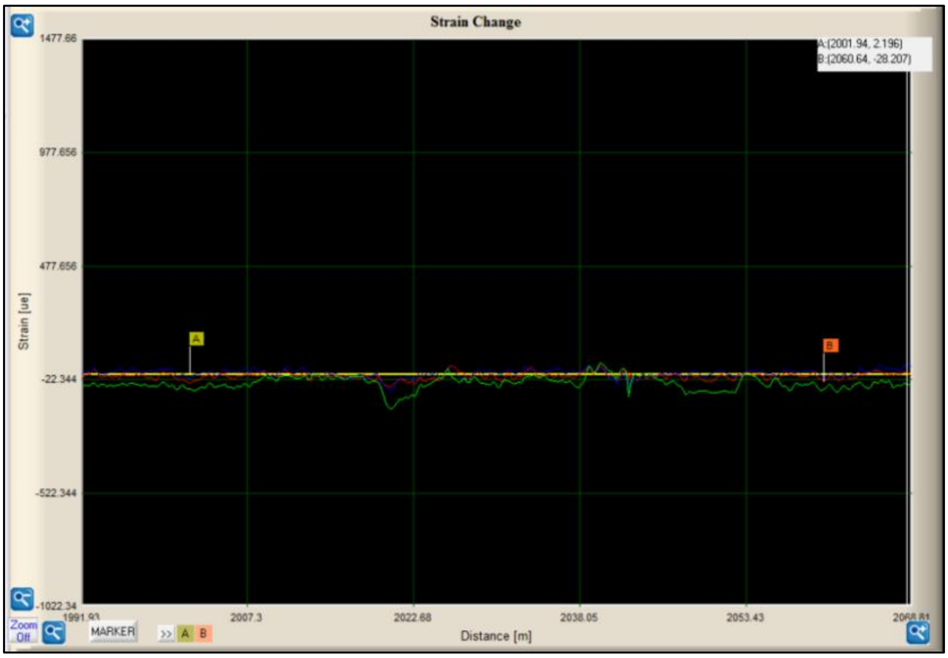

Figure 56: A close up view of the related portion of the cable along with the representative daily measurements taken during three days

Table 12 gives the microstrain results reached by the measurements performed in the field. The corresponding part of the cable is between the markers A and B as shown in the graph and the displacement results were obtained by the end of a three day monitoring in the field.

Table 12: Microstrain results gathered from field monitoring and corresponding displacements

Measurement Location	Displacement (cm)	Microstrain
2020.51 m	0.84	-530.42
	0.83	-532.3
	0.59	-580.21
2042.57 m	0.90	-519.16
	0.68	-561.017
	0.62	-572.72
2046-2053 m	0.87	-524.77
	0.85	-526.651
	0.71	-555.21

According to the deformation measurements obtained at the initial stage of the monitoring in Bahçecik Landslide, it is difficult to reach a concrete result such a short period of time. When the results of the numerical analysis and recorded strains are compared, it can be said that the field test results are relatively consistent with the numerical analysis results. However, it should be noted that the main reason of the deformation analysis is to detect the most critical failure surface area of the slope to determine the field monitoring boundaries and to test different groundwater level conditions that can be encountered during the field applications. As natural, the strain measurement obtained by BOTDA gives relatively lower strain than the deformation analysis. This may be a result of the emplacement time required for the cable to settle after the system was deployed. Therefore, in order to come up with firm results, sensitivity analysis should be continued in the field and the monitoring should be implemented for a longer period such as 3 or 5 months.

CHAPTER 6

DISCUSSION AND CONCLUSIONS

The main aim of the thesis study is to construct an early warning system by using optical fiber technology. Optical fiber systems were preferred because of their advantages over other methods like small size, wide bandwidth, immunity to electromagnetic interference, resistance to environmental conditions, easy data transfer, low cost, and real time monitoring. Although, the adopted technology has not been used as an early warning system yet, the conducted laboratory and field experiments show that it is capable of determining any type of mass movement.

At the initial stages of the study which had started with the Techno-Initiative Capital Support Program of Ministry of Science, Industry and Technology and continued with Research and Development, Innovation and Industrial Application Support Program of Republic of Turkey Small and Medium Enterprises Development Organization supports, an optical fiber system using the OTDR as a measurement device was used with bare fibers. The experiment with the OTDR system led to determine the sensor generation stage, test stage of its usefulness in the laboratory and the field implementation stage. The sensors were generated and the system was tested in laboratory scale by using a landslide simulation model having an inclination mechanism designed to represent a slope.

The system utilized with the OTDR was very sensitive as a point sensor and it was capable of measuring the strain in terms of centimeters. Although the system was sufficient for laboratory studies, it was not applicable to the field as power loss based measurement caused only three sensors to be used. In order to overcome the limitations of the OTDR, a new system based on the Brillouin frequency shift was used by the support of the National Earthquake Research Program (UDAP) of Republic of Turkey, Prime Ministry Disaster and Emergency Management Authority (AFAD). By the BOTDA system, the same procedure was followed. First, the system was tested in the laboratory simulator and then applied to field study. Laboratory studies performed led to a conclusion that the system was suitable for a landslide monitoring study and measurements resulted with a nonlinear relation between the strain and displacement. Following the laboratory scale studies, the system was applied to a landslide region in the Kocaeli Province, Başiskele District, Bahçecik Settlement Area. This area was selected, because of its critical situation in terms of landslide risk. In 2010, a landslide occurred and the region was announced as a hazard prone area by the Republic of Turkey Prime Ministry Disaster and Emergency Management Authority (AFAD) as the landslide was threatening a house that was located in the crown area. The BOTDA monitoring system was implemented to the landslide by deploying optical fiber cables with the help of fixing points and measurements were collected for few days.

The study area is located in a valley that lies within the stream bed of the Sarılık stream that is situated in a shear zone and the field observations showed that the units present in the area is the Paleocene-Eocene aged İncebel formation composed of sandstone-siltstone-marl alternation. The engineering geological assessment of the region was made by a field discontinuity scan-line survey and engineering geological boring logs. According to obtained field data, the formation is classified as very poor rock mass having soil-like lithology characteristics and it was highly weathered. The GSI rock mass classification system was used to reach the rock mass parameters required for the deformation analysis.

In order to understand the triggering mechanism of the landslide, initially, the seismic activity around the study area was examined and it was concluded that there has not been any important seismic activity that was capable of triggering the landslide. After this information, the Turkish State Meteorological Service database revealed that in December, 2010 there was a drastic increase in the rainfall precipitation values at Kocaeli. The average precipitation was 124.5 mm for December, 2010 while the average of the December precipitation was 108 mm. In addition, the precipitation reached a peak value with a daily precipitation of 28.4 mm on December 10, 2010 which might have been the triggering mechanism of the landslide.

The displacements take place in a small scale laboratory landslide simulator is rather obvious; however this is not the case for field application. Therefore, slope stability analyses were conducted.For this particular objective, a back analysis was implemented to reach the mobilized shear strength parameters of the moved mass by using three profiles. The back analysis was implemented by considering saturated condition at the time of failure and the surcharge of the houses that are located at the crown of the landslide. Then, the landslide was modeled based on deformation analysis via the finite element method to compute the displacements. The main purpose of applying finite element solution was to understand deformation characteristics of the field and to locate the place where the most deformation might occur. Accordinly, the monitoring system was deployed to the region to monitor the slope movement determined by deformation analysis. Another aim of the finite element solution was to evaluate the effect of grounwater level that can possibly be changed the stability results during the field monitoring study.

These results showed that the displacement values calculated were in fairly well agreement with those obtained through field monitoring within a small period of time. Although the field measurements performed was the preliminary study and the area should be monitored for a longer time period to reach the conclusive deformation results, the limited data measured in the study area was quite reasonable. The optical fiber monitoring system detected a displacement interval of

0.59-0.90 cm and the deformation analysis gave displacement values between 0.72-0.99 cm.

CHAPTER 7

RECOMMENDATIONS

This thesis study demonstrated that the optical fiber system is a reasonable tool as a landslide monitoring. At the end of the thesis, the monitoring result that is suitably compare with the deformation analysis was obtained. Also, calculated deformation results will be useful to understand anticipated excessive precipitation conditions in the future for the monitoring study. As mentioned previously, this study will continue to characterize slope movement through monitoring for a prolonged period of time as needed.

During the study period, preliminary results were gathered from the monitoring. Besides, deformation analysis conducted to locate the most critical failure surface in the study area. Results obtained from the both analysis present similar results but may not be representative as cables require an emplacement time to settle after the system was deployed. Therefore, in order to come up with firm results, sensitivity analysis should be continued in the field and the monitoring results should be implemented for a longer period of time. In addition, groundwater level on the region should be monitored as the landslided has triggered by precipitation of rainfall. For this purpose, a few piozometers might be deployed in the study area to control the results. In this period, deformation analysis will be detailed and monitoring system will be converted to an early warning system by asigning treshold displacement values to the system and controlling it with a GPRS system for remotely access monitoring or any other system that can replace it.

REFERENCES

Abramson, L., W., Lee, T., S., Sharma, S. & Boyce, G., M. (2002), Slope Stability and Stabilization Methods, John Wiley & Sons, Inc., New York, p. 712.

Akgün, A. & Bulut, F. (2007). GIS-Based Landslide Susceptibility For Arsin-Yomra (Trabzon, North Turkey) Region. Environmental Geology 51, pp. 1377-1387.

Al-Azzawi, A. (2007). Fiber Optics Principles and Practices. Taylor & Francis Group: Boca Raton.

Altuğ, G. (2007). Fiber Optik Grating Sensörler. Yüksek Lisans Tezi, Gazi Üniversitesi.

Ambraseys, N.N. & Zatopek, A. (1969). The Mudurnu Valley, West Anatolia, Turkey, Earthquake of 22 July 1967. Bull. Seismol. Soc. America, 59, 521-589.

Arslan, A., Kelam, M. A., Eker, A. M., Akgün, H. & Koçkar, M. K., (2014). Optical Fiber Technology To Monitor Slope Movement. Engineering Geology For Society And Territory Volume 2: Landslide Processes. Springer (eBook).

Barnoski, J. K. & Jensen, S. M. (1976). Fiber Waveguides: A Novel Technique For İnvestigating Attenuation Characteristics. Applied Optics,vol. 15, no.9, optical society of America.

Barka, A. (1996). Slip Distribution Along The North Anatolian Fault Associated With The Large Earthquakes Of The Period 1939 To 1967. Bull. Seismol. Soc. America, 86, pp. 1238-1254.

Barka, A., Akyüz, H.S., Altunel, E., Sunal, G. & Çakır, Z., (2002). The Surface Rupture And Slip Distribution Of The 17 August 1999 Izmit Earthquake (M 7.4), North Anatolian Fault. Bull. Seismol. Soc. America, 92, 43–60.

Bromhead, E., N. (1992). The Stability of Slopes, Blacky Academic & Professional, London, p. 411.

Cambazoğlu, S. (2012). Preparation Of A Source Model For The Eastern Marmara Region Along The North Anatolian Fault Segments And Probabilistic Seismic Hazard Assessment Of Düzce Province. Master Thesis, METU, Ankara, p. 154.

Cruden, D. M. (1991). A Simple Definition of a Landslide. Bulletin of the International Association of Engineering Geology, 43, pp. 27-29.

Cruden, D. M. & Varnes, D. J. (1996). Landslide Types And Processes (Chapter 3). In A. K. Turner & R. L. Schuster (Eds.), Landslides: Investigations and Mitigation. Transportation Research Board Special Report, 247. National Research Council. Washington, D. C.: National Academy Press.

Duman, T. Y., Emre, O., Doğan, A., Özalp, S. (2005). Step-Over And Bend Structures Along The 1999 Düzce Earthquake Surface Rupture, North Anatolian Fault, Turkey. Bull. Seismol. Soc. America, 95, 1250 – 1262.

Duman, T. Y., Nefeslioğlu, H. A., Çan, T., Ateş, Ş., Durmaz, S., Olgun, Ş., Hamzaçebi, S. & Keçer, M. (2006). Türkiye Heyelan Envateri Haritası 1/500 000 ölçekli İstanbul paftası. Maden Tetkik Arama Genel Müdürlüğü Özel yayın serisi-6.

Emre, Ö., Erkal, T., Tchepalyga, A., Kazanci, N., Keçer, M. & Ünay, E. (1998). Doğu Marmara Bölgesinin Neojen-Kuvaternerdeki Evrimi, Maden Tetkik ve Arama Dergisi, 120, pp. 233-258.

Emre, Ö., Doğan, A., Duman, T.Y. & Özalp, T. (2011). 1:250.000 Scale Active Fault Map Series of Turkey. General Directorate of Mineral Research and Exploration. Ankara-Turkey.

Erendil, M., Göncüoğlu, M. C., Tekeli, O., Aksay, A., Kuşçu, İ., Ürgün, B. M., Tunay, G. & Temren, A. (1991). Armutlu Yarımadasının Jeolojisi. MTA Rapor No. 9165. MTA, Ankara.

Fang, Z., Chin, K. K., Qu, R. & Cai, H. (2012). Fundamentals of Optical Fiber Sensors. John Wiley & Sons, Inc.: New Jersey.

Gedik İ., Pehlivan, Ş., Timur, E., Duru, M., Altun, İ., Akbaş, B., Özcan, İ. & Alan, İ. (2005). Kocaeli Yarımadasının Jeolojisi. MTA Rapor No. 10774. MTA, Ankara.

Geolab Geotecnics. (2012). Heyelan ve Şev Duraylılığının Risk Değerlendirme, İzleme ve Erken Uyarı Sistemi, Sanayi Bakanlığı TGSD Projesi Sonuç Raporu.

Gökçe, O., Özden, Ş. & Demir, A. (2008). Türkiye'de Afetlerin Mekansal Ve İstatistiksel Dağılımı Afet Bilgi Envanteri. T.C. Bayındırlık ve İskan Bakanlığı Afet İşleri Genel Müdürlüğü Afet Etüt ve Hasar Tespit Daire Başkanlığı. Ankara, p. 117

Göncüoğlu, M.C., Erendil, M., Tekeli, O., Ürgün, B.M., Aksay, A. & Kuşçu, G. (1986). Armutlu Yarımadası'nın Doğu Kesiminin Jeolojisi. MTA Rapor, No. 7786. MTA, Ankara.

Göncüoğlu, M. C., Erendil, M., Tekeli O., Aksay, A., Kuşçu İ. & Ürgün, B.M. (1992). Introduction to the Geology Of Armutlu Peninsula. ISGB-92 Guide Book. Ankara-Turkey.

Görür, N., Şengör, A.M.C., Akkök, R. & Yılmaz, Y. (1983), Pontidlerde Neo-Tetis'in Kuzey Kolunun Açılmasına Ilişkin Sedimentolojik Veriler. TJK Bülteni, 26, 11-20.

Grattan, K., T., V. & Meggitt, B., T. (eds.). (2000). Optical Fiber Sensor Technology Fundamentals. Kluwer Academic Publishers, Dordrecht, Netherlands. pp. 1-44.

Gupta, S. C. (2012). Textbook On Optical Fiber Communication And İts Applications (2nd Edition). PHI Learning Private Limited. New Delhi.

Halley, P. (1987). Fibre optic systems. John Wiley & Sons, United Kingdom.

HAMA Engineering. (2014). Heyelan Risk Analizi, Takip ve Erken Uyarı Sistemi (HERATEUS), Kosgeb Ar-Ge İnovasyon Desteği Gelişme Raporu.

Hayes, J. (2006). Fiber Optics Technician's Manual (third ed.). Thomson Delmar Learning: Canada.

Hoek E, & Bray JW, (1981). Rock Slope Engineering. London: Institution of Mining, Metallurgy, p. 358.

Horiguchi, T. , Kurashima, T. & Tateda, M. (1989). Tensile Strain Dependence of Brillouin Frequency Shift in Silica Optical Fibers. IEEE Photonics Technology Letters, vol. 1, No. 5, pp. 107-108.

Horiguchi, T., Shimizu, K., Kurashima T., Tateda, M. & Koyamada, Y. (1995). Development of a Distributed Sensing Technique Using Brillouin Scattering. Ournal of Lightwave Technology, vol. 13, No. 7.

ISRM. (1981). Suggested Methods For The Quantitative Description Of Discontinuities In Rock Masses. In: Barton T, editor. Rock Characterization, Testing And Monitoring. Oxford, London: Pergamon Press, p. 221.

Iten, M. (2011). Novel Applications of Distributed Fiber-Optic Sensing in Geotechnical Engineering. A Dissertation Submitted To Eth Zurich For The Degree Of Doctor Of Sciences.

Kandilli Observatory and Earthquake Research Institute (KOERI). (2015). Earthquake Catalogue, retrieved from Deprem Kataloğu: http://www.koeri.boun.edu.tr/sismo/2/deprem-verileri/deprem-katalogu/

Kelam, M. A., Eker, A. M., Akgün, H., Arslan, A. & Koçkar, M. K. (2013). A New Method For Monitoring Landslide And Slope Stability: Optical Fiber Technology. Proceedings of 66. Turkish Geological Symposium. Ankara, pp 312-313. (Abstract only).

Ketin, I. (1969). Uber die Nordanatolische Horizontalverschiebung. Bull Mineral Res. Explor. Inst. (MTA) Turkey. 72, 1-28.

Kocaeli Environment and Urbanization Directorate. (2011). Kocaeli Environment Information Report. Retrieved from http://www.csb.gov.tr/turkce/dosya/ced/icdr2011/kocaeli_icdr2011.pdf (accessed July 15,2015).

Lettis, W., Bachhuber, J., Witter, R., Brankman, C., Randolph, C.E., Barka, A., Page, W.D. & Kaya, A. (2002). Influence Of Releasing Step-Overs On Surface Fault Rupture And Fault Segmentation: Examples from the 17 August 1999 Izmit earthquake on the North Anatolian Fault, Turkey. Bull. Seismol. Soc. America, 92(1), 19-42.

Li, F., Du, Y., Zhang, W., Sun, B. & Li, F. (2012). Monitoring System For High Steep Slope Based On Optical Fiber Sensing Technology. Advanced Sensor Systems snd Applications V, v. 8561, 85610F.

Liu, Y., Dai, Z., Zhang, X., Peng, Z., Li, J., Ou, Z. & Liu, Y. (2010). Optical Fiber Sensors For Landslide Monitoring. Semiconductor Lasers and Applications IV, v. 7844, 78440D.

Mafang, S. F. (2011). Brillouin Echos for Advanced Distributed Sensing in Optical Fibres, Phd. Thesis, Ecole Polytechnique Federale DE Lausanne.

Marinos, P. & Hoek, E. (2000). GSI: A Geologically Friendly Tool for Rock Mass Strength Estimation. Proc. International Conference on Geotechnical and Geological Engineering, GeoEng2000, Technomic publ., pp. 1422-1442

Marinos, V., Marinos, P. & Hoek, E. (2005). The Geological Strength Index: Applications and Limitations. Bull. Eng. Geol. Env., v. 64, pp. 55-65.

Measures, R., M. (2001). Structural Monitoring With Fiber Optic Technology. Academic Press, USA.

Mohammed, Z. F. & Fatth, A. Y. (2013). Digital Signal Processing for Cancellation of Fiber Optic Impairments: Design and Simulation Using OptiSystem and Matlab. Lambert Academic Publishing: Germany.

MTA. (2003). Atlas of North Anatolian Fault: Special Publications Series:2. MTA Press, Ankara.

Ohno, H., Naruse, H., Kihara, M. & Shimada, A. (2001). Industrial Applications of the BOTDR Optical Fiber Strain Sensor. Optical Fiber Technology, 7, pp. 45-64.

Öztürk, A., İnan, S. & Tutkun, Z. (1985). Abant-Yeniçağa Yöresinin Tektoniği, Bull. Earth Sci. Cumhuriyet Univ.2, 35-52.

Pei, H., Cui, P., Yin, J., Zhu, H., Chen, X., Pei, L. & Xu D., (2011). Monitoring And Warning Of Landslides And Debris Flows Using An Optical Fiber Sensor Technology. J. Mount. Sci., v. 8, pp. 728-738.

Powers, J. (1997). An Introduction to Fiber Optic Systems (second ed.). McGraw-Hill Professional: USA

Rocscience. (2010). Slide Version 6, Slope Stability and Groundwater Seepage Analysis, Rocscience Inc. 31 Balsam Ave., Toronto, Ontario M4E 1B2, Canada.

Rocscience. (2011). Phase2 Version 8, Finite Element Analysis for Excavations and Slopes, Rocscience Inc. 31 Balsam Ave., Toronto, Ontario M4E 1B2, Canada.

Rocscience. (2012). DIPS Version 6, Graphical and Statistical Analysis of Orientation Data, Rocscience Inc. 31 Balsam Ave., Toronto, Ontario M4E 1B2, Canada.

Rocscience. (2014). RocLab Version 1, Rock Mass Strength Analysis Program Using The Hoek–Brown Failure Criterion, Rocscience Inc. 31 Balsam Ave., Toronto, Ontario M4E 1B2, Canada.

Savvaidis, P. D. (2003). Existing Landslide Monitoring Systems And Techniques. From Stars To Earth And Culture. School of Rural and Surveying Engineering, The Aristotle University of Thessaloniki, pp. 242-258.

Schuster, R. L. (1996). Socioeconomic Significance of Landslides (Chapter 2). In A. K. Turner & R. L. Schuster (Eds.), Landslides: Investigations and Mitigation. Transportation Research Board Special Report, 247. National Research Council. Washington, D. C.: National Academy Press.

Shiqing, N. & Qian, G. (2011). Application of Distributed Optical Fiber Sensor Technology Based on BOTDR in Similar Model Test of Backfill Mining. Procedia Earth and Planetary Science, 2, pp. 34-39.

Thyagarajan, K. S. & Ghatak A. (2007). Fiber Optic Essentials. Wiley-IEEE Press.

Turkish State Meteorological Service (2014). Annual Areal Precipitation, Kocaeli. Retrieved from http://www.mgm.gov.tr/veridegerlendirme/yillik-toplam-yagis-verileri.aspx?m=kocaeli#sfB (accessed July 10, 2015).

Turkish State Meteorological Service (2014). Statistics for Provinces, Kocaeli. Retrieved from http://www.mgm.gov.tr/veridegerlendirme/il-ve-ilceler-istatistik.aspx?m=KOCAELI#sfB (accessed July 10, 2015).

Varnes, D.J. (1978). Slope Movement Types and Processes. In Special Report 176: Landslides: Analysis and Control (R. L. Schuster and R. J. Krizek, eds.), Transportation and Road Research Board, National Research Council, Washington, D. C., pp.11-33.

Wang, B., Li, K., Shi, B. & Wei, G., (2008). Test On Application Of Distributed Fiber Optic Sensing Technique Into Soil Slope Monitoring. Landslides, v.6, pp. 61-68.

Watanabe K., Tajima, K. & Kubota, Y. (2000). Macrobending Characteristics of a Hetero-Core Splice Fiber Optic Sensor for Displacement and Liquid Detection. IEICE Trans. Electron., v.E83-C, no. 3.

Wu, Z. S. & Xu, B. (2002). Infrastructural Health Monitoring with BOTDR Fiber Optic Sensing Technique. Proceedings of the First International Workshop on Structural Health Monitoring of Innovative Civil Engineering Structures. ISIS Canada Research Network, pp. 217-226.

Xiaofei, Z., Wenjie, H., Qing, Z., Yanxin, S., Xianwei, M. & Yongwen, H., (2011). Development Of Optical Fiber Strain Monitoring System Based On BOTDR. The Tenth International Conference on Electronic Measurement & Instruments (ICEMI), IEEE, v. 4, pp. 38-41.

Yan, E., Song, K. & Li, H. (2010). Applicability Of Time Domain Refelectometry For Yuhuangge Landslide Monitoring. Journal ofr Earth Sciences, vol. 21, No.6, pp. 856-860.

Yin, Y., Wang, H., Gao, Y. & Li, X., (2010). Real-Time Monitoring And Early Warning Of Landslides At Relocated Wushan Town, The Three Gorges Reservoir, China. Landslides, v. 7, pp. 339-349.

Yücel, M., Göktaş, H. H., Yücel, M. & Öztürk, N.F. (2014). Brillouin Saçılması Tabanlı Fiber Optik Algılama. IEEE 22. Sinyal İşleme ve İletişim Uygulamaları Kurultayı Trabzon.

APPENDIX A

DAILY PRECIPITATION GRAPHS OF KOCAELI FOR DECEMBER, 2010

Figure A 1: Precipitation graph of December 5, 2010

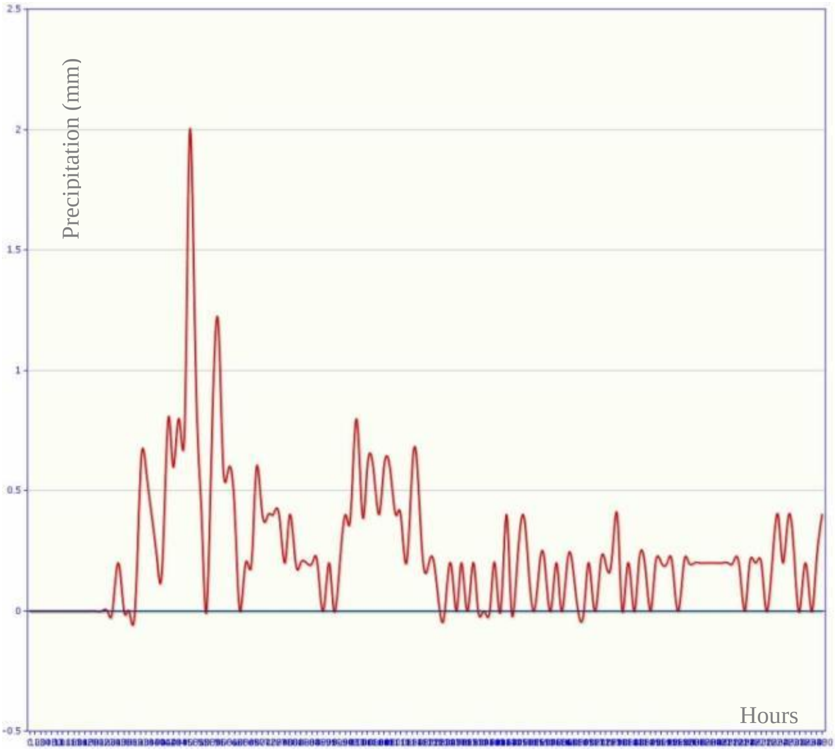

Figure A 2: Precipitation graph of December 10, 2010

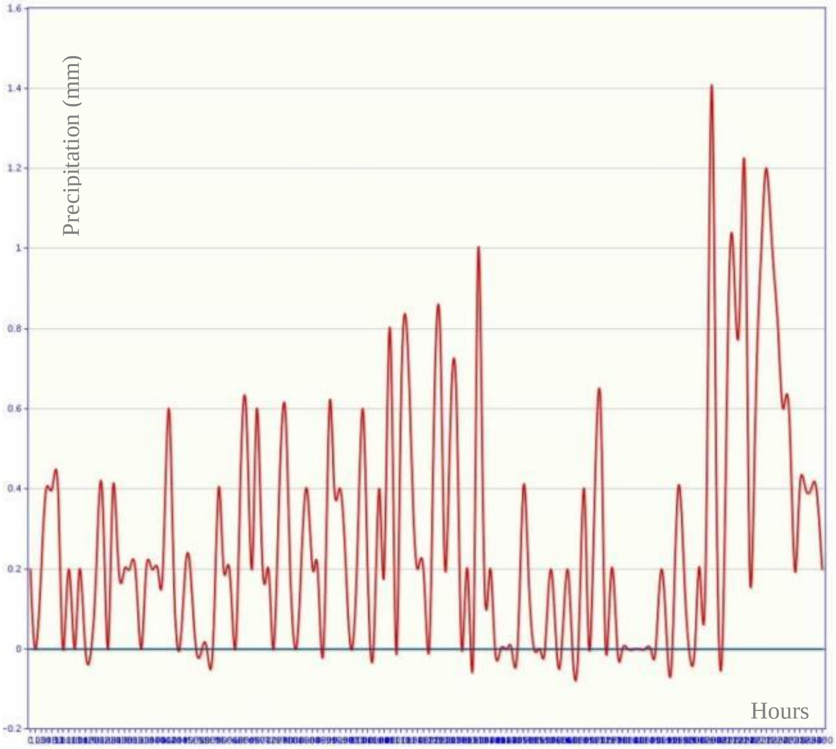

Figure A 3: Precipitation graph of December 11, 2010

Figure A 4: Precipitation graph of December 12, 2010

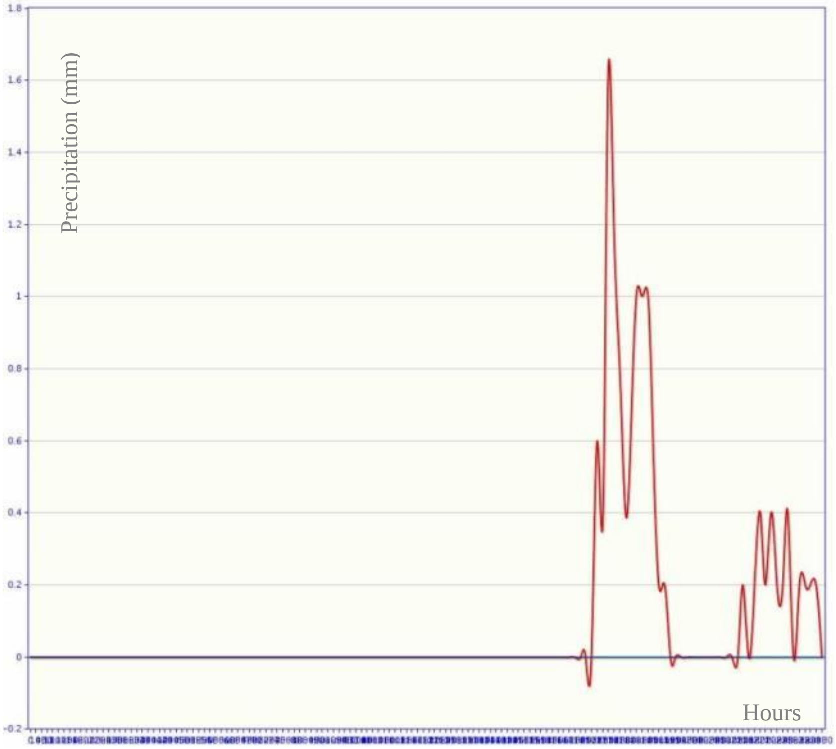

Figure A 5: Precipitation graph of December 13, 2010

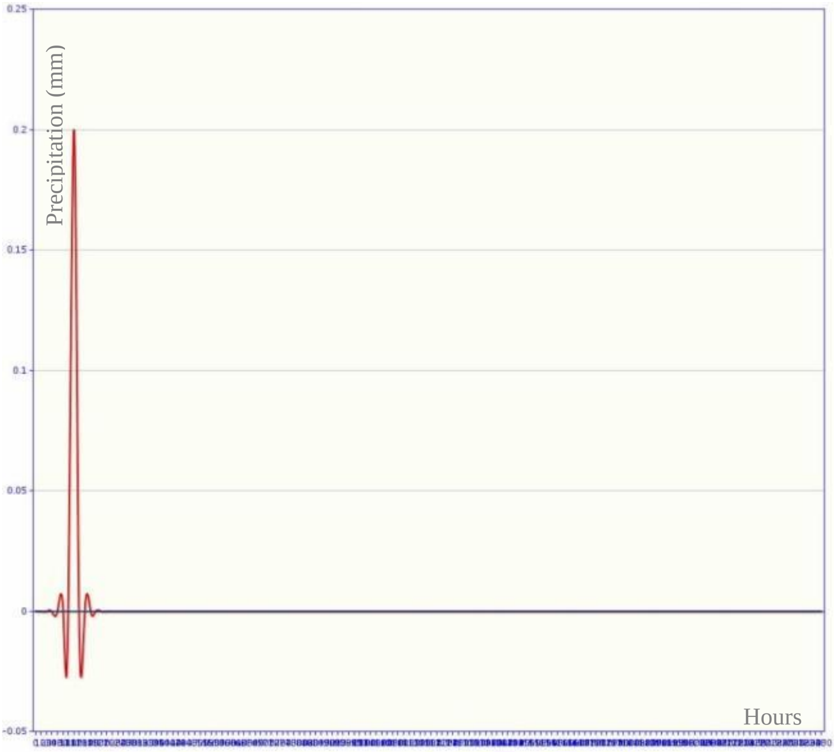

Figure A 6: Precipitation graph of December 14, 2010

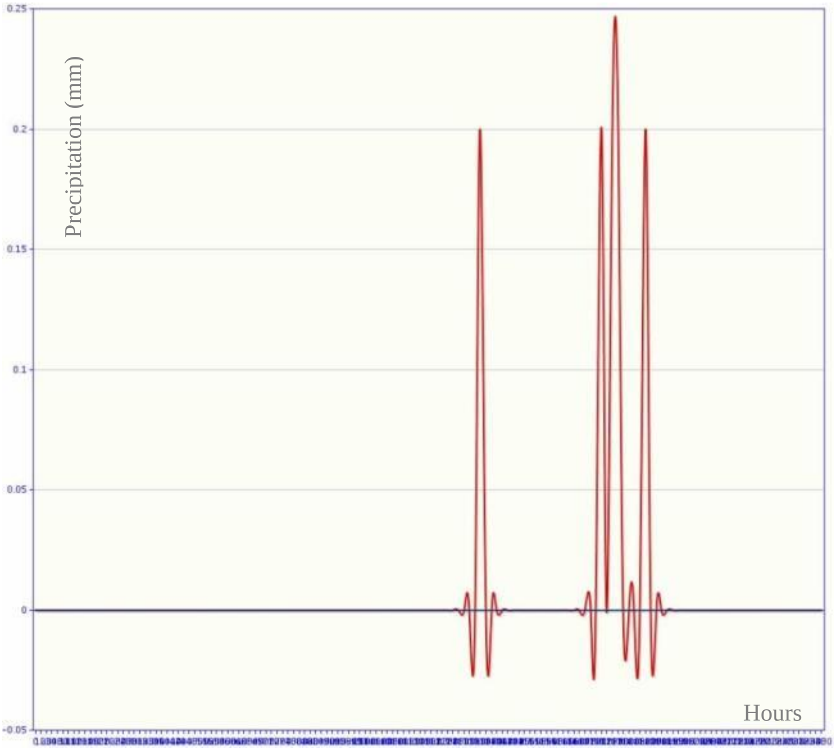

Figure A 7: Precipitation graph of December 16, 2010

Figure A 8: Precipitation graph of December 17, 2010

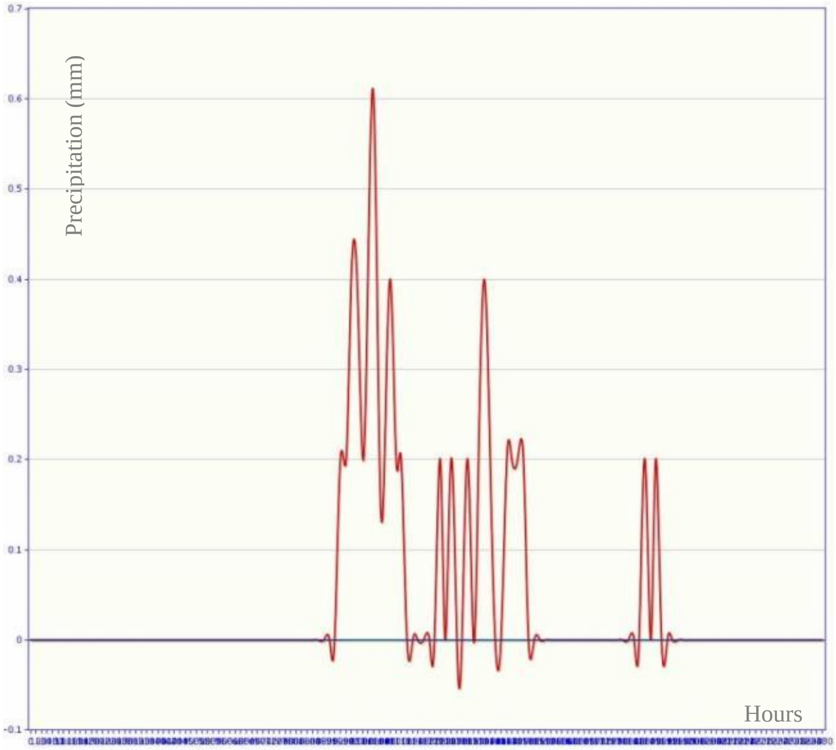

Figure A 9: Precipitation graph of December 19, 2010

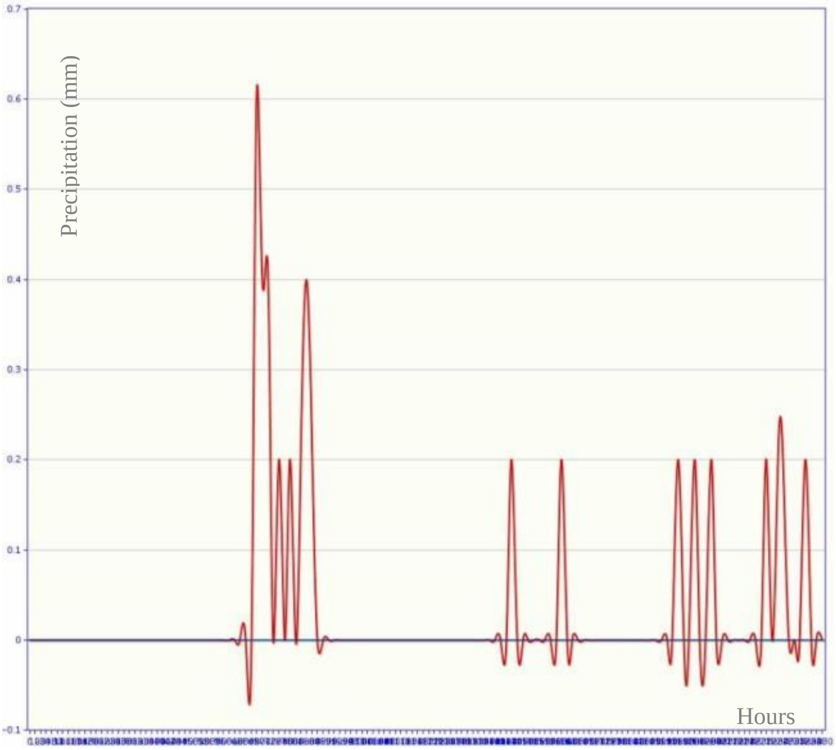

Figure A 10: Precipitation graph of December 26, 2010

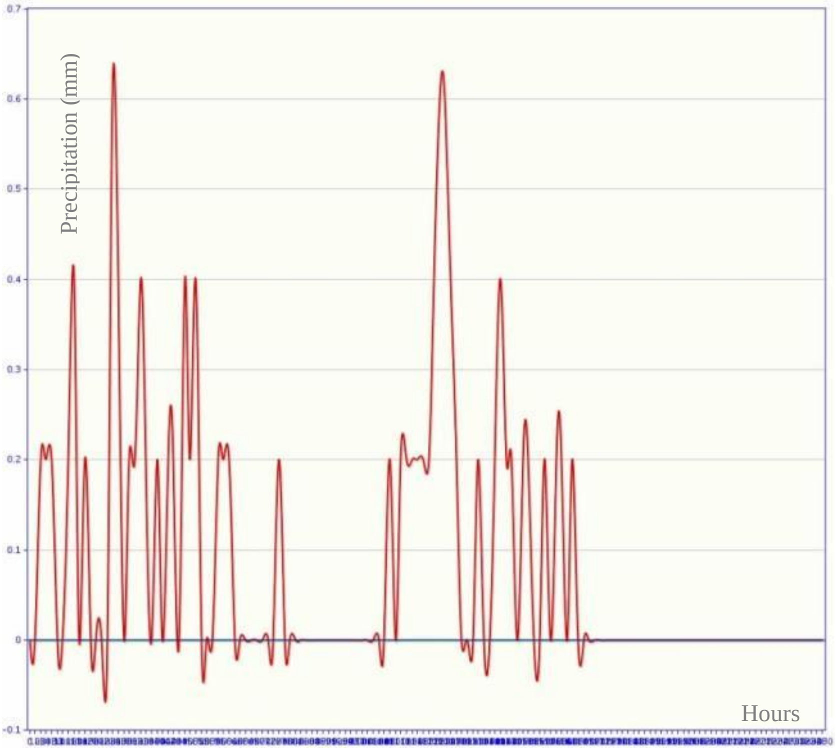

Figure A 11: Precipitation graph of December 27, 2010

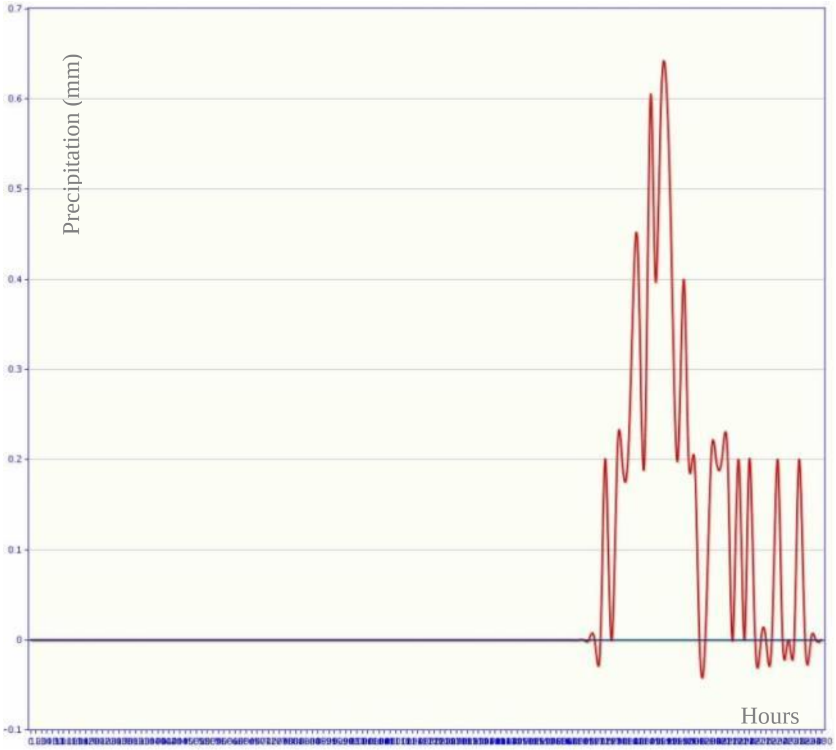

Figure A 12: Precipitation graph of December 28, 2010

Figure A 13: Precipitation graph of December 29, 2010

APPENDIX B

BOREHOLE LOGS

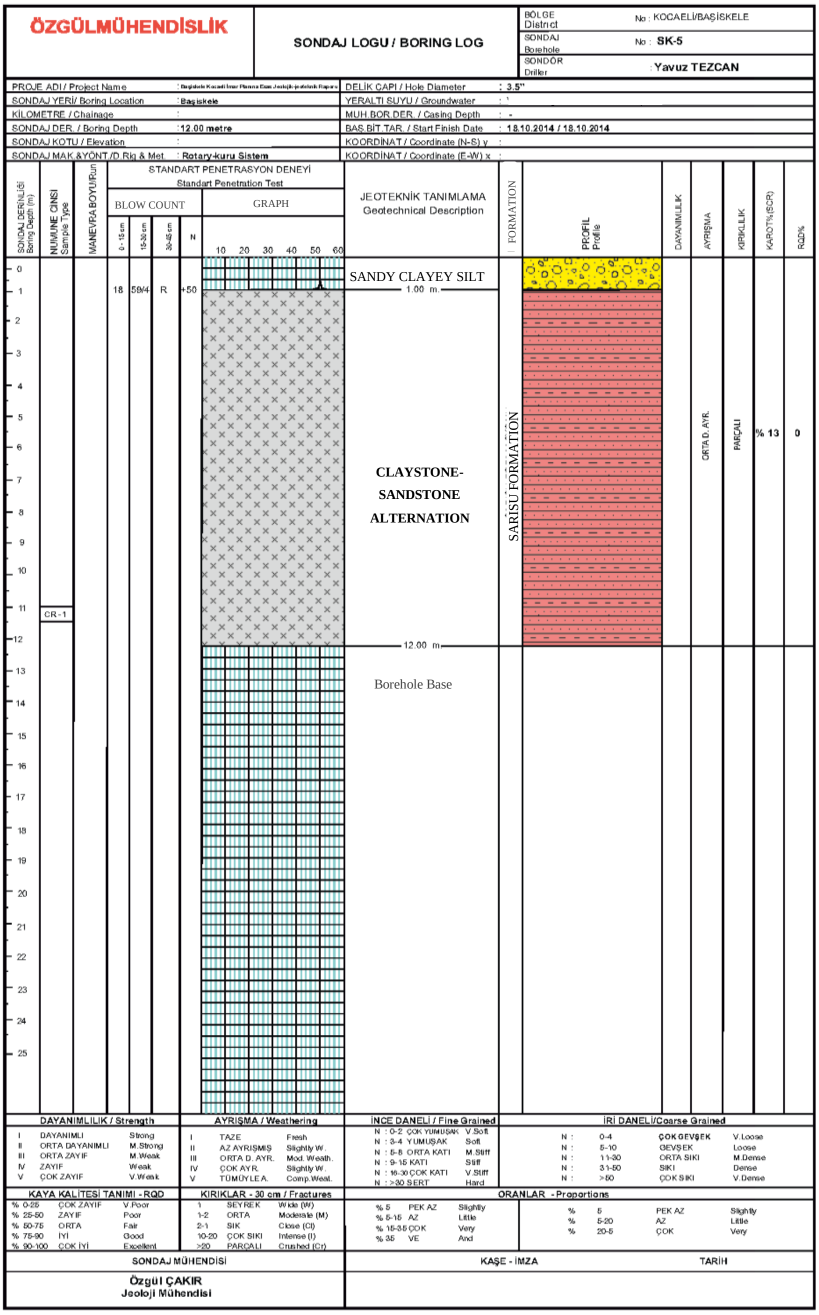

ÖZGÜLMÜHENDİSLİK

SONDAJ LOGU / BORING LOG

BÖLGE District No : KOCAELİ/BAŞİSKELE
SONDAJ Borehole No : **SK-5**
SONDÖR Driller : **Yavuz TEZCAN**

PROJE ADI / Project Name	: Başiskele Kocaeli İmar Planına Esas Jeolojik-jeoteknik Raporu	DELİK ÇAPI / Hole Diameter	: **3.5"**
SONDAJ YERİ/ Boring Location	: **Başiskele**	YERALTI SUYU / Groundwater	: '
KİLOMETRE / Chainage	:	MUH.BOR.DER. / Casing Depth	: -
SONDAJ DER. / Boring Depth	: **12.00 metre**	BAŞ.BİT.TAR. / Start Finish Date	: **18.10.2014 / 18.10.2014**
SONDAJ KOTU / Elevation	:	KOORDİNAT / Coordinate (N-S) y	:
SONDAJ MAK.&YÖNT./D.Rig & Met.	: **Rotary-kuru Sistem**	KOORDİNAT / Coordinate (E-W) x	:

SONDAJ DERİNLİĞİ Boring Depth (m)	NUMUNE CİNSİ Sample Type	MANEVRA BOYU/Run	STANDART PENETRASYON DENEYİ Standart Penetration Test — BLOW COUNT 0 - 15 cm	15-30 cm	30-45 cm	N	GRAPH 10 20 30 40 50 60	JEOTEKNİK TANIMLAMA Geotechnical Description	FORMATION	PROFİL Profile	DAYANIMLILIK	AYRIŞMA	KIRIKLILIK	KAROT%(SCR)	RQD%
0 – 1			18	50/4	R	+50		SANDY CLAYEY SILT							
1.00 m. – 12.00 m.	CR - 1							**CLAYSTONE-SANDSTONE ALTERNATION**	SARISU FORMATION			ORTA D. AYR.	PARÇALI	% 13	0
12.00 m								Borehole Base							

DAYANIMLILIK / Strength		
I	DAYANIMLI	Strong
II	ORTA DAYANIMLI	M.Strong
III	ORTA ZAYIF	M.Weak
IV	ZAYIF	Weak
V	ÇOK ZAYIF	V.Weak

AYRIŞMA / Weathering		
I	TAZE	Fresh
II	AZ AYRIŞMIŞ	Slightly W.
III	ORTA D. AYR.	Mod. Weath.
IV	ÇOK AYR.	Slightly W.
V	TÜMÜYLE A.	Comp.Weat.

İNCE DANELİ / Fine Grained		
N : 0-2	ÇOK YUMUŞAK	V.Soft
N : 3-4	YUMUŞAK	Soft
N : 5-8	ORTA KATI	M.Stiff
N : 9-15	KATI	Stiff
N : 16-30	ÇOK KATI	V.Stiff
N : >30	SERT	Hard

İRİ DANELİ/Coarse Grained			
N :	0-4	**ÇOK GEVŞEK**	V.Loose
N :	5-10	GEVŞEK	Loose
N :	11-30	ORTA SIKI	M.Dense
N :	31-50	SIKI	Dense
N :	>50	ÇOK SIKI	V.Dense

KAYA KALİTESİ TANIMI - RQD		
% 0-25	ÇOK ZAYIF	V.Poor
% 25-50	ZAYIF	Poor
% 50-75	ORTA	Fair
% 75-90	İYİ	Good
% 90-100	ÇOK İYİ	Excellent

KIRIKLAR - 30 cm / Fractures		
1	SEYREK	Wide (W)
1-2	ORTA	Moderate (M)
2-1	SIK	Close (Cl)
10-20	ÇOK SIKI	Intense (I)
>20	PARÇALI	Crushed (Cr)

ORANLAR - Proportions

% 5	PEK AZ	Slightly
% 5-15	AZ	Little
% 15-35	ÇOK	Very
% 35	VE	And

%	5	PEK AZ	Slightly
%	5-20	AZ	Little
%	20-5	ÇOK	Very

SONDAJ MÜHENDİSİ	KAŞE - İMZA	TARİH
Özgül ÇAKIR **Jeoloji Mühendisi**		

ÖZGÜLMÜHENDİSLİK

SONDAJ LOGU / BORING LOG

BÖLGE District	No : KOCAELİ/BAŞİSKELE
SONDAJ Borehole	No : **SK- 9**
SONDÖR Driller	: **Yavuz TEZCAN**

PROJE ADI / Project Name	: Başiskele Kocaeli İmar Planına Esas Jeolojik-jeoteknik Raporu	DELİK ÇAPI / Hole Diameter	: **3.5"**
SONDAJ YERİ/ Boring Location	: **Başiskele**	YERALTI SUYU / Groundwater	:
KİLOMETRE / Chainage	:	MUH.BOR.DER. / Casing Depth	: **-**
SONDAJ DER. / Boring Depth	: **12.00 metre**	BAŞ.BİT.TAR. / Start Finish Date	: **22.10.2014 / 22.10.2014**
SONDAJ KOTU / Elevation	:	KOORDİNAT / Coordinate (N-S) y	:
SONDAJ MAK.&YÖNT./D.Rig & Met.	: **Rotary-kuru Sistem**	KOORDİNAT / Coordinate (E-W) x	:

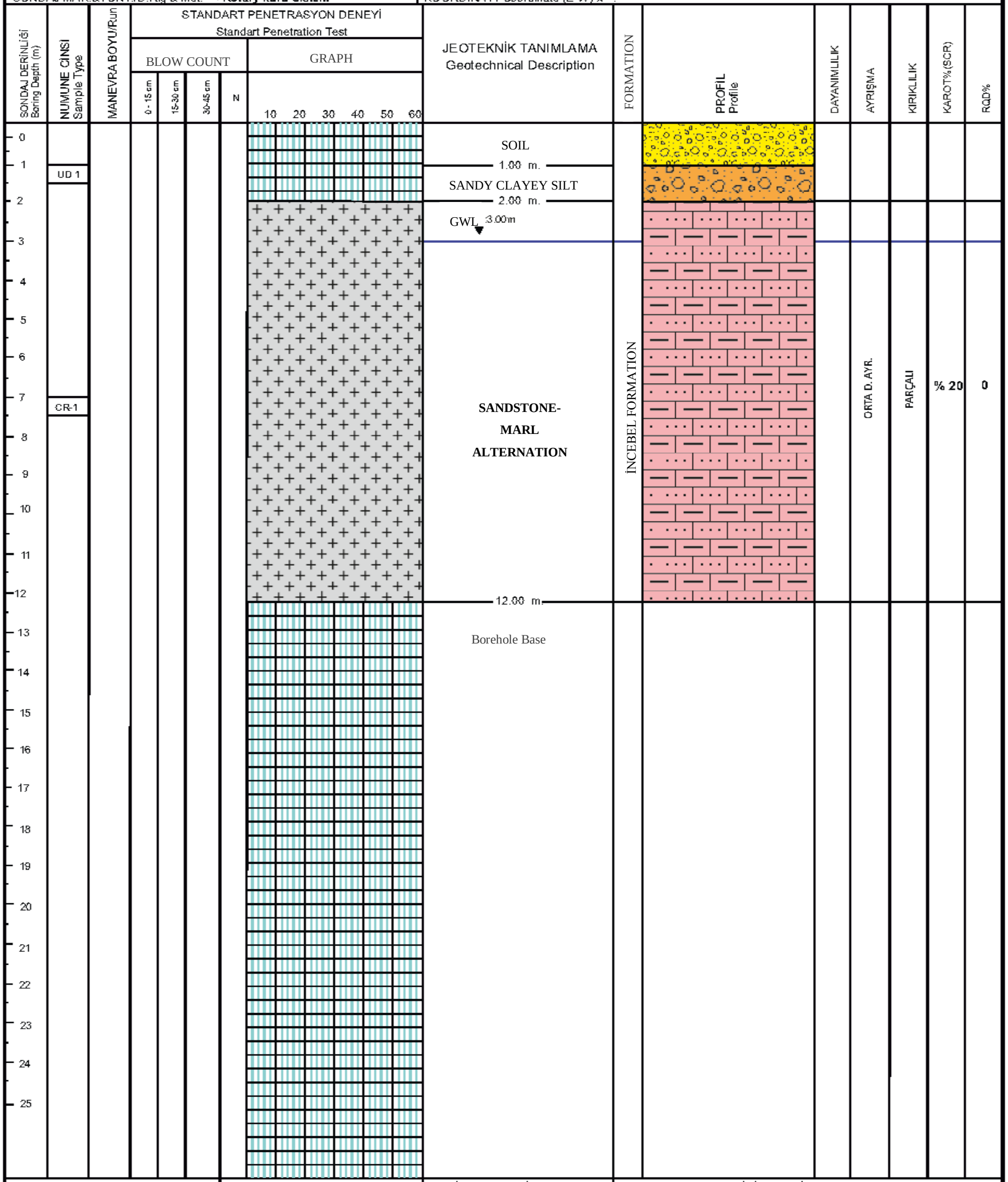

DAYANIMLILIK / Strength		
I	DAYANIMLI	Strong
II	ORTA DAYANIMLI	M.Strong
III	ORTA ZAYIF	M.Weak
IV	ZAYIF	Weak
V	ÇOK ZAYIF	V.Weak

AYRIŞMA / Weathering		
I	TAZE	Fresh
II	AZ AYRIŞMIŞ	Slightly W.
III	ORTA D. AYR.	Mod. Weath.
IV	ÇOK AYR.	Slightly W.
V	TÜMÜYLE A.	Comp.Weat.

İNCE DANELİ / Fine Grained		
N : 0-2	ÇOK YUMUŞAK	V.Soft
N : 3-4	YUMUŞAK	Soft
N : 5-8	ORTA KATI	M.Stiff
N : 9-15	KATI	Stiff
N : 16-30	ÇOK KATI	V.Stiff
N : >30	SERT	Hard

İRİ DANELİ/Coarse Grained			
N :	0-4	ÇOK GEVŞEK	V.Loose
N :	5-10	GEVŞEK	Loose
N :	11-30	ORTA SIKI	M.Dense
N :	31-50	SIKI	Dense
N :	>50	ÇOK SIKI	V.Dense

KAYA KALİTESİ TANIMI - RQD		
% 0-25	ÇOK ZAYIF	V.Poor
% 25-50	ZAYIF	Poor
% 50-75	ORTA	Fair
% 75-90	İYİ	Good
% 90-100	ÇOK İYİ	Excellent

KIRIKLAR - 30 cm / Fractures		
1	SEYREK	Wide (W)
1-2	ORTA	Moderate (M)
2-1	SIK	Close (Cl)
10-20	ÇOK SIKI	Intense (I)
>20	PARÇALI	Crushed (Cr)

ORANLAR - Proportions

% 5	PEK AZ	Slightly
% 5-15	AZ	Little
% 15-35	ÇOK	Very
% 35	VE	And

%	5	PEK AZ	Slightly
%	5-20	AZ	Little
%	20-5	ÇOK	Very

SONDAJ MÜHENDİSİ	KAŞE - İMZA	TARİH
Özgül ÇAKIR **Jeoloji Mühendisi**		

ÖZGÜLMÜHENDİSLİK

SONDAJ LOGU / BORING LOG

BÖLGE District	No : KOCAELİ/BAŞİSKELE		
SONDAJ Borehole	No : **SK- 10**		
SONDÖR Driller	: **Yavuz TEZCAN**		
PROJE ADI / Project Name	: Başiskele Kocaeli İmar Planına Esas Jeolojik-jeoteknik Raporu	DELİK ÇAPI / Hole Diameter	: **3.5"**
SONDAJ YERİ/ Boring Location	: **Başiskele**	YERALTI SUYU / Groundwater	:
KİLOMETRE / Chainage	:	MUH.BOR.DER. / Casing Depth	: **-**
SONDAJ DER. / Boring Depth	: **12.00 metre**	BAŞ.BİT.TAR. / Start Finish Date	: **24.10.2014 / 24.10.2014**
SONDAJ KOTU / Elevation	:	KOORDİNAT / Coordinate (N-S) y	:
SONDAJ MAK.&YÖNT./D.Rig & Met.	: **Rotary-kuru Sistem**	KOORDİNAT / Coordinate (E-W) x	:

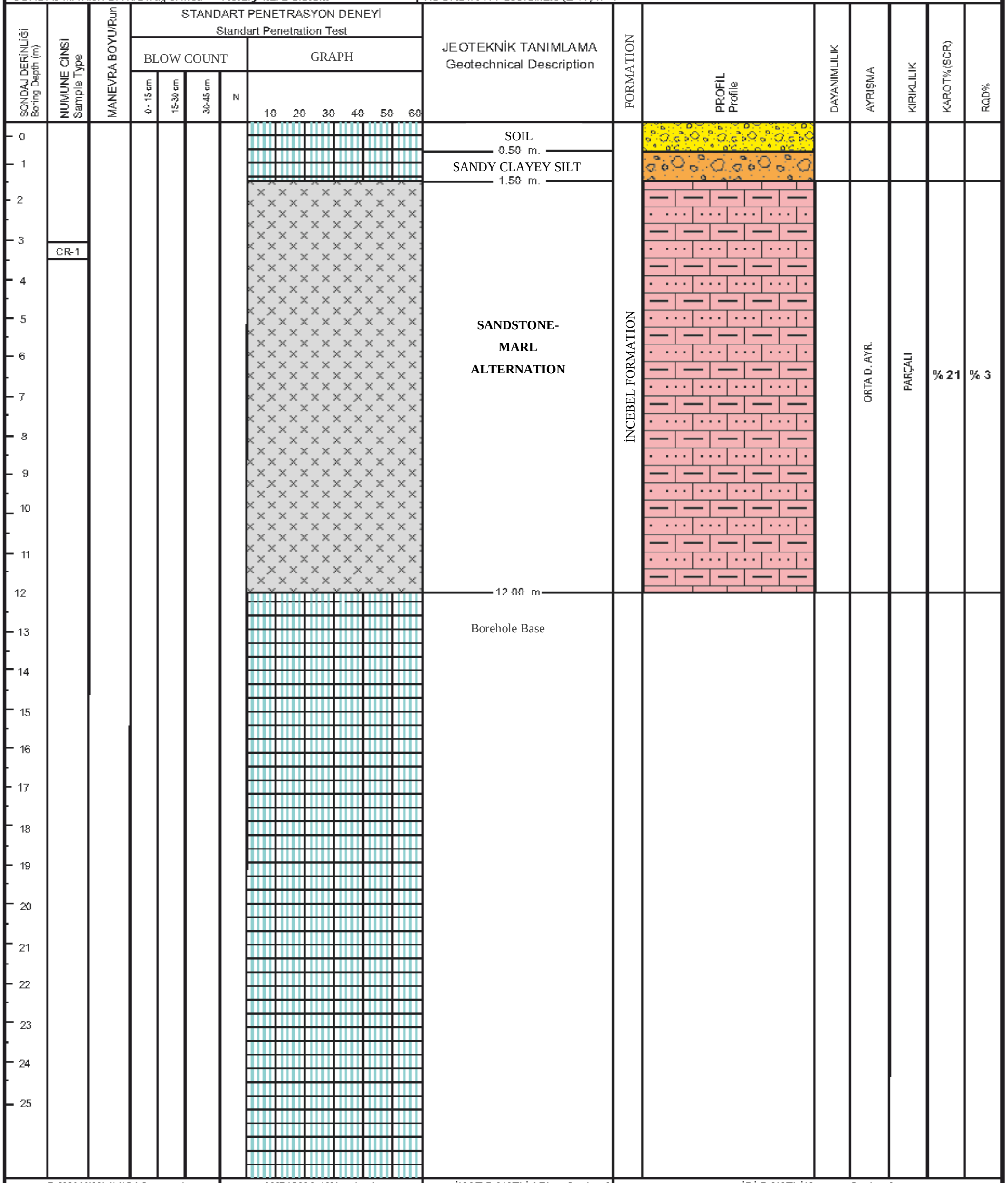

DAYANIMLILIK / Strength		
I	DAYANIMLI	Strong
II	ORTA DAYANIMLI	M.Strong
III	ORTA ZAYIF	M.Weak
IV	ZAYIF	Weak
V	ÇOK ZAYIF	V.Weak

AYRIŞMA / Weathering		
I	TAZE	Fresh
II	AZ AYRIŞMIŞ	Slightly W.
III	ORTA D. AYR.	Mod. Weath.
IV	ÇOK AYR.	Slightly W.
V	TÜMÜYLE A.	Comp.Weat.

İNCE DANELİ / Fine Grained		
N : 0-2	ÇOK YUMUŞAK	V.Soft
N : 3-4	YUMUŞAK	Soft
N : 5-8	ORTA KATI	M.Stiff
N : 9-15	KATI	Stiff
N : 16-30	ÇOK KATI	V.Stiff
N : >30	SERT	Hard

İRİ DANELİ/Coarse Grained			
N :	0-4	**ÇOK GEVŞEK**	V.Loose
N :	5-10	GEVŞEK	Loose
N :	11-30	ORTA SIKI	M.Dense
N :	31-50	SIKI	Dense
N :	>50	ÇOK SIKI	V.Dense

KAYA KALİTESİ TANIMI - RQD		
% 0-25	ÇOK ZAYIF	V.Poor
% 25-50	ZAYIF	Poor
% 50-75	ORTA	Fair
% 75-90	İYİ	Good
% 90-100	ÇOK İYİ	Excellent

KIRIKLAR - 30 cm / Fractures		
1	SEYREK	Wide (W)
1-2	ORTA	Moderate (M)
2-1	SIK	Close (Cl)
10-20	ÇOK SIKI	Intense (I)
>20	PARÇALI	Crushed (Cr)

ORANLAR - Proportions						
% 5	PEK AZ	Slightly	%	5	PEK AZ	Slightly
% 5-15	AZ	Little	%	5-20	AZ	Little
% 15-35	ÇOK	Very	%	20-5	ÇOK	Very
% 35	VE	And				

SONDAJ MÜHENDİSİ	KAŞE - İMZA	TARİH
Özgül ÇAKIR **Jeoloji Mühendisi**		

ÖZGÜLMÜHENDİSLİK

SONDAJ LOGU / BORING LOG

BÖLGE District	No : KOCAELİ/BAŞİSKELE
SONDAJ Borehole	No : **SK- 11**
SONDÖR Driller	: **Yavuz TEZCAN**

PROJE ADI / Project Name	: Başiskele Kocaeli İmar Planına Esas Jeolojik-jeoteknik Raporu	DELİK ÇAPI / Hole Diameter	: **3.5"**
SONDAJ YERİ/ Boring Location	: **Başiskele**	YERALTI SUYU / Groundwater	: [illegible]
KİLOMETRE / Chainage	:	MUH.BOR.DER. / Casing Depth	: -
SONDAJ DER. / Boring Depth	: **12.00 metre**	BAŞ.BİT.TAR. / Start Finish Date	: **25.10.2014 / 25.10.2014**
SONDAJ KOTU / Elevation	:	KOORDİNAT / Coordinate (N-S) y	:
SONDAJ MAK.&YÖNT./D.Rig & Met.	: **Rotary-kuru Sistem**	KOORDİNAT / Coordinate (E-W) x	:

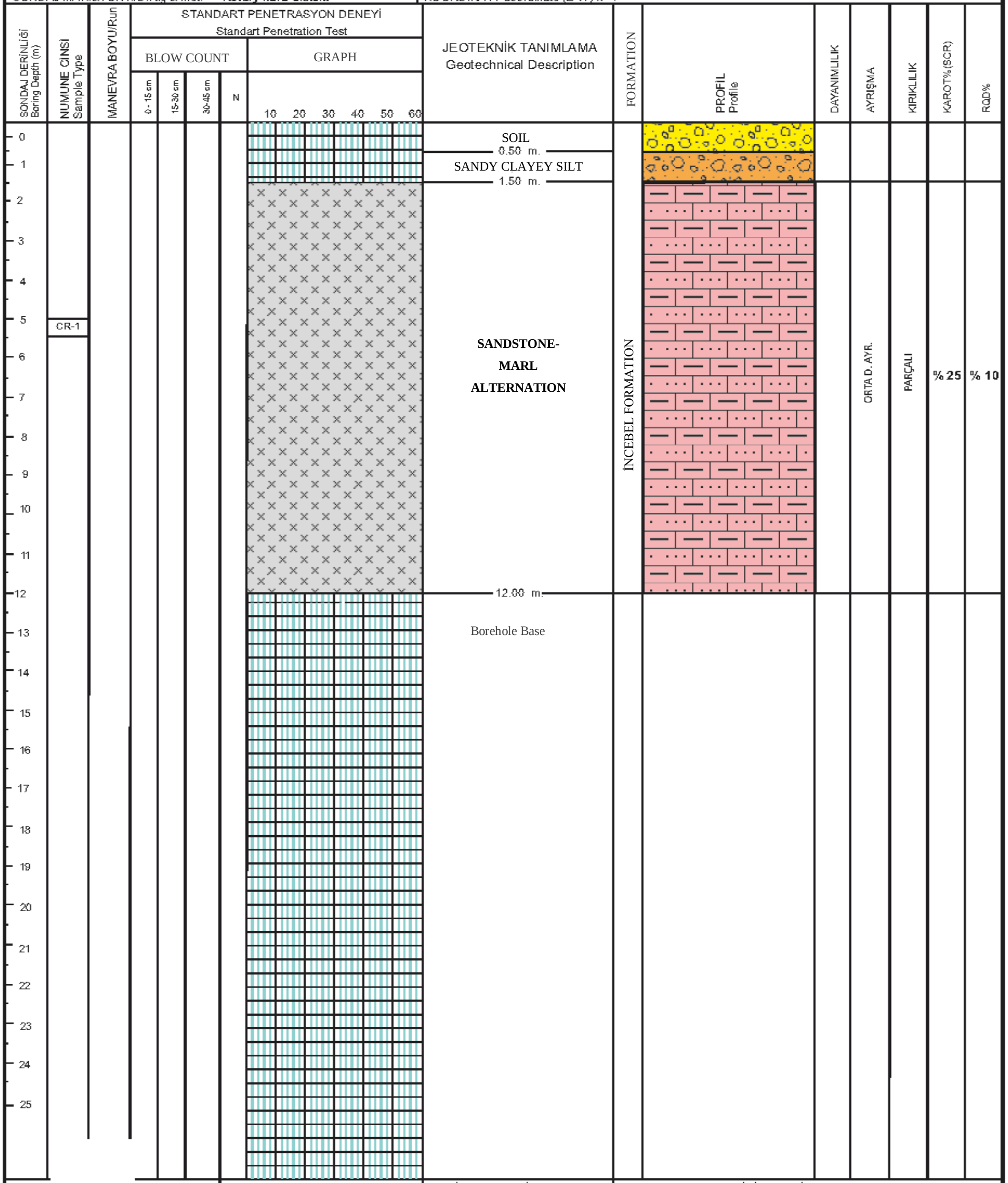

DAYANIMLILIK / Strength		
I	DAYANIMLI	Strong
II	ORTA DAYANIMLI	M.Strong
III	ORTA ZAYIF	M.Weak
IV	ZAYIF	Weak
V	ÇOK ZAYIF	V.Weak

AYRIŞMA / Weathering		
I	TAZE	Fresh
II	AZ AYRIŞMIŞ	Slightly W.
III	ORTA D. AYR.	Mod. Weath.
IV	ÇOK AYR.	Slightly W.
V	TÜMÜYLE A.	Comp.Weat.

İNCE DANELİ / Fine Grained		
N : 0-2	ÇOK YUMUŞAK	V.Soft
N : 3-4	YUMUŞAK	Soft
N : 5-8	ORTA KATI	M.Stiff
N : 9-15	KATI	Stiff
N : 16-30	ÇOK KATI	V.Stiff
N : >30	SERT	Hard

İRİ DANELİ/Coarse Grained			
N :	0-4	**ÇOK GEVŞEK**	V.Loose
N :	5-10	GEVŞEK	Loose
N :	11-30	ORTA SIKI	M.Dense
N :	31-50	SIKI	Dense
N :	>50	ÇOK SIKI	V.Dense

KAYA KALİTESİ TANIMI - RQD		
% 0-25	ÇOK ZAYIF	V.Poor
% 25-50	ZAYIF	Poor
% 50-75	ORTA	Fair
% 75-90	İYİ	Good
% 90-100	ÇOK İYİ	Excellent

KIRIKLAR - 30 cm / Fractures		
1	SEYREK	Wide (W)
1-2	ORTA	Moderate (M)
2-1	SIK	Close (Cl)
10-20	ÇOK SIKI	Intense (I)
>20	PARÇALI	Crushed (Cr)

ORANLAR - Proportions

% 5	PEK AZ	Slightly
% 5-15	AZ	Little
% 15-35	ÇOK	Very
% 35	VE	And

%	5	PEK AZ	Slightly
%	5-20	AZ	Little
%	20-5	ÇOK	Very

SONDAJ MÜHENDİSİ	KAŞE - İMZA	TARİH
Özgül ÇAKIR **Jeoloji Mühendisi**		

ÖZGÜLMÜHENDİSLİK

SONDAJ LOGU / BORING LOG

BÖLGE District	No : KOCAELİ/BAŞİSKELE
SONDAJ Borehole	No : **SK- 12**
SONDÖR Driller	: **Yavuz TEZCAN**

PROJE ADI / Project Name	: Başiskele Kocaeli İmar Planına Esas Jeolojik-jeoteknik Raporu	DELİK ÇAPI / Hole Diameter	: **3.5"**
SONDAJ YERİ/ Boring Location	: **Başiskele**	YERALTI SUYU / Groundwater	:
KİLOMETRE / Chainage	:	MUH.BOR.DER. / Casing Depth	: **-**
SONDAJ DER. / Boring Depth	: **18.00 metre**	BAŞ.BİT.TAR. / Start Finish Date	: **26.10.2014 / 26.10.2014**
SONDAJ KOTU / Elevation	:	KOORDİNAT / Coordinate (N-S) y	:
SONDAJ MAK.&YÖNT./D.Rig & Met.	: **Rotary-kuru Sistem**	KOORDİNAT / Coordinate (E-W) x	:

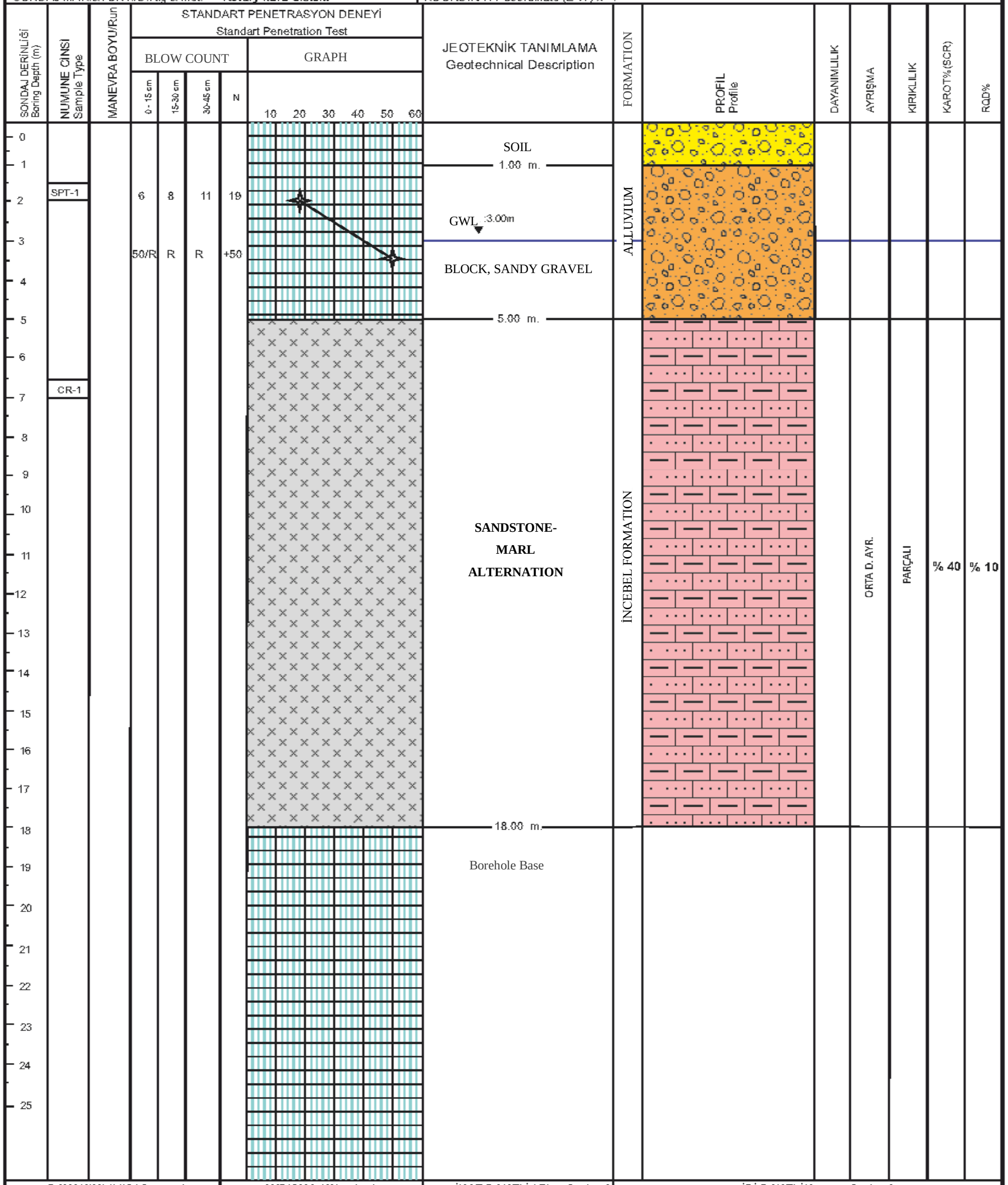

DAYANIMLILIK / Strength		
I	DAYANIMLI	Strong
II	ORTA DAYANIMLI	M.Strong
III	ORTA ZAYIF	M.Weak
IV	ZAYIF	Weak
V	ÇOK ZAYIF	V.Weak

AYRIŞMA / Weathering		
I	TAZE	Fresh
II	AZ AYRIŞMIŞ	Slightly W.
III	ORTA D. AYR.	Mod. Weath.
IV	ÇOK AYR.	Slightly W.
V	TÜMÜYLE A.	Comp.Weat.

İNCE DANELİ / Fine Grained		
N : 0-2	ÇOK YUMUŞAK	V.Soft
N : 3-4	YUMUŞAK	Soft
N : 5-8	ORTA KATI	M.Stiff
N : 9-15	KATI	Stiff
N : 16-30	ÇOK KATI	V.Stiff
N : >30	SERT	Hard

İRİ DANELİ/Coarse Grained			
N :	0-4	**ÇOK GEVŞEK**	V.Loose
N :	5-10	GEVŞEK	Loose
N :	11-30	ORTA SIKI	M.Dense
N :	31-50	SIKI	Dense
N :	>50	ÇOK SIKI	V.Dense

KAYA KALİTESİ TANIMI - RQD		
% 0-25	ÇOK ZAYIF	V.Poor
% 25-50	ZAYIF	Poor
% 50-75	ORTA	Fair
% 75-90	İYİ	Good
% 90-100	ÇOK İYİ	Excellent

KIRIKLAR - 30 cm / Fractures		
1	SEYREK	Wide (W)
1-2	ORTA	Moderate (M)
2-1	SIK	Close (Cl)
10-20	ÇOK SIKI	Intense (I)
>20	PARÇALI	Crushed (Cr)

ORANLAR - Proportions

% 5	PEK AZ	Slightly
% 5-15	AZ	Little
% 15-35	ÇOK	Very
% 35	VE	And

%	5	PEK AZ	Slightly
%	5-20	AZ	Little
%	20-5	ÇOK	Very

SONDAJ MÜHENDİSİ	KAŞE - İMZA	TARİH
Özgül ÇAKIR **Jeoloji Mühendisi**		

ÖZGÜLMÜHENDİSLİK

SONDAJ LOGU / BORING LOG

BÖLGE District	No :	KOCAELİ/BAŞİSKELE
SONDAJ Borehole	No :	**SK- 13**
SONDÖR Driller	:	**Yavuz TEZCAN**

PROJE ADI / Project Name	: Başiskele Kocaeli İmar Planına Esas Jeolojik-jeoteknik Raporu	DELİK ÇAPI / Hole Diameter	: **3.5"**
SONDAJ YERİ/ Boring Location	: **Başiskele**	YERALTI SUYU / Groundwater	:
KİLOMETRE / Chainage	:	MUH.BOR.DER. / Casing Depth	: **-**
SONDAJ DER. / Boring Depth	: **18.00 metre**	BAS.BİT.TAR. / Start Finish Date	: **26.10.2014 / 27.10.2014**
SONDAJ KOTU / Elevation	:	KOORDİNAT / Coordinate (N-S) y	:
SONDAJ MAK.&YÖNT./D.Rig & Met.	: **Rotary-kuru Sistem**	KOORDİNAT / Coordinate (E-W) x	:

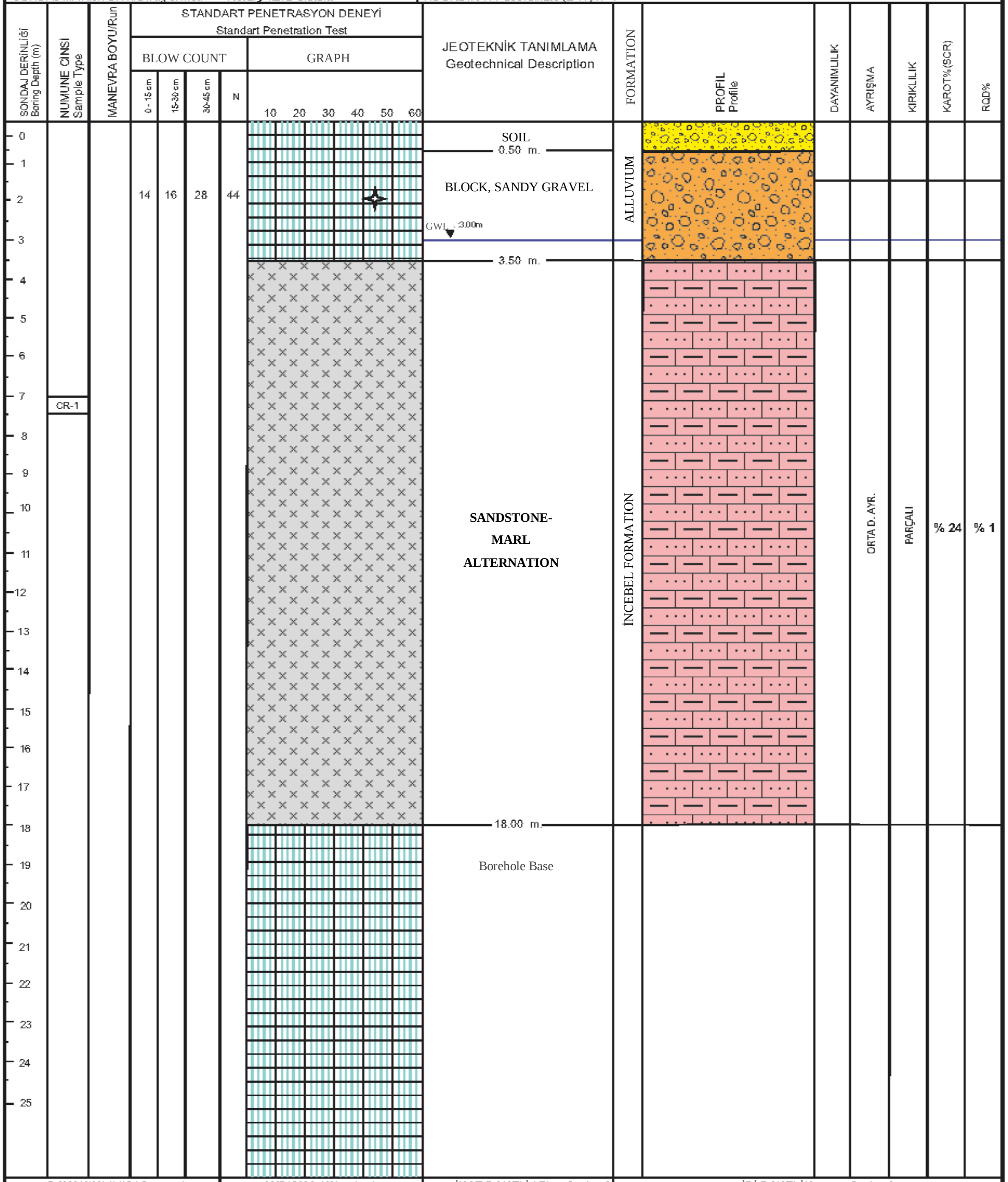

DAYANIMLILIK / Strength		
I	DAYANIMLI	Strong
II	ORTA DAYANIMLI	M.Strong
III	ORTA ZAYIF	M.Weak
IV	ZAYIF	Weak
V	ÇOK ZAYIF	V.Weak

AYRIŞMA / Weathering		
I	TAZE	Fresh
II	AZ AYRIŞMIŞ	Slightly W.
III	ORTA D. AYR.	Mod. Weath.
IV	ÇOK AYR.	Slightly W.
V	TÜMÜYLE A.	Comp.Weat.

İNCE DANELİ / Fine Grained		
N : 0-2	ÇOK YUMUŞAK	V.Soft
N : 3-4	YUMUŞAK	Soft
N : 5-8	ORTA KATI	M.Stiff
N : 9-15	KATI	Stiff
N : 16-30	ÇOK KATI	V.Stiff
N : >30	SERT	Hard

İRİ DANELİ/Coarse Grained			
N :	0-4	**ÇOK GEVŞEK**	V.Loose
N :	5-10	GEVŞEK	Loose
N :	11-30	ORTA SIKI	M.Dense
N :	31-50	SIKI	Dense
N :	>50	ÇOK SIKI	V.Dense

KAYA KALİTESİ TANIMI - RQD		
% 0-25	ÇOK ZAYIF	V.Poor
% 25-50	ZAYIF	Poor
% 50-75	ORTA	Fair
% 75-90	İYİ	Good
% 90-100	ÇOK İYİ	Excellent

KIRIKLAR - 30 cm / Fractures		
1	SEYREK	Wide (W)
1-2	ORTA	Moderate (M)
2-1	SIK	Close (Cl)
10-20	ÇOK SIKI	Intense (I)
>20	PARÇALI	Crushed (Cr)

ORANLAR - Proportions

% 5	PEK AZ	Slightly
% 5-15	AZ	Little
% 15-35	ÇOK	Very
% 35	VE	And

%	5	PEK AZ	Slightly
%	5-20	AZ	Little
%	20-5	ÇOK	Very

SONDAJ MÜHENDİSİ	KAŞE - İMZA	TARİH
Özgül ÇAKIR **Jeoloji Mühendisi**		

ÖZGÜLMÜHENDİSLİK

SONDAJ LOGU / BORING LOG

BÖLGE District	No : KOCAELİ/BAŞİSKELE
SONDAJ Borehole	No : **SK- 14**
SONDÖR Driller	: **Yavuz TEZCAN**

PROJE ADI / Project Name	: Başiskele Kocaeli İmar Planına Esas Jeolojik-jeoteknik Raporu	DELİK ÇAPI / Hole Diameter	: **3.5"**
SONDAJ YERİ/ Boring Location	: **Başiskele**	YERALTI SUYU / Groundwater	: '
KİLOMETRE / Chainage	:	MUH.BOR.DER. / Casing Depth	: **-**
SONDAJ DER. / Boring Depth	: **18.00 metre**	BAŞ.BİT.TAR. / Start Finish Date	: **27.10.2014 / 28.10.2014**
SONDAJ KOTU / Elevation	:	KOORDİNAT / Coordinate (N-S) y	:
SONDAJ MAK.&YÖNT./D.Rig & Met.	: **Rotary-kuru Sistem**	KOORDİNAT / Coordinate (E-W) x	:

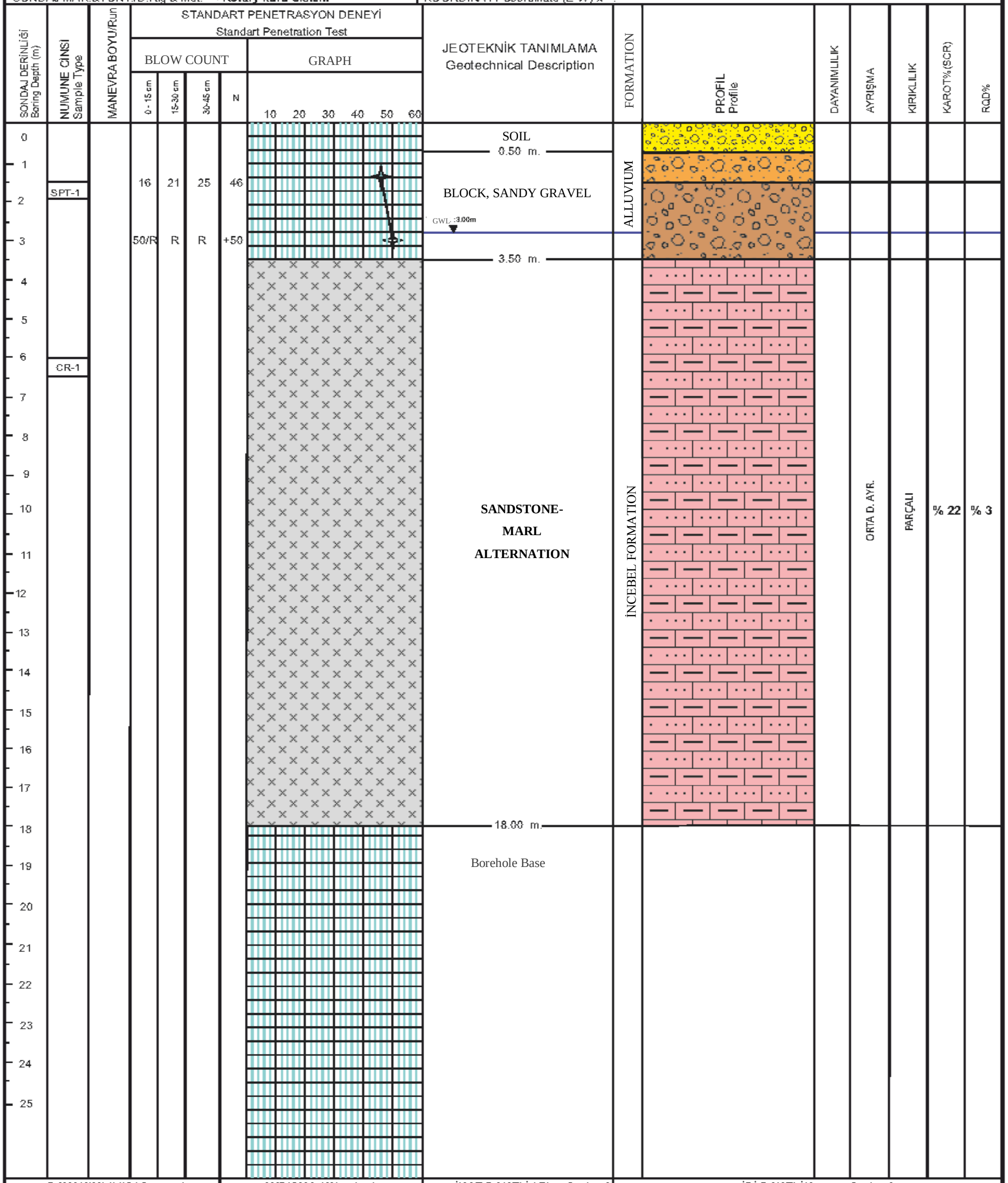

NUMUNE CİNSİ Sample Type	0 - 15 cm	15-30 cm	30-45 cm	N
SPT-1	16	21	25	46
	50/R	R	R	+50
CR-1				

SOIL

0.50 m.

BLOCK, SANDY GRAVEL

3.50 m.

SANDSTONE-
MARL
ALTERNATION

18.00 m.

Borehole Base

AYRIŞMA	KIRIKLILIK	KAROT%(SCR)	RQD%
ORTA D. AYR.	PARÇALI	% 22	% 3

DAYANIMLILIK / Strength		
I	DAYANIMLI	Strong
II	ORTA DAYANIMLI	M.Strong
III	ORTA ZAYIF	M.Weak
IV	ZAYIF	Weak
V	ÇOK ZAYIF	V.Weak

AYRIŞMA / Weathering		
I	TAZE	Fresh
II	AZ AYRIŞMIŞ	Slightly W.
III	ORTA D. AYR.	Mod. Weath.
IV	ÇOK AYR.	Slightly W.
V	TÜMÜYLE A.	Comp.Weat.

İNCE DANELİ / Fine Grained		
N : 0-2	ÇOK YUMUŞAK	V.Soft
N : 3-4	YUMUŞAK	Soft
N : 5-8	ORTA KATI	M.Stiff
N : 9-15	KATI	Stiff
N : 16-30	ÇOK KATI	V.Stiff
N : >30	SERT	Hard

İRİ DANELİ/Coarse Grained			
N :	0-4	**ÇOK GEVŞEK**	V.Loose
N :	5-10	GEVŞEK	Loose
N :	11-30	ORTA SIKI	M.Dense
N :	31-50	SIKI	Dense
N :	>50	ÇOK SIKI	V.Dense

KAYA KALİTESİ TANIMI - RQD		
% 0-25	ÇOK ZAYIF	V.Poor
% 25-50	ZAYIF	Poor
% 50-75	ORTA	Fair
% 75-90	İYİ	Good
% 90-100	ÇOK İYİ	Excellent

KIRIKLAR - 30 cm / Fractures		
1	SEYREK	Wide (W)
1-2	ORTA	Moderate (M)
2-1	SIK	Close (Cl)
10-20	ÇOK SIKI	Intense (I)
>20	PARÇALI	Crushed (Cr)

ORANLAR - Proportions

% 5	PEK AZ	Slightly
% 5-15	AZ	Little
% 15-35	ÇOK	Very
% 35	VE	And

%	5	PEK AZ	Slightly
%	5-20	AZ	Little
%	20-5	ÇOK	Very

SONDAJ MÜHENDİSİ	KAŞE - İMZA	TARİH
Özgül ÇAKIR **Jeoloji Mühendisi**		

ÖZGÜLMÜHENDİSLİK

SONDAJ LOGU / BORING LOG

BÖLGE District	No : KOCAELİ/BAŞİSKELE
SONDAJ Borehole	No : **SK- 15**
SONDÖR Driller	: **Yavuz TEZCAN**

PROJE ADI / Project Name	: Başiskele Kocaeli İmar Planına Esas Jeolojik-jeoteknik Raporu	DELİK ÇAPI / Hole Diameter	: **3.5"**
SONDAJ YERİ/ Boring Location	: **Başiskele**	YERALTI SUYU / Groundwater	: [illegible]
KİLOMETRE / Chainage	:	MUH.BOR.DER. / Casing Depth	: **-**
SONDAJ DER. / Boring Depth	: **10.00 metre**	BAŞ.BİT.TAR. / Start Finish Date	: **28.10.2014 / 28.10.2014**
SONDAJ KOTU / Elevation	:	KOORDİNAT / Coordinate (N-S) y	:
SONDAJ MAK.&YÖNT./D.Rig & Met.	: **Rotary-kuru Sistem**	KOORDİNAT / Coordinate (E-W) x	:

SONDAJ DERİNLİĞİ Boring Depth (m)	NUMUNE CİNSİ Sample Type	MANEVRA BOYU/Run	STANDART PENETRASYON DENEYİ Standart Penetration Test					JEOTEKNİK TANIMLAMA Geotechnical Description	FORMATION	PROFİL Profile	DAYANIMLILIK	AYRIŞMA	KIRIKLILIK	KAROT%(SCR)	RQD%
			BLOW COUNT				GRAPH								
			0 - 15 cm	15-30 cm	30-45 cm	N	10 20 30 40 50 60								
0 – 0.50								ROAD EMBANKMENT							
0.50 m. – 4.00 m.								EMBANKMENT							
4.00 m. – 10.00 m.	CR-1							**SANDSTONE-MARL ALTERNATION**	İNCEBEL FORMATION			ORTA D. AYR.	PARÇALI	**% 15**	**% 2**
10.00 m.								Borehole Base							

Depth scale: 0, 1, 2, 3, 4, 5, 6, 7, 8, 9, 10, 11, 12, 13, 14, 15, 16, 17, 18, 19, 20, 21, 22, 23, 24, 25

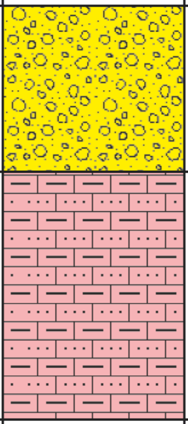

DAYANIMLILIK / Strength			AYRIŞMA / Weathering			İNCE DANELİ / Fine Grained			İRİ DANELİ/Coarse Grained			
I	DAYANIMLI	Strong	I	TAZE	Fresh	N : 0-2	ÇOK YUMUŞAK	V.Soft	N :	0-4	**ÇOK GEVŞEK**	V.Loose
II	ORTA DAYANIMLI	M.Strong	II	AZ AYRIŞMIŞ	Slightly W.	N : 3-4	YUMUŞAK	Soft	N :	5-10	GEVŞEK	Loose
III	ORTA ZAYIF	M.Weak	III	ORTA D. AYR.	Mod. Weath.	N : 5-8	ORTA KATI	M.Stiff	N :	11-30	ORTA SIKI	M.Dense
IV	ZAYIF	Weak	IV	ÇOK AYR.	Slightly W.	N : 9-15	KATI	Stiff	N :	31-50	SIKI	Dense
V	ÇOK ZAYIF	V.Weak	V	TÜMÜYLE A.	Comp.Weat.	N : 16-30	ÇOK KATI	V.Stiff	N :	>50	ÇOK SIKI	V.Dense
						N : >30	SERT	Hard				

KAYA KALİTESİ TANIMI - RQD			KIRIKLAR - 30 cm / Fractures			ORANLAR - Proportions						
% 0-25	ÇOK ZAYIF	V.Poor	1	SEYREK	Wide (W)	% 5	PEK AZ	Slightly	%	5	PEK AZ	Slightly
% 25-50	ZAYIF	Poor	1-2	ORTA	Moderate (M)	% 5-15	AZ	Little	%	5-20	AZ	Little
% 50-75	ORTA	Fair	2-1	SIK	Close (Cl)	% 15-35	ÇOK	Very	%	20-5	ÇOK	Very
% 75-90	İYİ	Good	10-20	ÇOK SIKI	Intense (I)	% 35	VE	And				
% 90-100	ÇOK İYİ	Excellent	>20	PARÇALI	Crushed (Cr)							

SONDAJ MÜHENDİSİ	KAŞE - İMZA	TARİH
Özgül ÇAKIR **Jeoloji Mühendisi**		

ÖZGÜLMÜHENDİSLİK

SONDAJ LOGU / BORING LOG

BÖLGE District	No : KOCAELİ/BAŞİSKELE
SONDAJ Borehole	No : **SK- 16**
SONDÖR Driller	: **Yavuz TEZCAN**

PROJE ADI / Project Name	: Başiskele Kocaeli İmar Planına Esas Jeolojik-jeoteknik Raporu	DELİK ÇAPI / Hole Diameter	: **3.5"**
SONDAJ YERİ/ Boring Location	: **Başiskele**	YERALTI SUYU / Groundwater	:
KİLOMETRE / Chainage	:	MUH.BOR.DER. / Casing Depth	: **-**
SONDAJ DER. / Boring Depth	: **12.00 metre**	BAŞ.BİT.TAR. / Start Finish Date	: **02.11.2014 / 02.11.2014**
SONDAJ KOTU / Elevation	:	KOORDİNAT / Coordinate (N-S) y	:
SONDAJ MAK.&YÖNT./D.Rig & Met.	: **Rotary-kuru Sistem**	KOORDİNAT / Coordinate (E-W) x	:

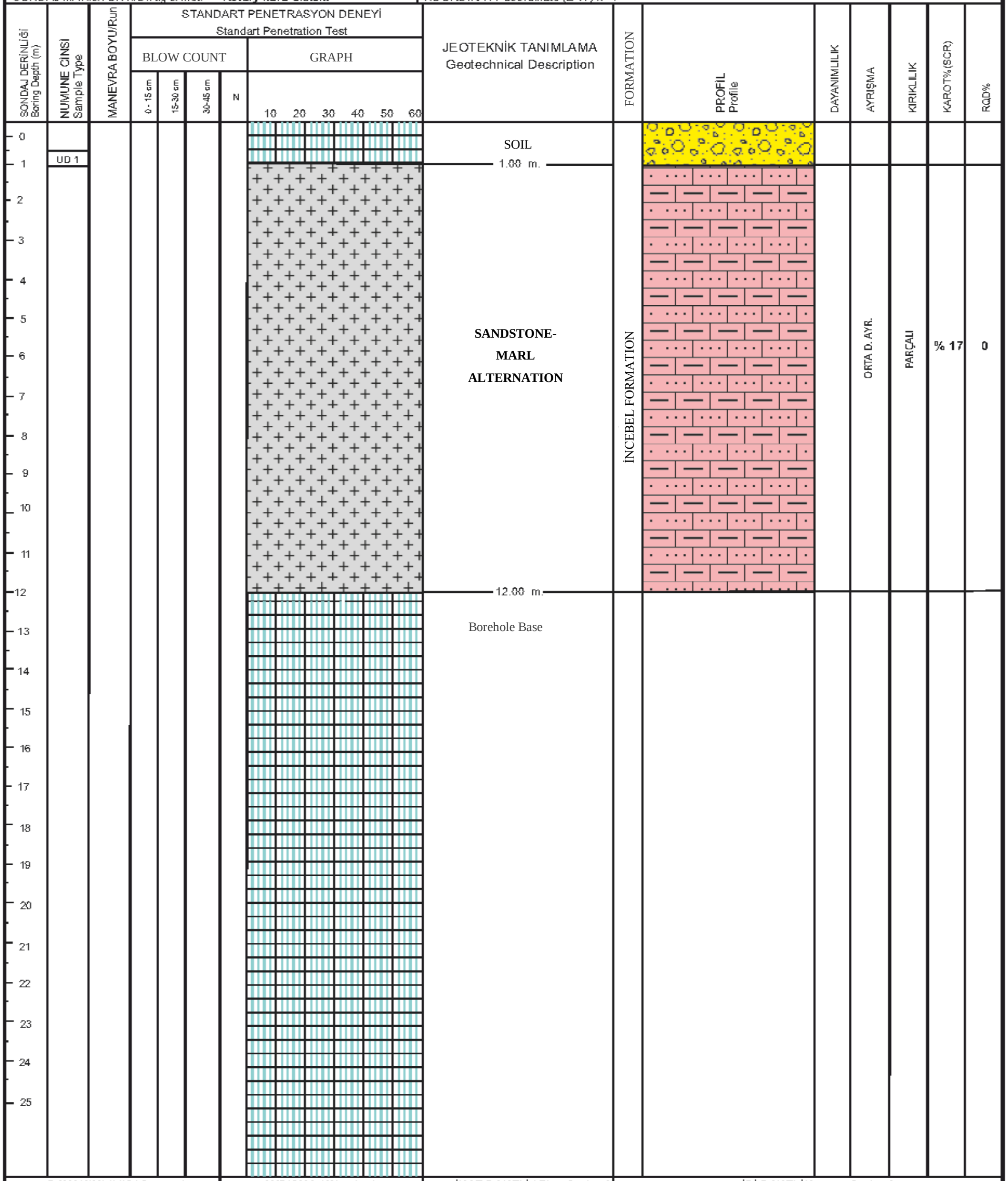

DAYANIMLILIK / Strength		
I	DAYANIMLI	Strong
II	ORTA DAYANIMLI	M.Strong
III	ORTA ZAYIF	M.Weak
IV	ZAYIF	Weak
V	ÇOK ZAYIF	V.Weak

AYRIŞMA / Weathering		
I	TAZE	Fresh
II	AZ AYRIŞMIŞ	Slightly W.
III	ORTA D. AYR.	Mod. Weath.
IV	ÇOK AYR.	Slightly W.
V	TÜMÜYLE A.	Comp.Weat.

İNCE DANELİ / Fine Grained		
N : 0-2	ÇOK YUMUŞAK	V.Soft
N : 3-4	YUMUŞAK	Soft
N : 5-8	ORTA KATI	M.Stiff
N : 9-15	KATI	Stiff
N : 16-30	ÇOK KATI	V.Stiff
N : >30	SERT	Hard

İRİ DANELİ/Coarse Grained			
N :	0-4	ÇOK GEVŞEK	V.Loose
N :	5-10	GEVŞEK	Loose
N :	11-30	ORTA SIKI	M.Dense
N :	31-50	SIKI	Dense
N :	>50	ÇOK SIKI	V.Dense

KAYA KALİTESİ TANIMI - RQD		
% 0-25	ÇOK ZAYIF	V.Poor
% 25-50	ZAYIF	Poor
% 50-75	ORTA	Fair
% 75-90	İYİ	Good
% 90-100	ÇOK İYİ	Excellent

KIRIKLAR - 30 cm / Fractures		
1	SEYREK	Wide (W)
1-2	ORTA	Moderate (M)
2-1	SIK	Close (Cl)
10-20	ÇOK SIKI	Intense (I)
>20	PARÇALI	Crushed (Cr)

ORANLAR - Proportions

% 5	PEK AZ	Slightly
% 5-15	AZ	Little
% 15-35	ÇOK	Very
% 35	VE	And

%	5	PEK AZ	Slightly
%	5-20	AZ	Little
%	20-5	ÇOK	Very

SONDAJ MÜHENDİSİ	KAŞE - İMZA	TARİH
Özgül ÇAKIR **Jeoloji Mühendisi**		

ÖZGÜLMÜHENDİSLİK

SONDAJ LOGU / BORING LOG

BÖLGE District	No :	KOCAELİ/BAŞİSKELE
SONDAJ Borehole	No :	**SK- 17**
SONDÖR Driller	:	**Yavuz TEZCAN**

PROJE ADI / Project Name	: Başiskele Kocaeli İmar Planına Esas Jeolojik-jeoteknik Raporu	DELİK ÇAPI / Hole Diameter	: 3.5"
SONDAJ YERİ/ Boring Location	: Başiskele	YERALTI SUYU / Groundwater	:
KİLOMETRE / Chainage	:	MUH.BOR.DER. / Casing Depth	: -
SONDAJ DER. / Boring Depth	: 21.00 metre	BAŞ.BİT.TAR. / Start Finish Date	: 03.11.2014 / 03.11.2014
SONDAJ KOTU / Elevation	:	KOORDİNAT / Coordinate (N-S) y	:
SONDAJ MAK.&YÖNT./D.Rig & Met.	: Rotary-kuru Sistem	KOORDİNAT / Coordinate (E-W) x	:

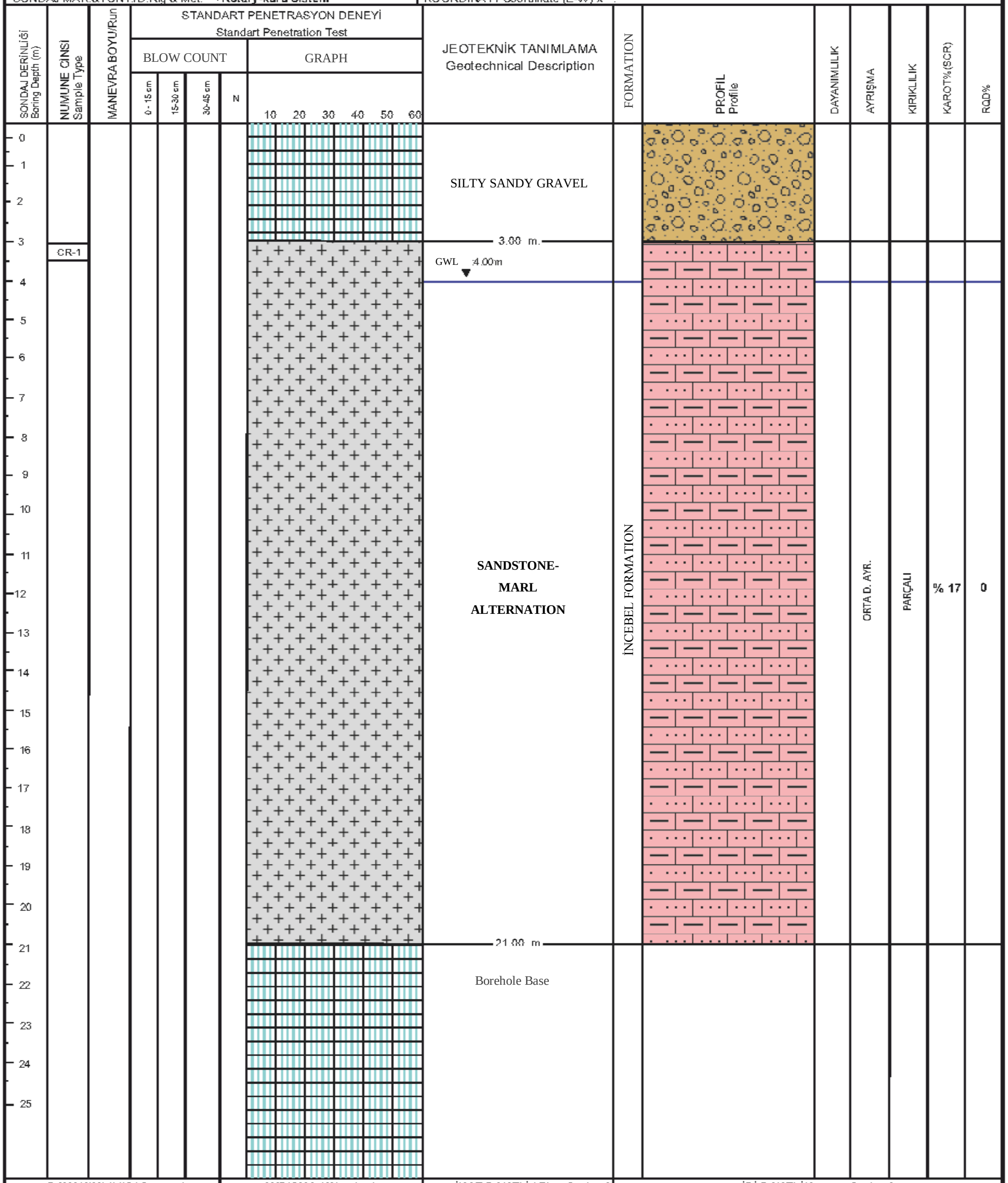

DAYANIMLILIK / Strength		
I	DAYANIMLI	Strong
II	ORTA DAYANIMLI	M.Strong
III	ORTA ZAYIF	M.Weak
IV	ZAYIF	Weak
V	ÇOK ZAYIF	V.Weak

AYRIŞMA / Weathering		
I	TAZE	Fresh
II	AZ AYRIŞMIŞ	Slightly W.
III	ORTA D. AYR.	Mod. Weath.
IV	ÇOK AYR.	Slightly W.
V	TÜMÜYLE A.	Comp.Weat.

İNCE DANELİ / Fine Grained		
N : 0-2	ÇOK YUMUŞAK	V.Soft
N : 3-4	YUMUŞAK	Soft
N : 5-8	ORTA KATI	M.Stiff
N : 9-15	KATI	Stiff
N : 16-30	ÇOK KATI	V.Stiff
N : >30	SERT	Hard

İRİ DANELİ/Coarse Grained			
N :	0-4	ÇOK GEVŞEK	V.Loose
N :	5-10	GEVŞEK	Loose
N :	11-30	ORTA SIKI	M.Dense
N :	31-50	SIKI	Dense
N :	>50	ÇOK SIKI	V.Dense

KAYA KALİTESİ TANIMI - RQD		
% 0-25	ÇOK ZAYIF	V.Poor
% 25-50	ZAYIF	Poor
% 50-75	ORTA	Fair
% 75-90	İYİ	Good
% 90-100	ÇOK İYİ	Excellent

KIRIKLAR - 30 cm / Fractures		
1	SEYREK	Wide (W)
1-2	ORTA	Moderate (M)
2-1	SIK	Close (Cl)
10-20	ÇOK SIKI	Intense (I)
>20	PARÇALI	Crushed (Cr)

ORANLAR - Proportions

% 5	PEK AZ	Slightly
% 5-15	AZ	Little
% 15-35	ÇOK	Very
% 35	VE	And

%	5	PEK AZ	Slightly
%	5-20	AZ	Little
%	20-5	ÇOK	Very

SONDAJ MÜHENDİSİ	KAŞE - İMZA	TARİH
Özgül ÇAKIR **Jeoloji Mühendisi**		

ÖZGÜLMÜHENDİSLİK	**SONDAJ LOGU / BORING LOG**	BÖLGE District	No : KOCAELİ/BAŞİSKELE
		SONDAJ Borehole	No : **SK- 18**
		SONDÖR Driller	: **Yavuz TEZCAN**

PROJE ADI / Project Name	: Başiskele Kocaeli İmar Planına Esas Jeolojik-jeoteknik Raporu	DELİK ÇAPI / Hole Diameter	: **3.5"**
SONDAJ YERİ/ Boring Location	: **Başiskele**	YERALTI SUYU / Groundwater	:
KİLOMETRE / Chainage	:	MUH.BOR.DER. / Casing Depth	: **-**
SONDAJ DER. / Boring Depth	: **21.00 metre**	BAŞ.BİT.TAR. / Start Finish Date	: **03.11.2014 / 04.11.2014**
SONDAJ KOTU / Elevation	:	KOORDİNAT / Coordinate (N-S) y	:
SONDAJ MAK.&YÖNT./D.Rig & Met.	: **Rotary-kuru Sistem**	KOORDİNAT / Coordinate (E-W) x	:

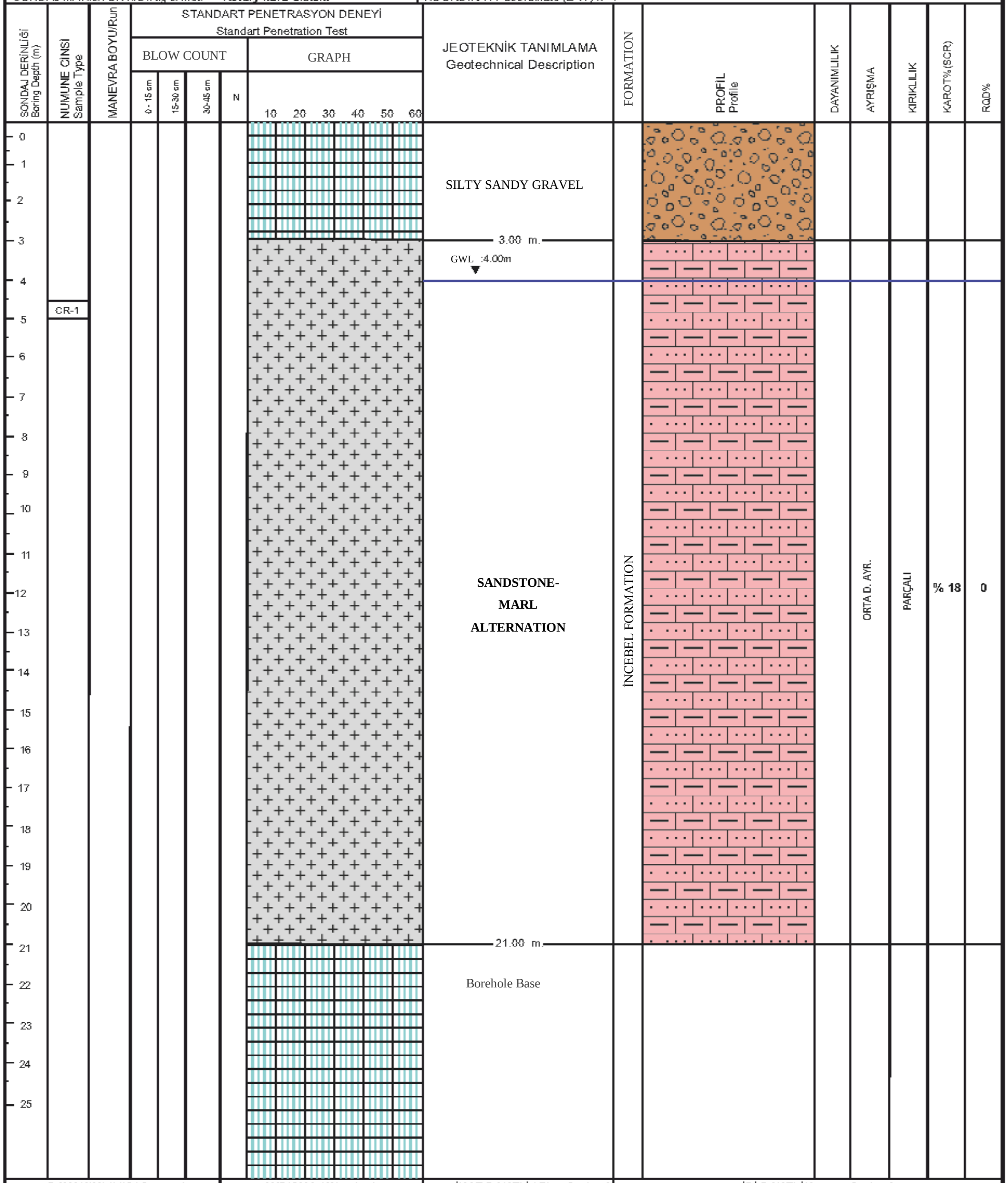

DAYANIMLILIK / Strength			AYRIŞMA / Weathering			İNCE DANELİ / Fine Grained		İRİ DANELİ/Coarse Grained			
I	DAYANIMLI	Strong	I	TAZE	Fresh	N : 0-2 ÇOK YUMUŞAK	V.Soft	N :	0-4	**ÇOK GEVŞEK**	V.Loose
II	ORTA DAYANIMLI	M.Strong	II	AZ AYRIŞMIŞ	Slightly W.	N : 3-4 YUMUŞAK	Soft	N :	5-10	GEVŞEK	Loose
III	ORTA ZAYIF	M.Weak	III	ORTA D. AYR.	Mod. Weath.	N : 5-8 ORTA KATI	M.Stiff	N :	11-30	ORTA SIKI	M.Dense
IV	ZAYIF	Weak	IV	ÇOK AYR.	Slightly W.	N : 9-15 KATI	Stiff	N :	31-50	SIKI	Dense
V	ÇOK ZAYIF	V.Weak	V	TÜMÜYLE A.	Comp.Weat.	N : 16-30 ÇOK KATI	V.Stiff	N :	>50	ÇOK SIKI	V.Dense
						N : >30 SERT	Hard				

KAYA KALİTESİ TANIMI - RQD			KIRIKLAR - 30 cm / Fractures			ORANLAR - Proportions					
% 0-25	ÇOK ZAYIF	V.Poor	1	SEYREK	Wide (W)	% 5	PEK AZ	Slightly	% 5	PEK AZ	Slightly
% 25-50	ZAYIF	Poor	1-2	ORTA	Moderate (M)	% 5-15	AZ	Little	% 5-20	AZ	Little
% 50-75	ORTA	Fair	2-1	SIK	Close (Cl)	% 15-35	ÇOK	Very	% 20-5	ÇOK	Very
% 75-90	İYİ	Good	10-20	ÇOK SIKI	Intense (I)	% 35	VE	And			
% 90-100	ÇOK İYİ	Excellent	>20	PARÇALI	Crushed (Cr)						

SONDAJ MÜHENDİSİ	KAŞE - İMZA	TARİH
Özgül ÇAKIR **Jeoloji Mühendisi**		

ÖZGÜLMÜHENDİSLİK	SONDAJ LOGU / BORING LOG	BÖLGE District	No : KOCAELİ/BAŞİSKELE
		SONDAJ Borehole	No : **SK- 19**
		SONDÖR Driller	: **Yavuz TEZCAN**

PROJE ADI / Project Name	: Başiskele Kocaeli İmar Planına Esas Jeolojik-jeoteknik Raporu	DELİK ÇAPI / Hole Diameter	: 3.5"
SONDAJ YERİ/ Boring Location	: **Başiskele**	YERALTI SUYU / Groundwater	:
KİLOMETRE / Chainage	:	MUH.BOR.DER. / Casing Depth	: -
SONDAJ DER. / Boring Depth	: **10.00 metre**	BAŞ.BİT.TAR. / Start Finish Date	: **04.11.2014 / 04.11.2014**
SONDAJ KOTU / Elevation	:	KOORDİNAT / Coordinate (N-S) y	:
SONDAJ MAK.&YÖNT./D.Rig & Met.	: **Rotary-kuru Sistem**	KOORDİNAT / Coordinate (E-W) x	:

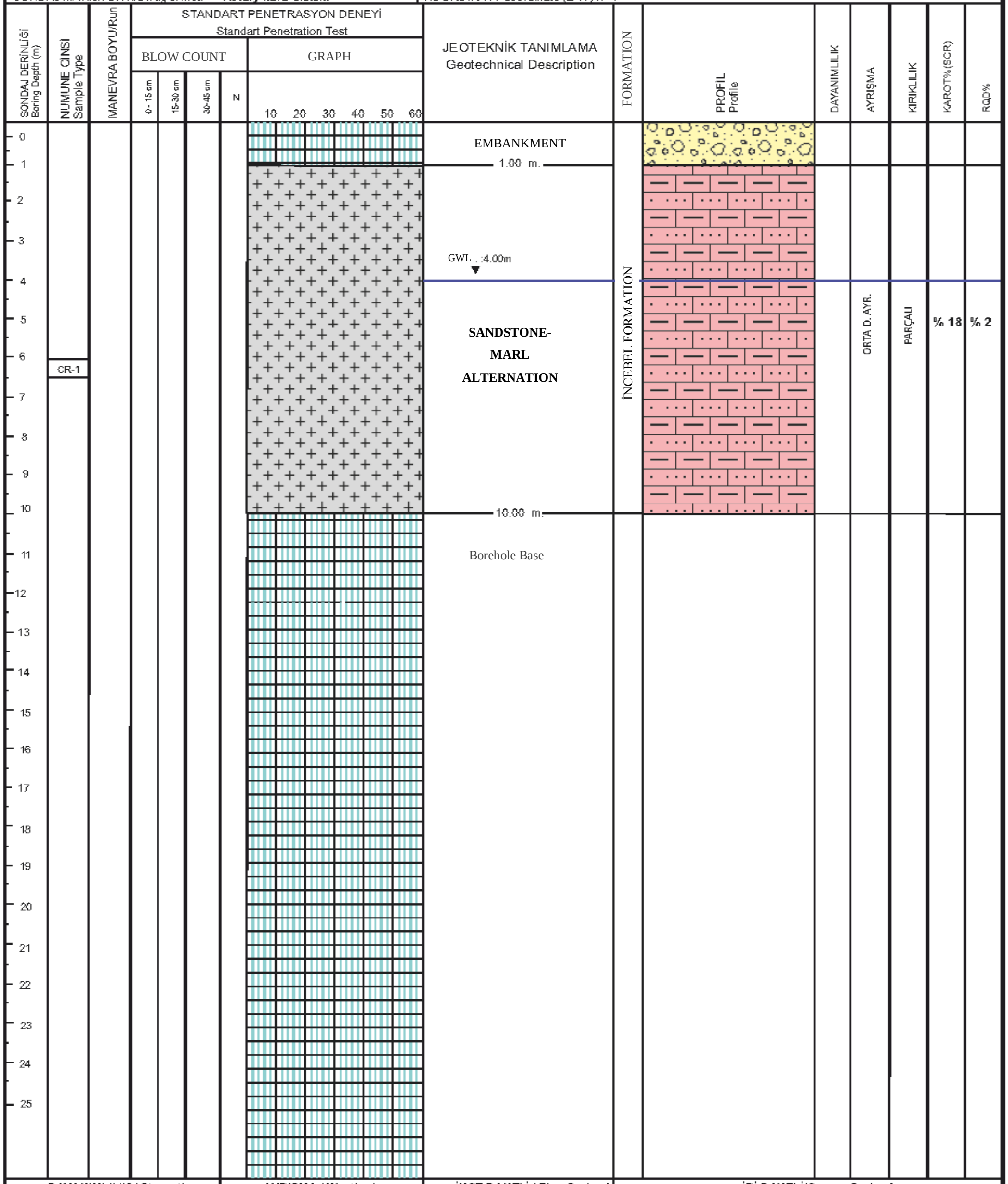

SONDAJ DERİNLİĞİ Boring Depth (m)	NUMUNE CİNSİ Sample Type	MANEVRA BOYU/Run	JEOTEKNİK TANIMLAMA Geotechnical Description	FORMATION	DAYANIMLILIK	AYRIŞMA	KIRIKLILIK	KAROT%(SCR)	RQD%
0 - 1.00 m.			EMBANKMENT						
1.00 - 10.00 m	CR-1		GWL :4.00m SANDSTONE-MARL ALTERNATION	INCEBEL FORMATION		ORTA D. AYR.	PARÇALI	% 18	% 2
10.00 m			Borehole Base						

DAYANIMLILIK / Strength		
I	DAYANIMLI	Strong
II	ORTA DAYANIMLI	M.Strong
III	ORTA ZAYIF	M.Weak
IV	ZAYIF	Weak
V	ÇOK ZAYIF	V.Weak

AYRIŞMA / Weathering		
I	TAZE	Fresh
II	AZ AYRIŞMIŞ	Slightly W.
III	ORTA D. AYR.	Mod. Weath.
IV	ÇOK AYR.	Slightly W.
V	TÜMÜYLE A.	Comp.Weat.

İNCE DANELİ / Fine Grained			
N :	0-2	ÇOK YUMUŞAK	V.Soft
N :	3-4	YUMUŞAK	Soft
N :	5-8	ORTA KATI	M.Stiff
N :	9-15	KATI	Stiff
N :	16-30	ÇOK KATI	V.Stiff
N :	>30	SERT	Hard

İRİ DANELİ/Coarse Grained			
N :	0-4	**ÇOK GEVŞEK**	V.Loose
N :	5-10	GEVŞEK	Loose
N :	11-30	ORTA SIKI	M.Dense
N :	31-50	SIKI	Dense
N :	>50	ÇOK SIKI	V.Dense

KAYA KALİTESİ TANIMI - RQD		
% 0-25	ÇOK ZAYIF	V.Poor
% 25-50	ZAYIF	Poor
% 50-75	ORTA	Fair
% 75-90	İYİ	Good
% 90-100	ÇOK İYİ	Excellent

KIRIKLAR - 30 cm / Fractures		
1	SEYREK	Wide (W)
1-2	ORTA	Moderate (M)
2-1	SIK	Close (Cl)
10-20	ÇOK SIKI	Intense (I)
>20	PARÇALI	Crushed (Cr)

ORANLAR - Proportions

% 5	PEK AZ	Slightly
% 5-15	AZ	Little
% 15-35	ÇOK	Very
% 35	VE	And

%	5	PEK AZ	Slightly
%	5-20	AZ	Little
%	20-5	ÇOK	Very

SONDAJ MÜHENDİSİ	KAŞE - İMZA	TARİH
Özgül ÇAKIR **Jeoloji Mühendisi**		

ÖZGÜLMÜHENDİSLİK	**SONDAJ LOGU / BORING LOG**	BÖLGE District	No : KOCAELİ/BAŞİSKELE
		SONDAJ Borehole	No : **SK- 21**
		SONDÖR Driller	: **Yavuz TEZCAN**

PROJE ADI / Project Name	: Başiskele Kocaeli İmar Planına Esas Jeolojik-jeoteknik Raporu	DELİK ÇAPI / Hole Diameter	: **3.5"**
SONDAJ YERİ/ Boring Location	: **Başiskele**	YERALTI SUYU / Groundwater	:
KİLOMETRE / Chainage	:	MUH.BOR.DER. / Casing Depth	: **-**
SONDAJ DER. / Boring Depth	: **13.00 metre**	BAŞ.BİT.TAR. / Start Finish Date	: **05.11.2014 / 05.11.2014**
SONDAJ KOTU / Elevation	:	KOORDİNAT / Coordinate (N-S) y	:
SONDAJ MAK.&YÖNT./D.Rig & Met.	: **Rotary-kuru Sistem**	KOORDİNAT / Coordinate (E-W) x	:

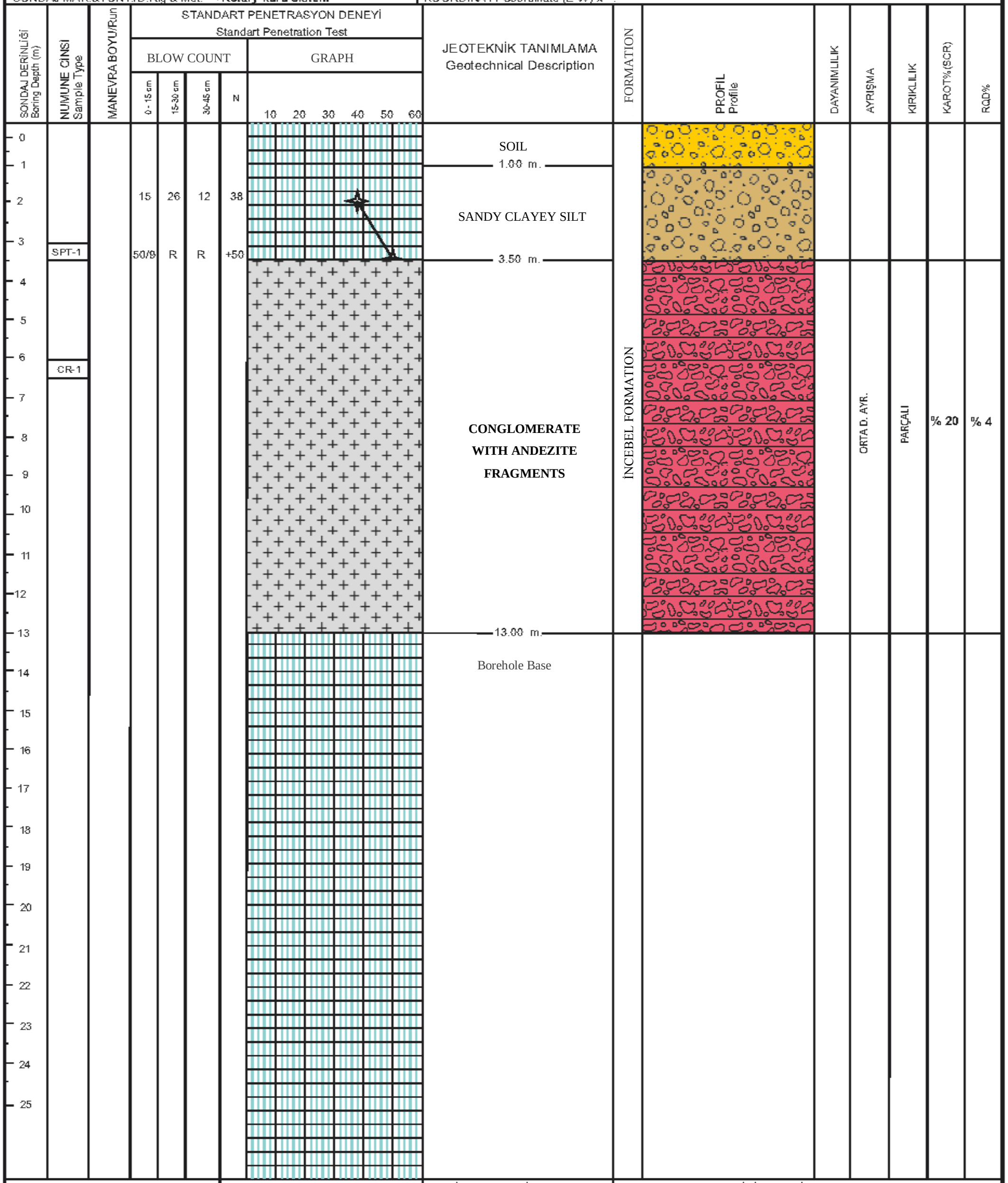

DAYANIMLILIK / Strength		
I	DAYANIMLI	Strong
II	ORTA DAYANIMLI	M.Strong
III	ORTA ZAYIF	M.Weak
IV	ZAYIF	Weak
V	ÇOK ZAYIF	V.Weak

AYRIŞMA / Weathering		
I	TAZE	Fresh
II	AZ AYRIŞMIŞ	Slightly W.
III	ORTA D. AYR.	Mod. Weath.
IV	ÇOK AYR.	Slightly W.
V	TÜMÜYLE A.	Comp.Weat.

İNCE DANELİ / Fine Grained		
N : 0-2	ÇOK YUMUŞAK	V.Soft
N : 3-4	YUMUŞAK	Soft
N : 5-8	ORTA KATI	M.Stiff
N : 9-15	KATI	Stiff
N : 16-30	ÇOK KATI	V.Stiff
N : >30	SERT	Hard

İRİ DANELİ/Coarse Grained			
N :	0-4	**ÇOK GEVŞEK**	V.Loose
N :	5-10	GEVŞEK	Loose
N :	11-30	ORTA SIKI	M.Dense
N :	31-50	SIKI	Dense
N :	>50	ÇOK SIKI	V.Dense

KAYA KALİTESİ TANIMI - RQD		
% 0-25	ÇOK ZAYIF	V.Poor
% 25-50	ZAYIF	Poor
% 50-75	ORTA	Fair
% 75-90	İYİ	Good
% 90-100	ÇOK İYİ	Excellent

KIRIKLAR - 30 cm / Fractures		
1	SEYREK	Wide (W)
1-2	ORTA	Moderate (M)
2-1	SIK	Close (Cl)
10-20	ÇOK SIKI	Intense (I)
>20	PARÇALI	Crushed (Cr)

ORANLAR - Proportions						
% 5	PEK AZ	Slightly	%	5	PEK AZ	Slightly
% 5-15	AZ	Little	%	5-20	AZ	Little
% 15-35	ÇOK	Very	%	20-5	ÇOK	Very
% 35	VE	And				

SONDAJ MÜHENDİSİ	KAŞE - İMZA	TARİH
Özgül ÇAKIR **Jeoloji Mühendisi**		

ÖZGÜLMÜHENDİSLİK

SONDAJ LOGU / BORING LOG

BÖLGE District	No : KOCAELİ/BAŞİSKELE
SONDAJ Borehole	No : **SK-22**
SONDÖR Driller	: **Yavuz TEZCAN**

PROJE ADI / Project Name	: Başiskele Kocaeli İmar Planına Esas Jeolojik-jeoteknik Raporu	DELİK ÇAPI / Hole Diameter	: **3.5"**
SONDAJ YERİ/ Boring Location	: **Başiskele**	YERALTI SUYU / Groundwater	:
KİLOMETRE / Chainage	:	MUH.BOR.DER. / Casing Depth	: **-**
SONDAJ DER. / Boring Depth	:**12.00 metre**	BAŞ.BİT.TAR. / Start Finish Date	: **06.11.2014 / 06.11.2014**
SONDAJ KOTU / Elevation	:	KOORDİNAT / Coordinate (N-S) y	:
SONDAJ MAK.&YÖNT./D.Rig & Met.	: **Rotary-kuru Sistem**	KOORDİNAT / Coordinate (E-W) x	:

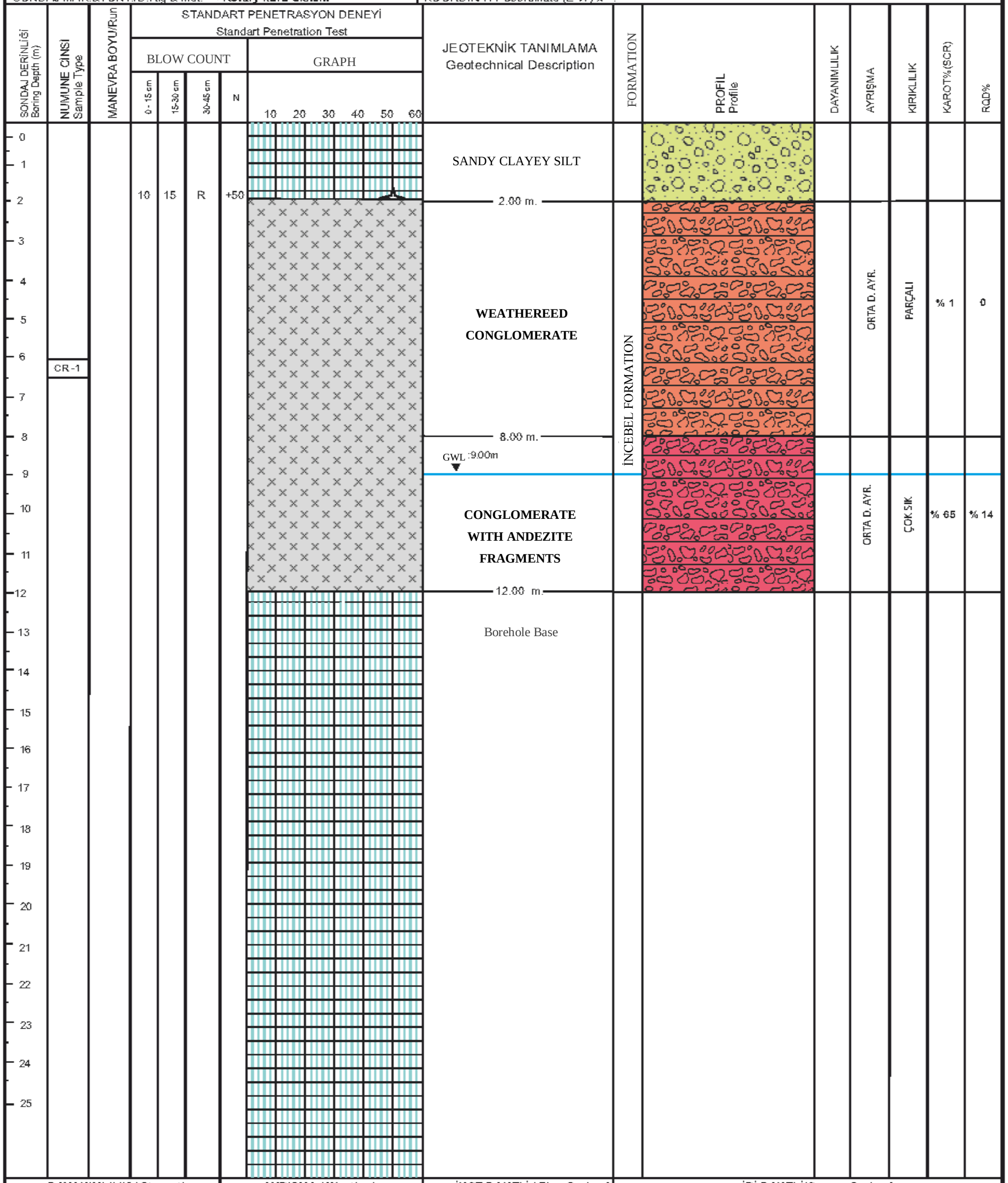

DAYANIMLILIK / Strength		
I	DAYANIMLI	Strong
II	ORTA DAYANIMLI	M.Strong
III	ORTA ZAYIF	M.Weak
IV	ZAYIF	Weak
V	ÇOK ZAYIF	V.Weak

AYRIŞMA / Weathering		
I	TAZE	Fresh
II	AZ AYRIŞMIŞ	Slightly W.
III	ORTA D. AYR.	Mod. Weath.
IV	ÇOK AYR.	Slightly W.
V	TÜMÜYLE A.	Comp.Weat.

İNCE DANELİ / Fine Grained		
N : 0-2	ÇOK YUMUŞAK	V.Soft
N : 3-4	YUMUŞAK	Soft
N : 5-8	ORTA KATI	M.Stiff
N : 9-15	KATI	Stiff
N : 16-30	ÇOK KATI	V.Stiff
N : >30	SERT	Hard

İRİ DANELİ/Coarse Grained			
N :	0-4	**ÇOK GEVŞEK**	V.Loose
N :	5-10	GEVŞEK	Loose
N :	11-30	ORTA SIKI	M.Dense
N :	31-50	SIKI	Dense
N :	>50	ÇOK SIKI	V.Dense

KAYA KALİTESİ TANIMI - RQD		
% 0-25	ÇOK ZAYIF	V.Poor
% 25-50	ZAYIF	Poor
% 50-75	ORTA	Fair
% 75-90	İYİ	Good
% 90-100	ÇOK İYİ	Excellent

KIRIKLAR - 30 cm / Fractures		
1	SEYREK	Wide (W)
1-2	ORTA	Moderate (M)
2-1	SIK	Close (Cl)
10-20	ÇOK SIKI	Intense (I)
>20	PARÇALI	Crushed (Cr)

ORANLAR - Proportions

% 5	PEK AZ	Slightly
% 5-15	AZ	Little
% 15-35	ÇOK	Very
% 35	VE	And

%	5	PEK AZ	Slightly
%	5-20	AZ	Little
%	20-5	ÇOK	Very

SONDAJ MÜHENDİSİ	KAŞE - İMZA	TARİH
Özgül ÇAKIR **Jeoloji Mühendisi**		

APPENDIX C

EARTHQUAKE CATALOGUE OF STUDY AREA AND ITS SURROUNDINGS FOR 2010

Table C 1: Earthquakes happened in 2010 with a moment magnitude equal and greater than 3.0

Date	Origin Time	Lat.	Long	Depth (km)	xM	MD	ML	Type	Location
26.01.2011	16:58:16.85	39.134	28.9993	5	3	3	0	Ke	HACIAHMETOGLU-SIMAV (KUTAHYA) [South West 1.3 km]
23.01.2011	22:01:11.13	40.4732	30.1672	5	3.1	3.1	0	Ke	CARDAK-PAMUKOVA (SAKARYA) [East 0.8 km]
20.01.2011	02:09:37.04	40.7042	29.7628	11.7	4.1	0	4.1	Ke	ORCUN-GOLCUK (KOCAELI) [West 2.7 km]
15.01.2011	16:00:22.25	40.7992	31.3677	3.3	3.2	3.2	0	Ke	DARIYERIHASANBEY-KAYNASLI (DUZCE) [North East 3.4 km]
12.01.2011	10:31:34.36	40.1412	31.7385	5	3.3	3.3	0	Ke	CANTIRLI-BEYPAZARI (ANKARA) [West 4.3 km]
16.12.2010	01:07:55.53	40.7258	29.8975	5.3	3	3	0	Ke	KOCAELI [South West 4.1 km]
12.12.2010	12:20:38.39	39.8082	30.5	5	3.1	3.1	0	Ke	TEPEBASI (ESKISEHIR) [North East 2.7 km]
11.12.2010	20:16:20.89	39.125	29.0658	5.4	3	3	0	Ke	SOGUT-SIMAV (KUTAHYA) [West 1.3 km]
08.12.2010	20:04:00.55	39.1167	29.1095	5.4	3.2	3.2	0	Ke	SENKOY-SIMAV (KUTAHYA) [North West 1.9 km]
02.12.2010	23:01:46.29	40.0853	31.6512	9.3	3	3	0	Ke	CAYIRHAN-NALLIHAN (ANKARA) [South West 2.7 km]
23.11.2010	22:16:51.14	39.1258	29.0437	5.4	3	3	0	Ke	KAPIKAYA-SIMAV (KUTAHYA) [South East 0.8 km]
20.11.2010	17:23:03.40	40.1038	31.6792	5	3	3	0	Ke	CAYIRHAN-NALLIHAN (ANKARA) [North 0.8 km]
19.11.2010	11:33:54.54	40.9503	29.2258	7.8	3	3	3	Ke	SULTANBEYLI (ISTANBUL) [South West 3.6 km]
12.11.2010	04:00:30.18	40.7258	28.9893	8.5	3	3	0	Ke	CINARCIK ACIKLARI-YALOVA (MARMARA DENIZI)
11.11.2010	23:03:26.58	40.0907	31.5948	8.7	3	3	0	Ke	DAVUTOGLAN-NALLIHAN (ANKARA) [South West 4.0 km]
31.10.2010	03:44:37.62	40.3798	30.0182	3.6	3.1	3.1	0	Ke	SELCIK-OSMANELI (BILECIK) [East 1.2 km]
26.10.2010	22:09:40.55	40.8023	27.6808	10.2	3.5	3.2	3.5	Ke	MARMARA DENIZI

25.10.2010	23:20:02.85	40.6955	30.5625	5	3.2	3.2	0	Ke	BUGDAYLI-AKYAZI (SAKARYA) [North East 2.0 km]
22.10.2010	03:15:26.44	39.1508	29.3088	5	3.2	0	3.2	Ke	ORENKOY-HISARCIK (KUTAHYA) [South East 1.3 km]
18.10.2010	06:07:15.65	39.5467	29.0985	5.2	3	3	0	Ke	DUMREKHUSEYINPASA-TAVSANLI (KワTAHYA) [South West 2.7 km]
16.10.2010	21:02:11.11	40.8233	31.324	5	3.1	0	3.1	Ke	DARIYERIYORUKLER-KAYNASLI (DUZCE) [North East 4.2 km]
14.10.2010	03:25:48.32	39.1312	29.056	5.4	3	3	0	Ke	KAPIKAYA-SIMAV (KUTAHYA) [East 1.4 km]
13.10.2010	11:31:30.40	40.7293	30.5827	6.2	3	3	0	Ke	BEDILTAHIRBEY-AKYAZI (SAKARYA) [South East 2.6 km]
03.10.2010	17:49:03.05	40.8402	28.1248	11.8	4.3	0	4.3	Ke	MARMARA DENIZI
29.09.2010	20:00:28.21	40.7338	30.1203	5	3	0	3	Ke	KETENCILER-KARTEPE (KOCAELI) [South West 3.6 km]
21.09.2010	10:11:10.96	39.9052	29.2063	7.7	3	3	0	Ke	BIYIKLIALANI-KELES (BURSA) [South East 1.7 km]
19.09.2010	15:05:04.69	40.7503	29.1665	9.4	3.1	3.1	0	Ke	YALOVA ACIKLARI (MARMARA DENIZI)
18.09.2010	17:17:15.11	40.8302	27.9902	17.8	3.1	3.1	0	Ke	MARMARA EREGLISI ACIKLARI-TEKIRDAG (MARMARA DENIZI)
14.09.2010	14:13:47.24	39.1088	29.0395	5.4	3	3	0	Ke	GOKCELER-SIMAV (KUTAHYA) [North East 1.2 km]
14.09.2010	14:05:27.66	39.135	29.078	2.5	3.7	0	3.7	Ke	SOGUT-SIMAV (KUTAHYA) [North West 1.0 km]
08.09.2010	20:51:54.50	40.1995	29.282	5	3	3	0	Ke	CATALTEPE-KESTEL (BURSA) [East 2.0 km]
05.09.2010	00:44:17.95	40.4663	28.9428	5.1	3	3	0	Ke	KAPAKLI-ARMUTLU (YALOVA) [West 2.3 km]
28.08.2010	18:15:05.93	40.0787	31.698	5	3	3	0	Ke	CAYIRHAN-NALLIHAN (ANKARA) [South East 2.6 km]
28.08.2010	17:35:54.52	39.9188	29.1605	5.2	3	3	0	Ke	HARMANALANI-KELES (BURSA) [West 1.7 km]
28.08.2010	01:03:19.52	40.1947	31.8303	5	3.2	3.2	0	Ke	CAKILOBA-BEYPAZARI (ANKARA) [South West 1.4 km]
26.08.2010	16:44:42.88	39.9617	29.1662	5	3	3	0	Ke	DELICE-KELES (BURSA) [South West 0.9 km]
26.08.2010	08:20:41.71	40.7688	30.9837	3.9	3	3	0	Ke	TASLIK-GOLYAKA (DUZCE) [North 1.2 km]
17.08.2010	00:27:14.50	40.8577	31.6353	5	3.1	3.1	0	Ke	CUKUROREN- (BOLU) [North 5.2 km]
16.08.2010	03:09:01.43	40.841	31.5838	5	3.9	0	3.9	Ke	KOZLU- (BOLU) [North West 4.8 km]
06.08.2010	02:43:14.56	40.6073	29.2097	3.7	3	3	0	Ke	YENIMAHALLE-TERMAL (YALOVA) [South East 0.3 km]
30.07.2010	13:34:43.49	39.4448	31.3462	7.3	3.1	3.1	0	Ke	BAHCECIK-SIVRIHISAR (ESKISEHIR) [North 1.6 km]
18.07.2010	02:54:58.27	38.9532	29.971	4.6	3	3	0	Ke	YESILYURT-ALTINTAS (KUTAHYA) [South East 2.2

									km]
17.07.2010	19:39:50.44	40.7115	29.1997	5	3.1	3.1	0	Ke	YALOVA ACIKLARI (MARMARA DENIZI)
09.07.2010	12:09:45.85	38.9662	29.9695	2	3	3	0	Ke	YESILYURT-ALTINTAS (KUTAHYA) [North East 2.1 km]
07.07.2010	10:24:49.31	40.8088	30.8817	9.2	3.3	0	3.3	Ke	YESILYAYLA-GUMUSOVA (DUZCE) [North East 1.6 km]
07.07.2010	04:02:07.35	39.1603	29.0348	5.2	3	3	0	Ke	KARACAOREN-SIMAV (KUTAHYA) [South East 1.1 km]
06.07.2010	16:01:33.27	40.425	28.428	2.3	3	3	0	Ke	BAYRAMDERE-KARACABEY (BURSA) [North East 5.6 km]
13.06.2010	02:13:25.17	39.1942	29.1212	5	3.1	3.1	0	Ke	TOKAT-HISARCIK (KUTAHYA) [South West 1.9 km]
11.06.2010	23:45:42.16	39.1155	29.1372	5	3	3	0	Ke	SENKOY-SIMAV (KUTAHYA) [North East 2.0 km]
09.06.2010	16:06:56.05	39.292	29.0838	5.4	3.3	0	3.3	Ke	KABAKLAR-EMET (KUTAHYA) [North West 2.5 km]
02.06.2010	19:09:32.85	39.4992	28.8588	6.9	3	0	3	Ke	MAHMUTCA-DURSUNBEY (BALIKESIR) [South West 0.2 km]
31.05.2010	16:08:20.25	39.0232	29.7352	5.3	3	3	0	Ke	CUKUROREN-GEDIZ (KUTAHYA) [North 3.1 km]
29.05.2010	22:36:04.04	40.946	31.7338	7.1	3	3	0	Ke	YAYLATEPE-YIGILCA (DUZCE) [South East 6.0 km]
29.05.2010	00:17:43.86	39.5007	28.8817	8.5	3.1	3.1	0	Ke	DEMIRCILER-DURSUNBEY (BALIKESIR) [North West 1.3 km]
27.05.2010	23:38:22.99	39.412	28.4905	5.4	3	3	0	Ke	YUKARIGOCEK-BIGADIC (BALIKESIR) [North East 3.2 km]
26.05.2010	08:07:32.11	39.2845	29.3003	5	3.1	3.1	0	Ke	KIRGIL-EMET (KUTAHYA) [North East 2.0 km]
25.05.2010	21:28:44.89	39.3158	29.3272	3.1	3.2	3.2	0	Ke	BAHATLAR-EMET (KUTAHYA) [South East 0.7 km]
21.05.2010	07:41:06.49	39.0953	29.0353	5.2	3.1	0	3.1	Ke	GOKCELER-SIMAV (KUTAHYA) [South East 0.5 km]
15.05.2010	14:08:22.17	41.1985	30.1332	5	4.2	0	4.2	Ke	KEFKEN-KANDIRA (KOCAELI) [North West 8.5 km]
11.05.2010	22:07:00.17	40.7035	29.2115	5	3.1	0	3.1	Ke	YALOVA ACIKLARI (MARMARA DENIZI)
07.05.2010	00:24:58.94	40.7042	29.2132	5.3	3.1	3.1	0	Ke	YALOVA ACIKLARI (MARMARA DENIZI)
04.05.2010	03:17:00.15	39.0835	29.0302	5.3	3	3	0	Ke	YESILKOY-SIMAV (KUTAHYA) [North East 1.7 km]
02.05.2010	18:37:36.87	39.5582	28.8472	5.3	3	3	0	Ke	AYVACIK-DURSUNBEY (BALIKESIR) [South East 2.7 km]
29.04.2010	09:14:13.03	39.4297	28.3015	10.1	3.3	3.3	0	Ke	HISARKOY-BIGADIC (BALIKESIR) [East 1.2 km]
26.04.2010	14:06:27.86	39.143	29.1108	5	3.1	3.1	0	Ke	SOGUT-SIMAV (KUTAHYA) [North East 3.1 km]

24.04.2010	15:29:13.61	40.7382	30.6393	4.4	3.2	0	3.2	Ke	DUZYAZI-AKYAZI (SAKARYA) [North West 1.5 km]
20.04.2010	23:26:06.51	40.934	31.5708	5.1	3.1	3.1	0	Ke	CUKUROREN-YIGILCA (DUZCE) [South East 3.7 km]
20.04.2010	05:00:18.79	39.0407	29.443	5	3.1	3.1	0	Ke	ALIAGA-GEDIZ (KUTAHYA) [West 2.3 km]
09.04.2010	11:27:10.85	40.4403	28.9353	5.4	3.3	0	3.3	Ke	KAPAKLI-ARMUTLU (YALOVA) [South West 3.9 km]
04.04.2010	03:54:05.24	39.4682	28.962	5	3	3	0	Ke	BEDIRLER-SIMAV (KUTAHYA) [South East 1.4 km]
04.04.2010	03:12:31.98	39.5447	28.8565	5	3	3	3	Ke	SARISIPAHILER-DURSUNBEY (BALIKESIR) [North East 2.7 km]
04.04.2010	03:04:51.01	39.5177	28.9113	5	3.1	3.1	0	Ke	YUNUSLAR-DURSUNBEY (BALIKESIR) [South West 0.6 km]
21.03.2010	07:11:38.50	39.239	29.2902	6.6	3	3	0	Ke	KIRGIL-EMET (KUTAHYA) [South 3.5 km]
21.03.2010	03:50:49.83	39.1178	29.0745	5	3	3	0	Ke	SOGUT-SIMAV (KUTAHYA) [South West 1.2 km]
18.03.2010	08:03:47.80	39.2785	29.1185	5	3	3	0	Ke	KABAKLAR-EMET (KUTAHYA) [East 0.9 km]
14.03.2010	19:55:55.95	39.3448	29.0872	5	3	3	0	Ke	SUDOSEGI-SIMAV (KUTAHYA) [South East 6.0 km]
08.03.2010	16:07:11.79	40.4482	29.1312	2.8	3.5	0	3.5	Ke	GEMLIK (BURSA) [North West 2.7 km]
06.03.2010	23:28:58.90	39.496	28.409	4.4	3.4	3.4	0	Ke	KURSU-BIGADIC (BALIKESIR) [North East 1.2 km]
05.03.2010	17:31:53.74	40.8603	27.9978	6.2	3.3	3.3	0	Ke	MARMARA EREGLISI ACIKLARI-TEKIRDAG (MARMARA DENIZI)
04.03.2010	19:08:09.73	39.5213	28.8222	8.4	3.2	3.2	0	Ke	POYRACIK-DURSUNBEY (BALIKESIR) [East 1.0 km]
04.03.2010	02:42:39.70	39.52	28.84	5	3.4	0	3.4	Ke	SARISIPAHILER-DURSUNBEY (BALIKESIR) [South West 0.4 km]
03.03.2010	22:42:57.19	39.5058	28.879	5.4	3.2	3.2	0	Ke	HINDIKLER-DURSUNBEY (BALIKESIR) [South 1.1 km]
03.03.2010	04:16:41.15	39.5238	28.8778	3.8	3.3	3.3	0	Ke	HINDIKLER-DURSUNBEY (BALIKESIR) [North 0.9 km]
03.03.2010	03:42:20.00	39.4968	28.8192	5.1	3.2	3.2	0	Ke	BOYALICA-DURSUNBEY (BALIKESIR) [South East 1.0 km]
02.03.2010	18:28:16.10	39.1003	29.0923	5	3.3	3.3	0	Ke	SENKOY-SIMAV (KUTAHYA) [West 2.5 km]
02.03.2010	15:43:24.65	40.6332	30.5465	11.8	3.1	3.1	0	Ke	MECIDIYE-KARAPURCEK (SAKARYA) [North East 0.9 km]
02.03.2010	05:08:43.10	39.0213	29.2348	5.4	3	3	0	Ke	SAPHANE (KUTAHYA) [South East 1.3 km]
02.03.2010	02:56:48.77	39.1175	29.1272	5.2	3	3	0	Ke	SENKOY-SIMAV (KUTAHYA) [North East 1.7 km]
02.03.2010	02:47:29.49	40.3945	30.2502	10.7	3	3	0	Ke	KARACAOREN-GEYVE (SAKARYA) [North East 1.3

									km]
02.03.2010	01:48:31.12	39.09	29.1758	5	3.1	3.1	0	Ke	BASKONAK-SIMAV (KUTAHYA) [South West 2.6 km]
02.03.2010	01:37:41.80	39.1185	29.1077	5.1	3.3	3.3	0	Ke	SENKOY-SIMAV (KUTAHYA) [North West 2.1 km]
02.03.2010	01:26:57.46	39.0875	29.171	5.4	3.1	3.1	0	Ke	BASKONAK-SIMAV (KUTAHYA) [South West 3.0 km]
02.03.2010	01:21:36.57	39.0967	29.1202	5.1	3.3	3.3	0	Ke	SENKOY-SIMAV (KUTAHYA) [South 0.7 km]
02.03.2010	00:59:43.08	39.1347	29.094	6.4	4.3	0	4.3	Ke	SOGUT-SIMAV (KUTAHYA) [North East 1.4 km]
02.03.2010	00:47:01.08	39.1037	29.0547	5	3.1	3.1	3.1	Ke	GOKCELER-SIMAV (KUTAHYA) [North East 2.0 km]
02.03.2010	00:36:10.90	39.11	29.073	2	3.3	3.3	0	Ke	SOGUT-SIMAV (KUTAHYA) [South West 2.0 km]
18.02.2010	17:48:09.06	39.032	29.621	4	3.1	3.1	0	Ke	GOYNUK-GEDIZ (KUTAHYA) [North West 2.6 km]
14.02.2010	20:25:04.77	39.737	30.5473	2.9	3	3	0	Ke	ODUNPAZARI (ESKISEHIR) [South East 3.8 km]
14.02.2010	18:44:57.61	40.8383	27.8238	4.9	3.1	3.1	0	Ke	MARMARA DENIZI
11.02.2010	10:21:01.58	39.7088	29.622	25.1	3	3	0	Ke	FINDICAK-DOMANIC (KUTAHYA) [North West 2.3 km]
10.02.2010	17:26:13.83	38.957	29.9792	5.4	3	3	0	Ke	ALLIOREN-DUMLUPINAR (KUTAHYA) [North West 1.9 km]
08.02.2010	02:46:05.96	40.4352	29.8735	5	3.2	3.2	0	Ke	KARATEKIN-IZNIK (BURSA) [South West 0.7 km]
07.02.2010	17:21:32.15	39.7695	30.587	5	3.7	0	3.7	Ke	SULTANDERE-ODUNPAZARI (ESKISEHIR) [North West 4.9 km]
04.02.2010	16:05:59.19	40.424	28.8528	6	3	3	0	Ke	GEMLIK KORFEZI (MARMARA DENIZI)
03.02.2010	21:57:55.00	40.4	28.85	9	3.5	0	3.5	Ke	KUMYAKA-MUDANYA (BURSA) [North East 2.6 km]
30.01.2010	12:28:10.40	39.18	28.9102	9.8	3	3	0	Ke	GUNEY-SIMAV (KUTAHYA) [South West 0.8 km]
29.01.2010	16:38:08.77	39.4968	28.902	5	3.1	3.1	0	Ke	DEMIRCILER-DURSUNBEY (BALIKESIR) [North East 1.1 km]
23.01.2010	07:15:04.04	39.9612	28.7815	4.2	3.2	3.2	0	Ke	OMERALTI-MUSTAFAKEMALPASA (BURSA) [South East 2.9 km]
20.01.2010	20:53:09.00	39.0765	29.1827	4.9	3.2	3.2	0	Ke	BASKONAK-SIMAV (KUTAHYA) [South West 3.0 km]
14.01.2010	04:11:40.05	40.765	31.636	5	3.2	3.2	0	Ke	YENIKOY- (BOLU) [South West 1.2 km]
13.01.2010	03:54:51.54	40.6378	28.769	10.6	3.4	0	3.4	Ke	ARMUTLU ACIKLARI-YALOVA (MARMARA DENIZI)
12.01.2010	22:46:11.19	40.6258	29.0125	6.7	3.2	3.2	0	Ke	SENKOY-CINARCIK (YALOVA) [South East 0.8 km]
12.01.2010	05:31:39.23	40.4797	28.149	7.6	3	3	0	Ke	BANDIRMA ACIKLARI-BALIKESIR (MARMARA DENIZI)

02.01.2010	04:14:34.66	40.8535	29.286	9	3	3	0	Ke	TUZLA (ISTANBUL) [North West 4.3 km]
01.01.2010	21:01:21.13	40.15	28.2928	4.7	3	3	0	Ke	YOLAGZI-KARACABEY (BURSA) [North West 1.9 km]

APPENDIX D

UNIFIED SOIL CLASSIFICATION SYSTEM

Table D 1: Unified Soil Classification System (based on Wagner, A.A. 1957) from Craig soil mechanics

Name			Group Symbols	Laboratory Criteria			
				Fines (%)	Grading	Plasticity	Notes
Coarse grained (more than 50% larger than 63 μm BS or No.200 US sieve size)	Gravels (more than 50% of coarse fraction of gravel size)	Well graded gravels, sandy gravels, with little or no fines	GW	0-5	$C_u>4$ $1<C_z<3$		
		Poorly graded gravels, sandy gravels, with little or no fines	GP	0-5	Not satisfying GW requirements		
		Silty gravels, silty sandy gravels	GM	>12		Below A-line or $I_p<4$	
		Clayey gravels, clayey sandy gravels	GC	>12		Below A-line or $I_p>7$	
	Sands (more than 50% of coarse fraction of sand size)	Well graded sands, gravelly sands, with little or no fines	SW	0-5	$C_u>6$ $1<C_z<3$		
		Poorly graded sands,	SP	0-5	Not satisfying SW		

		gravelly sands, with little or no fines			requirements		
		Silty sands	SM	>12		Below A-line or I_p<4	
		Clayey sands	SC	>12		Below A-line or I_p>7	
Fine grained (more than 50% smaller than 63 µm BS or No.200 US sieve size)	Silts and clays (liquid limit less than 50)	Inorganic silts, silty or clayey fine sands, with slight plasticity	ML	Use plasticity chart			
		Inorganic clays, silty clays, sandy clays of low plasticity	CL	Use plasticity chart			
		Organic silts and organic silty clays of low plasticity	OL	Use plasticity chart			
	Silts and clays (liquid limit greater than 50)	Inorganic silts of high plasticity	MH	Use plasticity chart			
		Inorganic clays of high plasticity	CH	Use plasticity chart			
		Organic clays of high plasticity	OH	Use plasticity chart			
Highly organic soils		Peat and other higgly organic soils	Pt				

APPENDIX E

DATASHEET OF THE CABLE USED IN FIELD APPLICATION

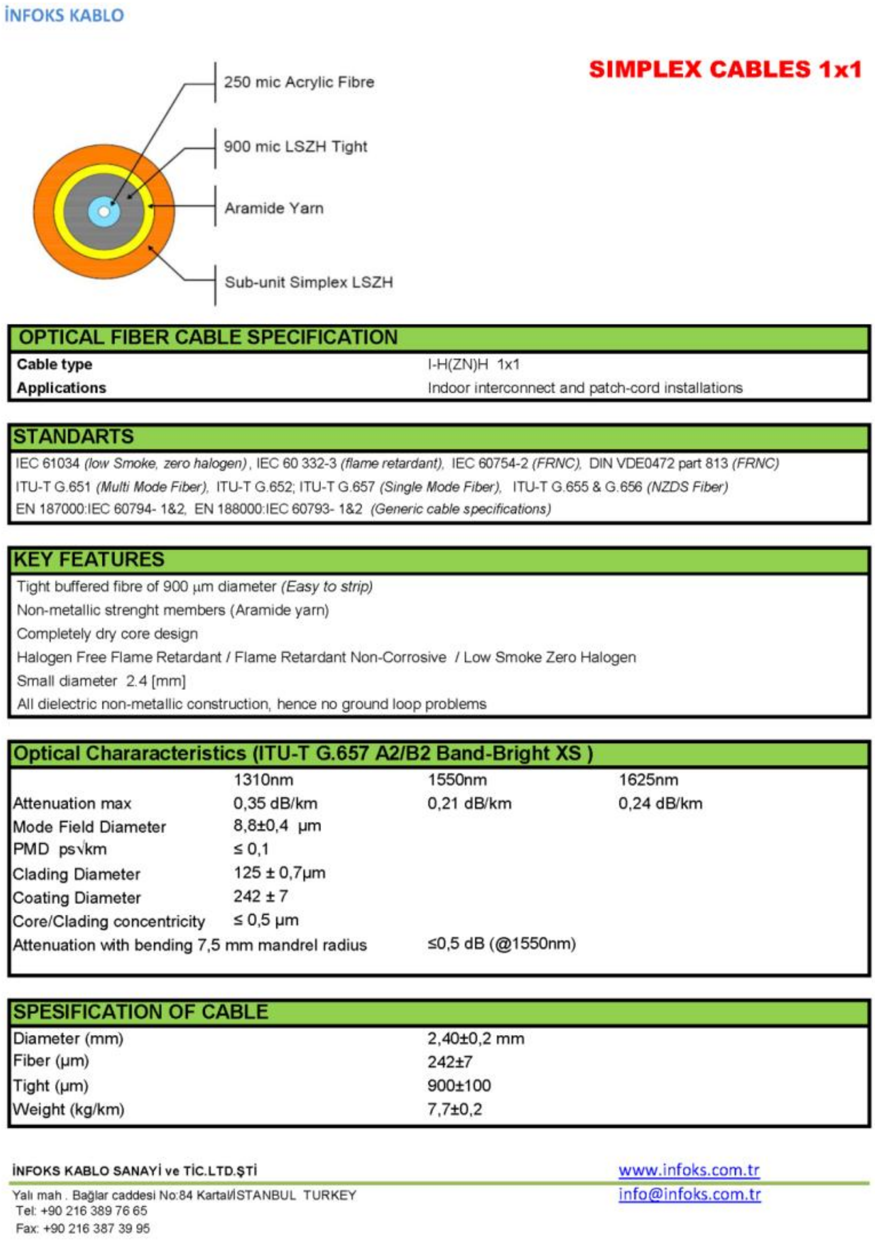

İNFOKS KABLO

SIMPLEX CABLES 1x1

OPTICAL FIBER CABLE SPECIFICATION	
Cable type	I-H(ZN)H 1x1
Applications	Indoor interconnect and patch-cord installations

STANDARTS

IEC 61034 *(low Smoke, zero halogen)*, IEC 60 332-3 *(flame retardant)*, IEC 60754-2 *(FRNC)*, DIN VDE0472 part 813 *(FRNC)*
ITU-T G.651 *(Multi Mode Fiber)*, ITU-T G.652; ITU-T G.657 *(Single Mode Fiber)*, ITU-T G.655 & G.656 *(NZDS Fiber)*
EN 187000:IEC 60794- 1&2, EN 188000:IEC 60793- 1&2 *(Generic cable specifications)*

KEY FEATURES

Tight buffered fibre of 900 μm diameter *(Easy to strip)*
Non-metallic strenght members (Aramide yarn)
Completely dry core design
Halogen Free Flame Retardant / Flame Retardant Non-Corrosive / Low Smoke Zero Halogen
Small diameter 2.4 [mm]
All dielectric non-metallic construction, hence no ground loop problems

Optical Chararacteristics (ITU-T G.657 A2/B2 Band-Bright XS)

	1310nm	1550nm	1625nm
Attenuation max	0,35 dB/km	0,21 dB/km	0,24 dB/km
Mode Field Diameter	8,8±0,4 μm		
PMD ps√km	≤ 0,1		
Clading Diameter	125 ± 0,7μm		
Coating Diameter	242 ± 7		
Core/Clading concentricity	≤ 0,5 μm		
Attenuation with bending 7,5 mm mandrel radius		≤0,5 dB (@1550nm)	

SPESIFICATION OF CABLE	
Diameter (mm)	2,40±0,2 mm
Fiber (μm)	242±7
Tight (μm)	900±100
Weight (kg/km)	7,7±0,2

İNFOKS KABLO SANAYİ ve TİC.LTD.ŞTİ
Yalı mah . Bağlar caddesi No:84 Kartal/İSTANBUL TURKEY
Tel: +90 216 389 76 65
Fax: +90 216 387 39 95

www.infoks.com.tr
info@infoks.com.tr

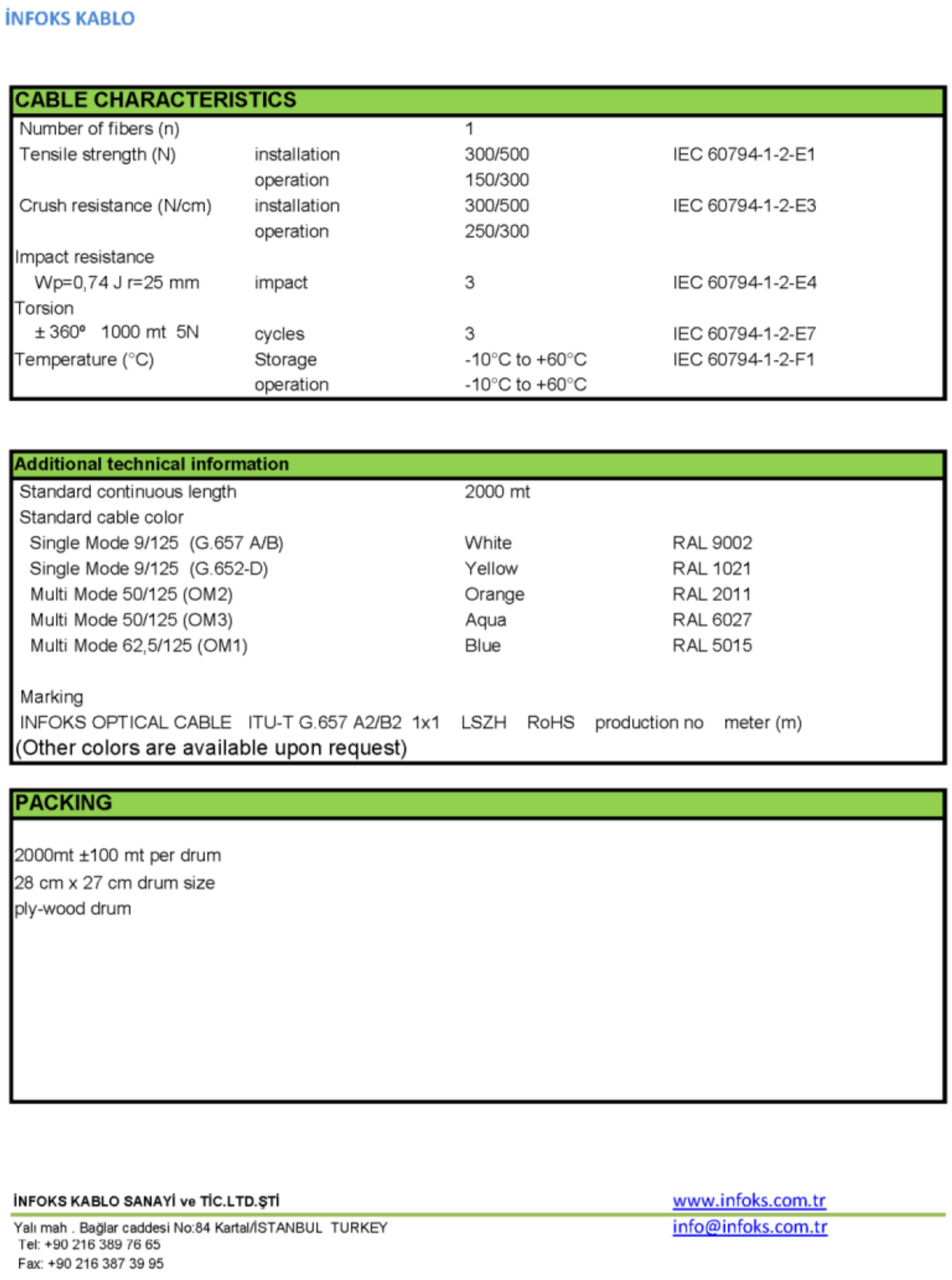

İNFOKS KABLO

CABLE CHARACTERISTICS

Number of fibers (n)		1	
Tensile strength (N)	installation	300/500	IEC 60794-1-2-E1
	operation	150/300	
Crush resistance (N/cm)	installation	300/500	IEC 60794-1-2-E3
	operation	250/300	
Impact resistance			
Wp=0,74 J r=25 mm	impact	3	IEC 60794-1-2-E4
Torsion			
± 360º 1000 mt 5N	cycles	3	IEC 60794-1-2-E7
Temperature (°C)	Storage	-10°C to +60°C	IEC 60794-1-2-F1
	operation	-10°C to +60°C	

Additional technical information

Standard continuous length	2000 mt	
Standard cable color		
Single Mode 9/125 (G.657 A/B)	White	RAL 9002
Single Mode 9/125 (G.652-D)	Yellow	RAL 1021
Multi Mode 50/125 (OM2)	Orange	RAL 2011
Multi Mode 50/125 (OM3)	Aqua	RAL 6027
Multi Mode 62,5/125 (OM1)	Blue	RAL 5015

Marking

INFOKS OPTICAL CABLE ITU-T G.657 A2/B2 1x1 LSZH RoHS production no meter (m)

(Other colors are available upon request)

PACKING

2000mt ±100 mt per drum

28 cm x 27 cm drum size

ply-wood drum

İNFOKS KABLO SANAYİ ve TİC.LTD.ŞTİ
Yalı mah . Bağlar caddesi No:84 Kartal/İSTANBUL TURKEY
Tel: +90 216 389 76 65
Fax: +90 216 387 39 95

www.infoks.com.tr
info@infoks.com.tr